Optimal Premium Pricing Strategy of General insurance in a competitive market with quadratic criteria

Athanasios Pantelous[1, 2] and Eudokia Passalidou[1]
[1]Institute for Financial and Actuarial Mathematics (IFAM), Department of Mathematical Sciences, University of Liverpool, Peach Street, L697ZL, Liverpool United Kingdom (e-mail: A.Pantelous@liverpool.ac.uk.)
[2]Institute For Risk and Uncertainty, University of Liverpool, Liverpool United Kingdom

Abstract. The main data source, on which premium pricing strategy is usually based, is company's own historical data on policies and claims, sometimes supplemented with data from external sources. Nevertheless, a firm which underwrites general insurance displays many of the features of a typical production firm, since it receives premium revenues to cover current cost of underwriting. Moreover, one needs to take also into consideration that individuals and corporations affront insurable and uninsurable risks in the non-life insurance market. On the other hand, it is commonly known that many lines of general insurance are highly competitive and as a result, in practice, the loading depends critically on the price that other insurers charge for comparable policies. Thus, the main idea of Pantelous and Passalidou [23, 24] papers was that company's premium is also affected by market's competition. Under the circumstances, the volume of business is related to the past year experience, the company's premium and reputation, the average premium of the market and a stochastic disturbance. Finally, using a linear discounted function for the company's wealth, an optimal premium strategy which maximizes its present value is derived.

Now, in the present paper, in order to examine the problem more effectively, a maximizing quadratic performance criterion concerning the utility function is suggested, considering a stochastic dynamic wealth function with a linear noise sequence, provided only that the mean value and the covariance matrix of the random vector is zero and a quadratic function of the control variables, respectively. In this covariance matrix, new parameters enrich the previous model, such as the income insurance elasticity of demand, number of consumers, inflation, market's financial risk and consumers' future expectations in addition to company's reputation. The quadratic utility function concerns the present value of wealth and also the marginal utility of insurance contracts. Finally, the derived optimal premium depends, among other factors, on company's wealth.
Keywords: Optimal Premium Strategies; Competitive Markets; Volume of Business; Quadratic performance criterion; Discrete time

1 Introduction

Non-life insurance pricing is the procedure of setting the price of a general insurance policy, taking into consideration various properties of the insured object and the policy holder. The main data source, on which pricing strategy is based, is the insurance company's own historical data on policies and claims, sometimes supplemented with data from external sources. Nevertheless, a firm which underwrites general insurance displays many of the features of a typical production firm, since it receives current premium revenues to cover the cost of underwriting. Needless to say that every company's objective is to maximize its wealth. Consequently, the main challenge that a company faces is to set a premium that comes up from a wealth maximization procedure which includes many different financial parameters.

In actuarial science, a premium principle connects the cost of a general insurance policy to the moments of the corresponding claim arrival and severity distributions. Insurers add a loading to this cost price in order to make a profit and cover their expenses. After this consideration, two main questions are raised; "*How an optimal premium can be calculated in order to maximize company's wealth?"* and "*How it is possible to find a premium strategy that takes into consideration all the different economic parameters that affect company's wealth except from the cost of a general insurance policy?"*

The usual approach concerning non-life insurance pricing is the use of generalized linear models (GLM); a number of key ratios are dependent on a set of rating factors according to Ohlsson and Johansson [22]. For personal lines (designed to be sold in large quantities) the key ratios are often claim frequency and severity (cost per claim), while for commercial lines (designed for relatively small legal entities) the loss ratio may be considered (claims costs per earned premium). Rating factors are grouped into classes (i.e. factor variables) and may include information about policyholder, the insured risk as well as geographic and demographic information. Generalized linear models (GLMs) consist of a rich class of statistical methods, which generalizes the ordinary linear models in two directions:

• *Probability distribution:* Instead of assuming the normal distribution, GLMs work with a general class of distributions, which contains a number of discrete and continuous distributions as special cases, in particular the normal, Poisson and gamma distributions.

• *Model for the mean:* In linear models the mean is a linear function of the covariates x. In GLMs, some monotone transformation of the mean is a linear function of the x's, with the linear and multiplicative models as special cases.

Nevertheless, it is essential to notice that individuals and corporations affront insurable and uninsurable risks in non-life insurance market. Insurable risks includes incidents such automobile damage and building fire while uninsurable risks include the volatility of share returns, variations in income and changes in economic conditions according to

Huang et al.[14]. As pointed out by Schlesinger and Doherty [25], uninsurable background risk might arise due to any number of the following reasons: social risks, general market risk, informational asymmetries, transaction costs of insurance, search costs for insurance, nonmarketable assets and risk versus uncertainty. Lee et al. [18, 19] study the impact of country risks, including political, financial and economic risks, on the income elasticity of insurance demand and concluded that there is a significant effect between them. In other words, these risks affect the company's premium pricing strategy through the income elasticity of insurance demand.

On the other hand, it is commonly known that many lines of insurance are highly competitive and as a result in practice the loading depends critically on the price that other insurers charge for comparable policies. In literature, the first papers concerning competition in insurance markets were written by Taylor [26, 27], who explores successfully the relation between the market's behaviour and the optimal response of an individual insurer, whose objective is to maximize the expected present value of the wealth arising over a pre-defined finite time horizon. He also assumes that the insurance products display a positive price-elasticity of demand. Thus, if the market as a whole begins underwriting at a loss, any attempt by a particular insurer to maintain profitability will result in a reduction of its volume of business. Therefore, he states that the optimal response depends upon various factors including:

(a) The predicted time which will elapse before a return of market rates into profitability,
(b) The price elasticity of demand for the insurance product under consideration, and
(c) The rate of return required on the capital supporting the insurance operation.

According to Taylor's results the optimal strategies do *not* follow what someone might forecast. For instance, it is not the case that profitability is best served by following the market during a period of premium rate depression. In particular, the optimal strategy may well involve underwriting for important profit margins at times when the average market premium rate is well short of breaking even.

A paper that extends significantly Taylor's ideas [26, 27] into a continuous-time stochastic framework is that of Emms et al. [10], since they use a stochastic process for modelling the market average premium and in particular a geometric Brownian motion. Emms et al. [10] handled the problem as a stochastic optimal control problem assuming that the premium policy is a control function and the utility function takes the linear form $U(w,t)=e^{-\beta t}w$, where β is the *inter-temporal* discount rate. Finally they determine a linear maximization problem $\max_{p} \mathrm{E}\int_0^T U\left(w(t),t\right)dt$ over a choice of strategies *p* and a finite time horizon T. Emms et al. [10] studies two premium strategies. In the first one the premium is proportional to the average markets premium and in the second, the premium policy *p* is a function of the break even premium π and the difference of the market's average premium $\bar{p}$ and the break even premium.

In this approach, the optimal strategies depend on (a) the ratio of initial market average premium to break-even premium, (b) the measure of the inverse elasticity of the demand function, and (c) the non-dimensional drift of the market average premium.

In Pantelous and Passalidou [23] paper, a stochastic demand function for the volume of business of an insurance company is formulated into a discrete-time framework extending further Taylor's ideas [26, 27]. Additionally, using the same linear discounted function for the wealth process of the company as in Emms et al. [9, 10], an analytical, endogenous formula for the optimal premium strategy of the insurance company is derived. Similar with Emms et al. [9, 10], a maximization problem for the wealth process of a company is set up, which is solved using stochastic dynamic programming into a discrete-time framework. Consequently, the optimal controller (i.e. the premium) is defined incorporating different parameters of the market into a competitive environment with the same characteristics as in Taylor [26, 27] and Emms et al. [9, 10] papers. In more details, the volume of business is equal to $V_k = V_{k-1}\left(\bar{p}_k / p_k\right)^{-\theta_k}$ where p_k denotes the premium charged by the insurer and $\bar{p}_k$ is the average premium of the market in year $[k,k+1)$; V_{k-1} is the volume of exposure underwritten by the insurer in year $k-1$, and θ_k denotes the set of all other stochastic variables (which are assumed to be independently distributed in time and Gaussian) and it is also considered to be relevant to the demand function in year $[k,k+1)$, such as inflation, interest rate, exchange rate, marketing etc. Finally, the optimal strategy process p_k^* is derived to be:

$$p_k^* = \left(\frac{1}{E\left(\theta_k\right)} \pi_k V_{k-1} E\left(\bar{p}_k\right) \right)^{1/2} \quad \text{for } k = 0,1,.....,T-1.$$

More recently, in Pantelous and Passalidou [24] paper, the volume of business is formed to be a general stochastic demand function extending further their previous suggestions making the model more realistic. Thus, the company's reputation is also considered to the formulation of the volume of business. According to Cretu and Brodie [6], company's reputation (or corporate reputation) has a strong influence on buying decisions or in other words, on the demand of the company's product. Thus, a general functional equation for the volume of business is proposed, which is related to the past years' experience, the average premium of the market, the company's premium, its reputation, and a stochastic disturbance. Then, using a linear discounted function for the company's wealth, an optimal premium strategy is found which maximizes the present value of a wealth function. Analytical solutions of some special and common cases are presented where the optimal premium depends endogenously on the dynamics of the insurance market.

In the last two mentioned above papers, the stochastic disturbance of the volume of business function denotes the set of all other stochastic variables (which are assumed to be independently distributed in time and Gaussian) that are considered to be relevant to the demand function. Analytically, this stochastic parameter consists of many micro-macro factors that affect company's volume of business and consequently the optimal premium strategy.

In order to examine the problem more effectively, a maximizing quadratic performance criterion concerning the utility function is suggested subject to a stochastic wealth function. The utility function concerns the present value of wealth plus the marginal utility of the insurance contracts. Following close Pantelous and Passalidou [23, 24], the volume of business in year k is proportional to the ratio of the markets *average* premium, to the *company*'s premium in year k times, the company's volume of business of the preceding year in addition to a function of the form $f_k(w_k, \tilde{p}_k, \theta_k)$ where $F_k(w_k, \tilde{p}_k) \equiv \mathrm{E}\left[f_k(w_k, \tilde{p}_k, \theta_k) f_k^{\mathrm{T}}(w_k, \tilde{p}_k, \theta_k) \right]$. The function $F_k(w_k, \tilde{p}_k)$ consists of micro-macro parameters which for the very first time, according to the authors' knowledge, are introduced in a competitive insurance pricing model, such as the income insurance elasticity of demand, numbers of consumers, inflation, financial risk of the market and future expectations of consumers in addition to fame of company. Since it will not be easy or accurate to define completely the function $f_k(w_k, \tilde{p}_k, \theta_k)$ because of its stochastic property, a rational approach is formulating the function $F_k(w_k, \tilde{p}_k)$.

To conclude, the contribution of this paper can be summarized on the following key points. Firstly, the optimal premium strategy is determined for a quadratic utility function. In this approach expect from the present value of company's wealth, the marginal utility-premium ratio is also included. Second, the stochastic parameter that affects company's volume of business is analysed into different micro-macro parameters which directly or indirectly affect the optimal premium. Finally, since the maximized criterion is quadratic the optimal premium found depends among other factors, on company's wealth.

The paper is organized as follows: In section 2, a discrete-time model for the insurance market is constructed. We discuss the utility and wealth function and model's main assumptions as long as their economic explanation. In the next section the calculation of the optimal premium is presented which concludes with tow Theorems. Section 4 consists of the discussion of the main results. Finally, section 5 presents a simple application of the model to complete the study.

2 Model Formulation

2.1 Basic Notation

In this part of the paper, following closely Taylor [26, 27], Emms et al. [9, 11], and Pantelous and Passalidou [23, 24] research work, the following notation is needed for what it follows.

V_k : denotes the *volume of business* (or *exposure*) underwritten by the insurer in year $[k, k+1)$. This volume can be measured in any meaningful unit, e.g. number of contracts, total man-hours at risk (for workers' compensation insurance). In our paper, we consider the number of contracts as the volume of exposure.

π_k : denotes the *break-even* premium in year $[k, k+1)$, i.e. risk premium plus expenses per unit exposure.

p_k : denotes the *premium* charged by the insurer in year $[k, k+1)$.

$\overline{p}_k$: denotes the "*average" premium* charged by the market in year $[k, k+1)$.

θ_k : denotes the set of all *other* stochastic variables (which are assumed to be independently distributed in time and follow a Gaussian distribution) and it is considered to be relevant to the demand function in year $[k, k+1)$.

Q_k : denotes the *present day value* factor of a wealth asset in year $[k, k+1)$.

R_k : denotes the *marginal* utility of insurance contracts in year $[k, k+1)$.

B_k^i : denotes the *income elasticity* of demand concerning insurance contracts in year $[k, k+1)$ and time period $i = 0, ..., n'$ and $n' = \left[n(n+1)/2 \right]$.

C_k^i : denotes the *inflation* rate in year $[k, k+1)$ and time period $i = 0, ..., n'$ and $n' = \left[n(n+1)/2 \right]$.

N_k^i : denotes *financial* risk of the market in year $[k, k+1)$ and time period $i = 0, ..., n'$ and $n' = \left[n(n+1)/2 \right]$.

M_k^i : denotes the *number* of consumers in year $[k, k+1)$ and time period $i = 0, ..., n'$ and $n' = \left[n(n+1)/2 \right]$.

g_k^i : denotes the *reputation's impact* to the volume of business in year $[k,k+1)$ and time period $i=0,.....,n'$ and $n'=\left[n(n+1)/2\right]$.

h_k^i : denotes the future *expectations* of consumers (concerning the premium) and time period $i=0,.....,n'$ and $n'=\left[n(n+1)/2\right]$.

2.2 Utility and wealth function

Utility function has a crucial role concerning company's optimal premium pricing. Borch [4, 5] showed how utility theory could be used to formulate and solve some problems that are relevant to insurance. Following Von Neuman and Morgenstern [28], who argued that the existence of a utility function could be derived from a set of axioms governing a preference ordering, the suggested wealth utility function has the following two basic properties following Gerber and Pafumi [11]:

(1) $U(W_k)$ is an increasing function of wealth W_k,

(2) $U(W_k)$ is a concave function of W_k or in other words it is a *risk-averse* utility function.

The first property deals with the required evidence that more wealth is better, which is a reasonable target of every company. Several reasons are given for the second property. The most obvious one is that an insurance company prefers to use a risk averse (or risk avoiding) utility function to equalize other potential risks (financial etc.) that it may confront. One way to justify this, is to require the marginal utility $U(W_k)$ to be a decreasing function of wealth W_k, or equivalently, that the gain of utility resulting from a monetary gain of g, $U(W_k+g)-U(W_k)$ to be a decreasing function of wealth W_k.

The utility function which is proposed is equal to the sum of the present value of company's wealth plus the marginal utility-premium ratio, from the starting year which is equal to zero till year $N-1$ times $1/2$ plus the present value of the company's wealth in year N times $1/2$.

The marginal utility-premium ratio indicates the fulfilment derived from the last money spent on the insurance. A client (insured) maximizes his utility function by equating the marginal utility-price ratio for each insurance contract purchased. A generic marginal utility-premium ratio is equal to the marginal utility of general insurance divided to the premium paid. Following closely the previous papers, in this paper, we also denote the wealth process w_k as the insurer's capital at time $[k,k+1)$, so we obtain

$$w_{k+1}=-a_k w_k+(p_k-\pi_k)V_k, \tag{2.1}$$

where $a_k\in[0,1]$ denotes the *excess return* on capital (i.e. return on capital required by the shareholders of the insurer whose strategy is under consideration). Thus, $-a_k w_k$ is the *cost* of holding w_k in the time interval $[k,k+1)$. Moreover, the basic assumption of our previous papers is maintained so the volume of business in year *k* is assumed to be proportional to the ratio of the markets *average* premium to the *company*'s premium in year *k* times the company's volume of business in the preceding year. Furthermore, the volume of business is stochastic due to the stochastic parameter θ_k which is assumed to be independently distributed in time and Gaussian and indirectly affects the premium and finally the company's wealth. This parameter's affection will be explained analytically in Assumption 2 (see next sub-section).

Consequently, we consider the problem of maximizing with respect to $\left\{\tilde{p}_k=p_k^{-1}\right\}$ the performance criterion

$$\mathrm{E}_{/w_0}\left\{\sum_{k=0}^{N-1}\frac{1}{2}\left(w_k^{\mathrm{T}}Q_k w_k+\tilde{p}_k^{\mathrm{T}}R_k\tilde{p}_k\right)+\frac{1}{2}w_N^{\mathrm{T}}Q_N w_N\right\}. \tag{2.2}$$

Subject to the stochastic dynamic system of the wealth function

$$w_{k+1}=-a_k w_k+m_k+Z_k\tilde{p}_k+f_k(w_{k,}\tilde{p}_k,\theta_k), \tag{2.3}$$

where $m_k=V_{k-1}\bar{p}_k$, $Z_k=-V_{k-1}\bar{p}_k\pi_k$, $w_k\in\mathbb{R}^n$, $\tilde{p}_k\in\mathbb{R}^m$, $\theta_k\in\mathbb{R}^q$, $f_k:\mathbb{R}^n\times\mathbb{R}^m\times\mathbb{R}^q\to\mathbb{R}^n$, and Q_k, Q_N, R_k, a_k, Z_k are matrices of appropriate dimensions and $m_k\in\mathbb{R}^n$. Since market's average premium is stochastic the elements of factor Z_k are stochastic parameters and m_k is also stochastic.

In other words $\mathrm{E}(m_k) = V_{k-1}\mathrm{E}(\bar{p}_k)$, $\mathrm{E}(Z_k) = -V_{k-1}\mathrm{E}(\bar{p}_k)\pi_k = -\mathrm{E}(m_k)\pi_k$.

2.3 Assumptions

The following assumptions are made:

Assumption 1: $f_k(w_k, \tilde{p}_k) \equiv \mathrm{E}[f_k(w_k, \tilde{p}_k, \theta_k)]$ is *zero* for all $w_k \in \mathbb{R}^n$, $u_k \in \mathbb{R}^m$, $k = 0, ..., N-1$. There is no loss of generality in assuming $f_k(w_k, \tilde{p}_k) \equiv 0$ because appropriate choices of $-a_k, Z_k, m_k$ will model any mean value of f_k which is linear in $w_k, \tilde{p}_k$.

Assumption 2: $F_k(w_k, \tilde{p}_k) \equiv \mathrm{E}\left[f_k(w_k, \tilde{p}_k, \theta_k) f_k^{\mathrm{T}}(w_k, \tilde{p}_k, \theta_k)\right]$ exists and is a general quadratic function of $w_k, \tilde{p}_k$ for $k = 0, ..., N-1$.

That is $F_k(w_k, \tilde{p}_k)$ has the representation

$$F_k(w_k, \tilde{p}_k) = B_k^0 + \sum_{i=1}^{n'} B_k^i \left(\frac{1}{2} w_k^{\mathrm{T}} C_k^i w_k + \tilde{p}_k^T N_k^i w_k + \frac{1}{2} \tilde{p}_k^{\mathrm{T}} M_k^i \tilde{p}_k + w_k^{\mathrm{T}} g_k^i + \tilde{p}_k^T h_k^i \right),$$

where $B_k^i, C_k^i, N_k^i, M_k^i$ are matrices of appropriate dimensions $g_k^i \in \mathbb{R}^n, h_k^i \in \mathbb{R}^m$ and B_k^i, C_k^i, M_k^i are symmetric $i = 0, ..., n'$, where $n' = \left[n(n+1)/2 \right]$.

The income elasticity of non-life insurance measures the responsiveness of the demand for general insurance contracts to a change in the income of the people demanding them *ceteris paribus* (all other factors held constant). Lee et al [18] conclude that insurance, like other developed financial services, has grown in quantitative importance as part of the general advancement of financial sectors and that there is a relationship between non-life insurance premiums and real income. According to their study income elasticity of non-life insurance premiums are larger than one. This means that non-life insurance is a luxury good.

A frequent reason given for the lack of depth in non-life insurance markets in developing countries is that consumers perceive insurance as a luxury item. Insurance penetration is clearly related to a country's income level. The link between a country's aggregate demand for insurance and level of gross domestic product (GDP) is clear, but the forces driving the demand for insurance at the micro level are not. The insurance-as-luxury assumption implies that income distribution in developing countries is such that insurance can only be consumed in small quantities. This is common sense after all, spending money to protect against losses is not feasible unless income is reasonably high and consumers have possessions to which they have title, and an interest in protecting them. The key is to determine when the income levels pass the 'reasonably high' mark, and when consumers believe that they have amassed enough property to merit protection. Traditional thinking holds that, especially in developing countries, personal insurance services are of interest largely to the top economic groups and, because this demographic is minuscule, the insurance market should be minuscule as well.

Moreover inflation can change dramatically company's wealth since inflation reflects a reduction in the purchasing power per unit of money or loss of real value in the medium of exchange and unit of account within the economy. A chief measure of price inflation is inflation rate. In fact, inflation rate is disadvantageous to the development both of life and non-life insurance in that it is detrimental to individual's purchasing power.

Several studies have documented the impact of inflation, especially on the property-liability insurance industry. Some of them are mentioned indicatively. D'Arcy [7] finds that both the underwriting profit margin and insurance investment returns were negatively correlated with the inflation rate during the period 1951-1976. Krivo [16] determines that although inflation and the underwriting profit margin were not significantly correlated over the subsequent period 1977-2006, investment returns and the year-to-year change in underwriting profit margin were both significantly negatively correlated with inflation over that period. Lowe and Warren [21] describe the negative impact of inflation on property-liability insurers' claim costs, loss reserves and asset portfolios. They express concern that most current actuaries, underwriters and claim staff have never experienced of severe inflation, so could be slow to adapt to any change in the economic environment. In other words, property-liability insurers are impacted by inflation in several ways. The clearest impact is the cost of future claims on current policies according to Ahlgrim and D' Arcy [1].

A critical factor that affects demand for non-life insurance and indirectly premium and wealth is the number of consumers in the market. As more or fewer consumers enter the market this has a direct effect on insurance contracts that consumers are willing and able to buy. An increase in the number of people means that there are more potential customers or in other words more individual demand curves to add up to get the general insurance demand curve, so markets demand increases. An increase in demand shifts the demand curve to the right so at each premium, the quantity of contracts demanded increases. The excess demand causes the premium to rise and equilibrium is restored at a different point.

Another variable that affects wealth function and premium is the financial risk of the market. Studies have documented a correlation between financial development and the development of the insurance market. Lorent [20] indicates that insurance and banking are increasingly intricate and Billio et al.[3] also show that the insurance sector has over time become highly interrelated with other sectors in financial system such as banks, hedge funds etc due to the

involvement of insurance companies in non-core activities such as credit defaults swaps, derivatives trading and investment management.

As it has been already mentioned, the reputation of the company affects the product's demand and consequently the optimal premium and company's wealth as well. The reputation of a business is essential to its survival. The trust and confidence of the client can have a direct and profound effect on a company's bottom line. While an intangible concept, having a good reputation can benefit a business in a multitude of ways including consumer preference, support for an organization in times of crisis or controversy and the future value of an organization in the marketplace.

Finally, the future expectation of consumers concerning the premiums can also affect how many contracts one is willing and able to buy. The expectations that clients have, concerning the future premium, are assumed constant when a demand curve is constructed. Clients' expectations are one of five demand determinants that shift the demand curve when they change. It is important to realize that clients (buyers) make buying decisions based on a comparison of current and future premiums. They are motivated to purchase a non-life insurance contract at the lowest possible price. If that lowest price is the one existing today, then they will buy today. If that lowest price is expected to occur in the future, then they will wait until later to buy. Thus, if a potential client thinks next month's premium will be higher than he had initially expected, he may buy an insurance contract today and not next month. That means that the demand for general insurance contracts today will increase.

Assumption 3: $F_k(w_k, \tilde{p}_k) \geq 0, \forall w_k \in \mathbb{R}^n, \tilde{p}_k \in \mathbb{R}^m$

Assumption 3 is necessary (hence not all restrictive) in order that $F_k(w_k, \tilde{p}_k)$ be a covariance matrix for each $w_k \in \mathbb{R}^n, \tilde{p}_k \in \mathbb{R}^m$. The optimal control sequence $\{\tilde{p}_k\}$ is to be drawn from sequences of closed loop controllers i.e. of the form $\tilde{p}_k = D_k(W_k);\ W_k \in \{w_0, w_1, ..., w_k\}$ where $D_k : \mathbb{R}^n \times \mathbb{R}^k \to \mathbb{R}^m; k = 0, ..., N-1$. Note that because θ_k is a sequence of random variables independently disturbed in time, knowledge of w_k is equivalent to knowledge of W_k so that the sequences of closed loop controllers can be written $\tilde{p}_k = D_k(w_k);\ k = 0, ..., N-1$.

Assumption 4: There is positive price-elasticity of demand, i.e. if the market as a whole begins underwriting as a whole begins underwriting at a loss, any attempt by a particular insurer to maintain profitability will result in a reduction of his volume of business.

Assumption 5: There is a finite time horizon.

Assumption 6: Demand in year $k+1$ is assumed to be proportional to demand in the preceding year k.

3 Main Results

Let's define first

$$\bar{C}_k(S_{k+1}) \equiv \frac{1}{2}\sum_{i=1}^{n'} tr\left(S_{k+1}B_k^i\right)C_k^i,\ \bar{N}_k(S_{k+1}) \equiv \frac{1}{2}\sum_{i=1}^{n'} tr\left(S_{k+1}B_k^i\right)N_k^i,\ \bar{M}_k(S_{k+1}) \equiv \frac{1}{2}\sum_{i=1}^{n'} tr\left(S_{k+1}B_k^i\right)M_k^i,$$

$$\bar{g}_k(S_{k+1}) \equiv \frac{1}{2}\sum_{i=1}^{n'} tr\left(S_{k+1}B_k^i\right)g_k^i,\ \bar{h}_k(S_{k+1}) \equiv \frac{1}{2}\sum_{i=1}^{n'} tr\left(S_{k+1}B_k^i\right)h_k^i, \text{ and}$$

$$\mathrm{E}\left(\tilde{R}_k\right) \equiv R_k + \mathrm{E}\left(Z_k^T\right)S_{k+1}\mathrm{E}\left(Z_k\right) + \bar{M}_k(S_{k+1}), \tag{3.1}$$

$$\mathrm{E}\left(\tilde{a}_k\right) \equiv \mathrm{E}\left(Z_k^T\right)S_{k+1}(-a_k) + \bar{N}_k(S_{k+1}), \tag{3.2}$$

$$\mathrm{E}\left(\tilde{m}_k\right) \equiv \mathrm{E}\left(Z_k^T\right)S_{k+1}\mathrm{E}\left(m_k\right) + \mathrm{E}\left(Z_k^T\right)d_{k+1} + \bar{h}_k(S_{k+1}). \tag{3.3}$$

Where

$$\mathrm{E}\left(S_k\right) = Q_k + \left(-a_k\right)^T S_{k+1}\left(-a_k\right) + \bar{C}_k(S_{k+1}) + \mathrm{E}\left(\tilde{a}_k^T\right)\mathrm{E}\left(\tilde{R}_k^{-1}\right)\mathrm{E}\left(\tilde{a}_k\right), S_N = Q_N \tag{3.4}$$

$$\mathrm{E}\left(d_k\right) = -a_k^T S_{k+1}\mathrm{E}\left(m_k\right) - a_k^T d_{k+1} + \bar{g}_k(S_{k+1}) + \mathrm{E}\left(\tilde{a}_k\right)\mathrm{E}\left(\tilde{R}_k^{-1}\right)\mathrm{E}\left(\tilde{m}_k\right), d_N = 0 \tag{3.5}$$

$$\mathrm{E}\left(e_k\right) = \frac{1}{2}tr\left(S_{k+1}B_k^0\right) + \frac{1}{2}\mathrm{E}\left(m_k^T\right)S_{k+1}\mathrm{E}\left(m_k\right) + d_{k+1}^T E\left(m_k\right) + e_{k+1} + \frac{1}{2}\mathrm{E}\left(\tilde{m}_k^T\right)\mathrm{E}\left(\tilde{R}_k^{-1}\right)\mathrm{E}\left(\tilde{m}_k\right), e_N = 0\ . \tag{3.6}$$

Theorem 1.

$$\textit{If}\quad \mathrm{E}\left(\tilde{R}_k\right) \geq 0 \quad \textit{for all}\quad k \in \{0, ..., N-1\}, \tag{3.7}$$

the optimal closed loop controller is

$$\tilde{p}_k^* = \mathrm{E}\left(\tilde{R}_k^{-1}\right)\left[\mathrm{E}\left(\tilde{a}_k\right)w_k + \mathrm{E}\left(\tilde{m}_k\right)\right];\ k = 0, ..., N-1, \tag{3.8}$$

and the maximum value is given by

$$\frac{1}{2}w_0^T S_0 w_0 + d_0^T w_0 + e_0 . \tag{3.9}$$

Proof. Let's define

$$J_k(w_k) \equiv \max_{p_k \cdots p_{N-1}} \mathrm{E}_{/w_k} \left\{ \sum_{t=k}^{N-1} \frac{1}{2}\left(w_t^T Q_t w_t + \tilde{p}_t^T R_t \tilde{p}_t \right) + \frac{1}{2} w_N^T Q_N w_N \right\}. \tag{3.10}$$

The optimal performance criterion satisfies Bellman equation

$$\begin{aligned}
J_k(w_k) &\equiv \max_{p_k \cdots p_{N-1}} \mathrm{E}_{/w_k} \left\{ \sum_{k=0}^{N-1} \frac{1}{2}\left(w_k^T Q_k w_k + \tilde{p}_k^T R_k \tilde{p}_k \right) + \frac{1}{2} w_N^T Q_N w_N \right\}, \\
J_k(w_k) &\equiv -\min_{p_k \cdots p_{N-1}} \mathrm{E}_{/w_k} \left\{ -\sum_{k=0}^{N-1} \frac{1}{2}\left(w_k^T Q_k w_k + \tilde{p}_k^T R_k \tilde{p}_k \right) - \frac{1}{2} w_N^T Q_N w_N \right\}, \\
J_k(w_k) &\equiv -\min_{p_k \cdots p_{N-1}} \mathrm{E}_{/w_k} \left\{ -\frac{1}{2} w_k^T Q_k w_k - \frac{1}{2} \tilde{p}_k^T R_k \tilde{p}_k - J_{k+1}(w_{k+1}) \right\}, \\
J_k(w_k) &\equiv -\min_{p_k \cdots p_{N-1}} \left\{ -\frac{1}{2} w_k^T Q_k w_k - \frac{1}{2} \tilde{p}_k^T R_k \tilde{p}_k - \mathrm{E}_{/w_k}\left(J_{k+1}(w_{k+1}) \right) \right\},
\end{aligned} \tag{3.11}$$

and $J_N(w_N) = \frac{1}{2} w_N^T Q_N w_N$. We now show by induction that

$$J_k(w_k) \equiv \frac{1}{2} w_k^T S_k w_k + d_k^T w_k + e_k \tag{3.12}$$

solves (3.11), by noting that (3.12) is true for $k = N$, assuming that (3.12) is true for $k+1$ and proving that is true for k. Substituting the assumed expression for $J_{k+1}(w_{k+1})$ into the right hand side of (3.11) yields

$$\begin{aligned}
&-\min_{p_k}\{ -\frac{1}{2} w_k^T Q_k w_k - \frac{1}{2} \tilde{p}_k^T R_k \tilde{p}_k - \mathrm{E}_{/w_k}\left[-a_k w_k + Z_k \tilde{p} + m_k + f_k(w_{k,} p_k, \theta_k) \right]^T \times S_{k+1}\left[-a_k w_k + Z_k \tilde{p} + m_k + f_k(w_{k,} \tilde{p}_k, \theta_k) \right] \\
&-\mathrm{E}_{/w_k} d_{k+1}^T \left[-a_k w_k + Z_k \tilde{p} + m_k + f_k(w_{k,} \tilde{p}_k, \theta_k) \right] - e_{k+1} \} \\
&= -\min_{p_k}\{ -\frac{1}{2} w_k^T Q_k w_k - \frac{1}{2} \tilde{p}_k^T R_k \tilde{p}_k - \frac{1}{2} w_k^T \left(-a_k^T \right) S_{k+1} \left(-a_k \right) w_k - \tilde{p}_k^T \mathrm{E}\left(Z_k^T \right) S_{k+1} \left(-a_k \right) w_k \\
&-\frac{1}{2} \tilde{p}_k^T \mathrm{E}\left(Z_k^T \right) S_{k+1} \mathrm{E}\left(Z_k \right) \tilde{p}_k - \mathrm{E}\left(m_k^T \right) S_{k+1} \left(-a_k \right) w_k - \mathrm{E}\left(m_k^T \right) S_{k+1} \mathrm{E}\left(Z_k \right) \tilde{p}_k \\
&-\frac{1}{2} \mathrm{E}\left(m_k^T \right) S_{k+1} \mathrm{E}\left(m_k \right) - \frac{1}{2} tr(S_{k+1} B_k^0) - \frac{1}{2} w_k^T \bar{C}_k \left(S_{k+1} \right) w_k - \tilde{p}_k^T \bar{N}_k \left(S_{k+1} \right) w_k \\
&-\frac{1}{2} \tilde{p}_k^T \bar{M}_k \left(S_{k+1} \right) \tilde{p}_k - w_k^T \bar{g}_k \left(S_{k+1} \right) - \tilde{p}_k^T \bar{h}_k \left(S_{k+1} \right) - d_{k+1}^T \left(-a_k \right) w_k - d_{k+1}^T E\left(Z_k \right) \tilde{p}_k - d_{k+1}^T E\left(m_k \right) - e_{k+1} \} \\
&= -\min_{p_k}\{ \frac{1}{2} w_k^T \left[-Q_k - (-a_k^T) S_{k+1} \left(-a_k \right) - \bar{C}_k(S_{k+1}) \right] w_k + w_k^T \left[-(-a_k^T) S_{k+1} E\left(m_k \right) - \bar{g}_k(S_{k+1}) - (-a_k^T) d_{k+1} \right] \\
&\qquad -\frac{1}{2} tr\left(S_{k+1} B_k^0 \right) - \frac{1}{2} \mathrm{E}\left(m_k^T \right) S_{k+1} \mathrm{E}\left(m_k \right) - d_{k+1}^T \mathrm{E}\left(m_k \right) - e_{k+1} - \frac{1}{2} \tilde{p}_k^T \mathrm{E}\left(\tilde{R}_k \right) \tilde{p}_k - \tilde{p}_k^T \mathrm{E}\left(\tilde{a}_k \right) w_k - \tilde{p}_k^T \mathrm{E}\left(\tilde{m}_k \right) \}.
\end{aligned} \tag{3.13}$$

Because of (3.7), the control that maximizes (3.13) is given by (3.8). When this is substituted into (3.13), we obtain

$$\begin{aligned}
&-\left[\frac{1}{2} w_k^T \left[-Q_k - (-a_k)^T S_{k+1} - \bar{C}_k(S_{k+1}) - \mathrm{E}\left(\tilde{a}_k^T \right) \mathrm{E}\left(\tilde{R}_k^{-1} \right) \mathrm{E}\left(\tilde{a}_k \right) \right] w_k \right] \\
&-w_k^T \left[-(-a_k^T) S_{k+1} \mathrm{E}\left(m_k \right) - \bar{g}_k(S_{k+1}) - (-a_k^T) d_{k+1} - \mathrm{E}\left(\tilde{a}_k^T \right) \mathrm{E}\left(\tilde{R}_k^{-1} \right) \mathrm{E}\left(\tilde{m}_k \right) \right] \\
&-\left[-\frac{1}{2} tr(S_{k+1} B_k^0) - \frac{1}{2} \mathrm{E}\left(m_k^T \right) S_{k+1} \mathrm{E}\left(m_k \right) - d_{k+1}^T \mathrm{E}\left(m_k \right) - e_{k+1} - \frac{1}{2} \mathrm{E}\left(\tilde{m}_k^T \right) \mathrm{E}\left(\tilde{R}_k^{-1} \right) \mathrm{E}\left(\tilde{m}_k \right) \right]
\end{aligned}$$

$$= \left[\frac{1}{2} w_k^T \left[Q_k + (-a_k)^T S_{k+1} (-a_k) + \bar{C}_k (S_{k+1}) + \mathrm{E}\left(\tilde{a}_k^T\right) \mathrm{E}\left(\tilde{R}_k^{-1}\right) \mathrm{E}\left(\tilde{a}_k\right) \right] w_k \right]$$

$$+ w_k^T \left[(-a_k^T) S_{k+1} \mathrm{E}\left(m_k\right) + \bar{g}_k (S_{k+1}) + (-a_k^T) d_{k+1} + \mathrm{E}\left(\tilde{a}_k^T\right) \mathrm{E}\left(\tilde{R}_k^{-1}\right) \mathrm{E}\left(\tilde{m}_k\right) \right]$$

$$+ \frac{1}{2} tr(S_{k+1} B_k^0) + \frac{1}{2} \mathrm{E}\left(m_k^T\right) S_{k+1} \mathrm{E}\left(m_k\right) + d_{k+1}^T \mathrm{E}\left(m_k\right) + e_{k+1} + \frac{1}{2} \mathrm{E}\left(\tilde{m}_k^T\right) \mathrm{E}\left(\tilde{R}_k^{-1}\right) \mathrm{E}\left(\tilde{m}_k\right). \quad (3.14)$$

Using (3.1), (3.2), (3.3) in (3.14) yields the fact that (3.12) is true. Thus the proof by induction is complete. □

The next theorem shows that under certain reasonable conditions inequality (3.7) is satisfied.

Theorem 2. *Suppose that* $Q_N \geq 0$ *and that* $Q_k \geq 0$ *and* $R_k > 0$ *for all* $k = 0, ..., N-1$

$$\textit{then} \quad \tilde{R}_k > 0 \textit{ and } S_{k+1} \geq 0; k = 0, ..., N-1. \quad (3.15)$$

Proof. We prove this by induction. First we note that because of Assumption 3 and the equation $F_k(w_k, \tilde{p}_k)$ which is mentioned in Assumption 2 we have

$$\bar{M}_k\left(S_{k+1}\right) \geq 0, \text{ if } S_{k+1} \geq 0 \ . \quad (3.16)$$

Now we proceed by induction. Clearly we have $\tilde{R}_{N-1} > 0$ and $S_N \geq 0$. We now assume

$$S_i \geq 0, \ i = k+1, ..., N, \quad (3.17)$$

which implies

$$\tilde{R}_{i-1} > 0, \ i = k+1, ..., N. \quad (3.18)$$

Because $S_{k+1} \geq 0$ it follows from (3.16) and (3.1) that $\tilde{R}_k > 0$.

This, by virtue of (3.4), permits the computation of S_k, d_k, e_k and (3.12) yields

$$J_k(w_k) = \frac{1}{2} w_k^T S_k w_k + d_k^T w_k + e_k = \max_{p_k ..... p_{N-1}} \mathrm{E}_{/w_k} \left\{ \sum_{t=\kappa}^{N-1} \frac{1}{2} \left(w_t^T Q_t w_t + \tilde{p}_t^T R_t \tilde{p}_t \right) + \frac{1}{2} w_N^T Q_N w_N \right\}. \quad (3.19)$$

Now because of our assumption on Q_N, Q_k, R_k; $k = 0, ..., N-1$, the right-hand side of (3.19) is nonnegative for all w_k which implies $S_k \geq 0$ and hence it follows from (3.16) and (3.1) that $\tilde{R}_{k-1} > 0$ so that (3.17), (3.18) are true for $i = k, ..., N$ and the proof by induction is complete. □

4 Discussion of main results

According to the derived results so far, the optimal premium is calculated endogenously by the market and derived quite naturally using elements of dynamic programming. First, based on Pantelous and Passalidou's [23] primary pricing model, the optimal premium depends on the break-even premium, the company's volume of business of the preceding year, the expectation of market's average premium and the expectation of the stochastic parameter θ_k. This stochastic parameter consists of all micro-macro parameters that affect company's volume of business.

The second model referred also to Pantelous and Passalidou [24] says that the optimal premium depends, as before, on the break-even premium, the volume of business of the previous year, the expected value of the average premium rate and also on the company's reputation raised to a factor b and the expected value of the natural exponential function of the stochastic parameter θ_k. In this model the optimal premium can be calculated for both negative and positive prices of θ_k.

Concerning the new results of the present paper, at first it is essential to mention that the optimal premium is calculated on three factors $\tilde{R}_k$, $\tilde{a}_k$, $\tilde{m}_k$ which all include, among others elements, the parameter Z_k. This parameter consists of the three following factors:

- *The break- even premium,*
- *The company's volume of business of the preceding year,*
- *The expectation of market's average premium*.

These factors are also appeared to the optimal premium calculated in our previous papers, remaining consistent in our main philosophy and staying faithful to the way of confronting the problem. The expectation of market's average premium is directly related to the market's competition which affects company's premium. Moreover the break-even

premium is directly related to the company's profitability as well as its wealth and the company's volume of business of the preceding year is indicative to the company's volume of business and optimal premium as well.

Except the parameter Z_k, two other parameters are appeared to these three main factors $\tilde{R}_k$, $\tilde{a}_k$, $\tilde{m}_k$ from which the optimal premium is calculated on. These are S_{k+1} and B_k^i. As we have mentioned earlier B_k^i denotes the income elasticity of demand which affects every financial factor of every market and every business in it since both are all related directly or indirectly to the consumer's income. The factor S_{k+1} is calculated based on the following:

- *The present day value factor,*
- *The market's inflation*.

These two economic factors play the most crucial role concerning company's wealth on which optimal premium is depended on. The present day value factor is used to simplify the calculation for finding the present value of a series of values in the future. It is based on the discount interest rate and the number of periods. Inflation and interest rates are linked, and frequently referenced in macroeconomics. Inflation refers to the rate at which prices for goods and services rises. In general, as interest rates are lowered, more people are able to borrow more money. The result is that consumers have more money to spend, causing the economy to grow and inflation to increase. The opposite holds true for rising interest rates. As interest rates are increased, consumers tend to have less money to spend. With less spending, the economy slows and inflation decreases.

These parameters are related to company's wealth directly since the main difference between the optimal premium calculated in this paper and the ones mentioned above is that the optimal premium is related directly to the company's wealth.

As we have already mentioned the optimal premium is depended on company's wealth and the parameters $\tilde{R}_k$, $\tilde{a}_k$, $\tilde{m}_k$. All these factors consists of parameters that are indicative to the financial conditions prevailing to a market and affect the company's wealth and consumer's marginal utility. We mentioned earlier that all these three parameters rely on Z_k, S_{k+1} and B_k^i.

Analytically, the factor $\tilde{a}_k$ depends also on:

- *The excess return of capital i.e. return on capital required by the shareholders of the insurer whose strategy is under consideration.*
- *The financial risk that the markets confronts.*

Excess return on capital refers to principal payments back to "capital owners" (shareholders, partners, unit holders) that exceed the growth (net income/taxable income) of an insurance business or investment. As the financial risk in a market becomes higher the shareholders probably will ask for a higher excess return of capital.

Moreover the optimal premium depends on the parameter $\tilde{m}_k$ which calculates on:

- *The parameter m_k which equals to the volume of business of the preceding year times market's average premium,*
- *The future expectation of the consumers concerning the company's premium,*
- *The parameter d_{k+1} which is related to the reputation's impact to the volume of business.*

Another crucial factor is the future expectations of clients. Buyers make buying decisions based on a comparison of current and future prices. They are motivated to purchase an insurance contract at the lowest price possible. If that lowest price is the one existing today, then they will buy today. If that lowest price is expected to occur in the future, then they will wait until later to buy.

Moreover, firms with strong positive reputations attract better people. They are perceived as providing more value, which often allows them to charge a premium. Their customers are more loyal and buy broader ranges of products and services. Because the market believes that such companies will deliver sustained earnings and future growth, they have higher price-earnings multiples and market values and lower costs of capital.

Finally the optimal premium depends on the parameter $\tilde{R}_k$ which calculates on:

- *The marginal utility of insurance contracts,*
- *The number of the consumers.*

Consequently, the main parameters that were suggested to affect the optimal premium pricing policy are still appeared to the present optimal premium calculation formula (break-even premium, previous year's volume and the expectation of the market's average premium). This formula is also enriched with company's wealth and consumer's utility which affection on the optimal premium depends on the three main parameters mentioned above. This optimal premium depends on many new introduced different parameters. Thus, the optimal premium is more close to the reality since take into consideration market's financial factors which indirectly affects the company's optimal premium strategy.

5 Application

In order to illustrate the main theoretical finding of this paper, a simple numerical example is presented. Unfortunately, that available real data in public are not analytic and several assumptions has to be made, thus the derived numerical results are subjective and they just illustrate the applicability of the model. The following table present the main parameters needed to calculate a company's optimal premium according this model.

$$E(\bar{p}_k) = 200\,€, \qquad N_k = \begin{bmatrix} 0,2 & 1,2 \\ -0,2 & -1,2 \end{bmatrix},$$

$$V_{k-1} = 1000, \qquad a_k = 0,8,$$

$$\pi_k = 60\,€, \qquad d_{k+1} = \begin{bmatrix} 2,1 & 4,1 \\ 3,2 & 4,2 \end{bmatrix},$$

$$R_k = \begin{bmatrix} 10 & 15 \\ 12 & 13 \end{bmatrix}, \qquad h_k = \begin{bmatrix} 0 & 1 \\ 1 & 0 \end{bmatrix},$$

$$S_{k+1} = \begin{bmatrix} 0,5 & 0,8 \\ 0,4 & 0,7 \end{bmatrix}, \qquad B_k^1 = \begin{bmatrix} 1,2 & 1,5 \\ 1,4 & 1,6 \end{bmatrix},$$

$$M_k = \begin{bmatrix} 10^6 & 1,5\times 10^6 \\ 1,2\times 10^6 & 1,7\times 10^6 \end{bmatrix}, \qquad w_k = 320.000\,€.$$

The expectation of market's average premium can be found following Pantelous and Passalidou's [23] two suggested premium strategies.

In the first premium strategy, the *average* premium is calculated considering all the competitors of the market, and their proportions regarding to the volume of business. In mathematical terms the expected *average* premium of the market is equal to $\mathrm{E}(\bar{p}) = \frac{1}{m}\sum_{i=1}^{K} b_{i,n}\, p_{i,n}$ where $b_{i,n} = V_{i,n}\left(\sum_{i=1}^{K} V_{i,n}\right)^{-1}$ and $\sum_{i=1}^{K} b_{i,n} = 1$ for every year *n*, $p_{i,n}$ is the premium of the company i^{th} for the year *n*; *K* is the number of the competitors (including also our company's premium) in the insurance market and m is the number of years for the available data (i.e. we assume that we have the uniform distribution for the weight of every year).

According the second premium strategy the *average* premium is calculated considering the premiums of the top K^+ competitors of the market (including the leading company of the market). In mathematical terms the expected *average* premium of the market is equal to $\mathrm{E}(\bar{p}) = \frac{1}{m}\sum_{i=1}^{K^+} b_{i,n}^{+}\, p_{i,n}^{+}$, where $b_{i,n}^{+} = V_{i,n}\left(\sum_{i=1}^{K^+} V_{i,n}\right)^{-1}$ and $\sum_{i=1}^{K^+} b_{i,n}^{+} = 1$ for every year *n*, $p_{i,n}^{+}$ is the premium of the i^{th} top company for the year *n*; K^+ is the number of the top competitors (including also our company's premium) in the insurance market and m is the number of years for the available data (i.e. we assume that we have the uniform distribution for the weight of every year).

The volume of business of the previous year and net premium can be found by company's own data.

The matrix R_k shows the marginal utility of insurance contracts in year $[k, k+1)$ for four different insured (clients) categories.

The matrix S_{k+1} can be calculated on the present day value factor of company's wealth, the market's inflation and the known, from the previous year, parameter S_k.

The matrix M_k denotes the number of consumers separated to four different group categories. Each element of matrix M_k is a different category of possible clients. Thus, each element of the matrix R_k denotes the marginal utility of insurance contract for each group category.

The matrix N_k denotes the financial risk of the market in year $[k, k+1)$. The elements of this matrix denote the possibility of a market to present increased financial risk. Positive values denote the existence of financial risk in the market and negative values the lack of it. The elements of this matrix can either derive from the market's data or can be a combination of different future scenarios concerning the market.

The factor a_k denotes the excess return of capital i.e. return on capital required by the shareholders of the insurer whose strategy is under consideration and is set by each company.

The matrix d_{k+1} can be calculated based on the reputation's impact to the company's volume of business and the known, from the previous year, parameter d_k.

The matrix h_k denotes the future expectations of the consumers. The element 1 means that clients expect that the premium is going to be higher to the near future and buy a general insurance contract today. On the other hand the element 0 means that clients expect that the premium is going to be smaller to the near future and do not buy a general insurance contract today.

The matrix B_k^1 denotes the income elasticity of demand concerning insurance contract in year $[k, k+1)$ for each group category.

After the calculations the optimal premium that comes up is calculated $\tilde{p}^* = \begin{bmatrix} 0,0047 & 0 \\ 0 & 0,0047 \end{bmatrix}$ and since $\tilde{p} = p^{-1}$ the optimal premium strategy is equal to $p^* = 212,76€$.

As we have mentioned earlier on important parameter that affects company's optimal premium is company's wealth. Table 1 and figure 1 presents the optimal premium for different levels of wealth ceteris paribus.

Company's Wealth	Premium
310.000 €	250 €
320.000 €	213 €
330.000 €	189 €
340.000 €	167 €
350.000 €	149 €

Table 1: Company's premium for different values of wealth

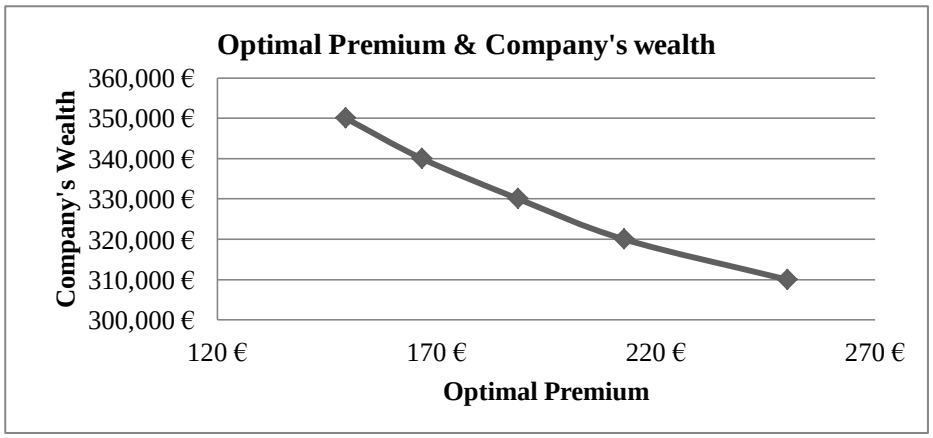

Figure 1: Company's premium for different values of wealth

As company's wealth becomes bigger the optimal premium becomes lower. This is quite rational since companies with smaller wealth have to charge their clients a higher premium in order to maximize their wealth. On the other hand companies with higher wealth can charge a smaller premium in order to have more clients and though more new customers to maximize their wealth.

6. Conclusions

Staying close to our original hypothesis that the company's premium is also affected by market's competition, we calculate a premium strategy which maximizes a quadratic performance criterion concerning a utility function, subject to a stochastic dynamic wealth function with a linear noise sequence provided only that the mean value of the random vector is zero and the covariance matrix of the random vector is a quadratic function of our control variables. In this covariance matrix, new parameters enrich our model, such as the income insurance elasticity of demand, number of consumers, inflation, market's financial risk and consumers' future expectations in addition to fame of company.

The stochastic parameter θ_k that was mentioned in our previous papers and affects the volume of business consists of many micro-macro parameters. These parameters are analysed and the way they affect directly or indirectly the optimal premium is explained.

The contribution of this paper can be summarized on the following. First, the utility function that is maximized in order to find the optimal premium is a quadratic function in which expect from the present value of company's wealth

that has mentioned to previous papers the marginal utility-premium ratio is also included. Second, the stochastic parameter that affects company's volume of business is analysed into different micro-macro parameters which directly or indirectly affect the optimal premium. Finally, since the maximized criterion is quadratic the optimal premium found depends among other factors, on company's wealth.

Finally, using a simple example based on Pantelous and Passalidou [23] paper, the relation between company's wealth and premium is shown. According to these results, as company's wealth becomes bigger the optimal premium becomes lower. In other words companies with bigger wealth want to maximize wealth new clients that will attract them with smaller premium while companies with lower wealth want to maximize their wealth trying to maintain their customers and charge them with higher premiums.

References

1. K.C. Ahlgrim and S.P. D'Arcy, The Effect of Deflation or High Inflation on the Insurance Industry, Casualty Actuarial Society, Canadian Institute of Actuaries and Society of Actuaries, 2012.
2. D.P. Bertzekas, Dynamic programming and control theory, Athens Scientific Press,USA, 2000.
3. M. Billio, M. Getmansky, A.W. Lo and L. Pelizzon, Econometric measures of connectedness and systemic risk in the finance and insurance sectors, Journal of Financial Economics, 104, 3 535–559, 2012.
4. K. Borch, The mathematical theory of insurance, DC Heath and Co, Lexington, Mass, 1974.
5. K. Borch, Economics of insurance, North-Holland Amsterdam, 1990.
6. A. Cretu and R.J. Brodie, The influence of brand image and company reputation where manufacturers market to small firms: A customer value perspective, Industrial Marketing Management, 36, 2, 230-240, 2007.
7. S.P. D'Arcy, A Strategy for Property-Liability Insurers in Inflationary Times, Proceedings of the Casualty Actuarial Society, 69, 163-186, 1982.
8. C.D. Daykin, T. Pentikainen and M. Pesonen, Practical risk theory for actuaries, Chapman and Hall, USA, 1994.
9. P. Emms and S. Haberman, Pricing general insurance using optimal control theory, ASTIN Bulletin, 35, 2, 427-453, 2005.
10. P. Emms, S. Haberman and I. Savoulli, Optimal strategies for pricing general insurance, Insurance: Mathematics and Economics, 40, 1, 15-34, 2007.
11. H.U. Gerber and G Pafumi, Utility functions: From risk theory to finance, North American Actuarial Journal, 2, 3, 74-100, 1999.
12. M. Gulumser, S. Roger, D. Tonkinb, and J. Johannes, Competition in the general insurance industry, Zeitschrift fr die gesamte Versicherungswissenschaft, 91, 3, 453-481, 2002.
13. Hellenic Association of Insurance Companies (2010), Statistical Tables (2006-2009), see http://www.eaee.gr/cms/.
14. H-H. Huang, Y-M. Shiu and C-P. Wang, Optimal insurance contract with stochastic background wealth, Scandinavian Actuarial Journal, 2, 119-13, 2011.
15. D.H. Jacobson, A General result in stochastic Optimal Control of Nonlinear Discrete-Time Systems with Quadratic Performance Criteria, Journal of Mathematical Analysis and Applications, 47, 153-161, 1974.
16. R. Krivo, An Update to D'Arcy's 'A Strategy for Property-Liability Insurers in Inflationary Times', Casualty Actuarial Society E-Forum, 2009.
17. H.J. Kushner, An introduction to stochastic control theory, John Wiley & Sons, USA, 1970.
18. C.-C. Lee and Y-B. Chiu, The impact of real income on insurance premiums: Evidence from panel data, International Review of Economics & Finance, 21, 1, 246–260, 2012.
19. C-C. Lee,Y-B. Chiu and C-H. Chang, Insurance demand and country risks: A nonlinear panel data analysis, Journal of International Money and Finance, 36, 68-85, 2013.
20. B. Lorent, The Link Between Insurance and Banking Sectors: an International Cross-section Analysis of Life Insurance Demand, CEB Working Paper No. 10/040, Solvay Brussels School of Economics and Management, 2010.
21. S. Lowe and R. Warren, Post-Recession Inflation: An Emerging Risk for P&C Insurers, Emphasis 3, pp. 24-29, 2010.
22. E. Ohlsson and B. Johansson, Non-Life Insurance Pricing with Generalized Linear Models, Springer Science & Business Media, 2010.
23. A.A. Pantelous and E. Passalidou, Optimal premium pricing policy in a competitive insurance market environment. Annals of Actuarial Science, 7, 2, 175-191, 2013.
24. A.A. Pantelous and E. Passalidou, Optimal Premium Pricing Strategies for Competitive General Insurance Markets, Applied Mathematics and Computation, 259, 858-874, 2015.
25. H. Schlesinger and N. Doherty, Incomplete Markets for Insurance : An overview, Journal of Risk and Insurance, 52, 402-423, 1985.
26. G.C. Taylor, Underwriting strategy in a competitive insurance environment, Insurance: Mathematics and Economics, 5, 1, 59-77, 1986.
27. G.C. Taylor, Expenses and underwriting strategy in competition, Insurance: Mathematics and Economics, 6, 4, 275-287, 1987.
28. J. Von Neumann and O. Morgenstern, Theory of games and economic behavior, Princeton, NJ, US: Princeton University Press, 1947.

Exponential Expansions for Perturbed Discrete Time Semi-Markov Processes

Mikael Petersson

Department of Mathematics, Stockholm University, SE-106 91 Stockholm, Sweden
(E-mail: mikpe@math.su.se)

Abstract. We consider a discrete time semi-Markov process where the characteristics defining the process depend on a small perturbation parameter. It is assumed that the state space consists of one finite communicating class of states and, in addition, one absorbing state. Our main object of interest is the asymptotic behaviour of the joint probabilities of the position of the semi-Markov process and the event of non-absorption as time tends to infinity and the perturbation parameter tends to zero. We give exponential expansions of these probabilities together with a recursive algorithm for computing the coefficients in the expansions. As an intermediate result, which is interesting in its own right, we obtain asymptotic power series expansions for moments of first hitting times.
Keywords: Semi-Markov process, Perturbation, Asymptotic Expansion, Regenerative process, Renewal equation, Solidarity property, First hitting time.

1 Introduction

The aim of this paper is to present a detailed asymptotic analysis of the long time behaviour of non-linearly perturbed discrete time semi-Markov processes with absorption.

We consider a discrete time semi-Markov process $\xi^{(\varepsilon)}(n)$, on a finite state space, depending on a small perturbation parameter $\varepsilon \geq 0$ in the sense that its transition probabilities are functions of ε. It is assumed that these functions are continuous at $\varepsilon = 0$ so that the process $\xi^{(\varepsilon)}(n)$ for $\varepsilon > 0$ can be interpreted as a perturbation of the process $\xi^{(0)}(n)$. Furthermore, we assume that for ε small enough, the state space can be partitioned into one communicating class of states $\{1, \ldots, N\}$ and one absorbing state 0. The absorption time, that is, the first hitting time of state 0, is denoted by $\mu_0^{(\varepsilon)}$. It will be assumed that absorption may, or may not be possible, both for the limiting process and the perturbed process.

We allow for smooth non-linear perturbations in the sense that certain moment functionals of transition probabilities may be non-linear functions of ε which up to some order k can be expanded in an asymptotic power series with respect to ε.

Under assumptions mentioned above and some additional Cramér type conditions on moments of transition probabilities and a non-periodicity condition

16^{th} *ASMDA Conference Proceedings, 30 June – 4 July 2015, Piraeus, Greece*

for the limiting semi-Markov process we obtain the following asymptotic relation:

$$\frac{\mathsf{P}_i\{\xi^{(\varepsilon)}(n^{(\varepsilon)}) = j,\ \mu_0^{(\varepsilon)} > n^{(\varepsilon)}\}}{\exp(-(\rho^{(0)} + c_1\varepsilon + \cdots + c_{r-1}\varepsilon^{r-1})n^{(\varepsilon)})} \to \frac{\widetilde{\pi}_{ij}^{(0)}}{e^{\lambda_r c_r}} \text{ as } \varepsilon \to 0,\ i, j \neq 0, \qquad (1)$$

where (i) $n^{(\varepsilon)}$ is a non-negative integer valued function of ε such that $n^{(\varepsilon)} \to \infty$ and $\varepsilon^r n^{(\varepsilon)} \to \lambda_r \in [0, \infty)$ as $\varepsilon \to 0$, for some $1 \leq r \leq k$; (ii) $\widetilde{\pi}_{ij}^{(0)}$ are positive constants given by explicit expressions; (iii) $\rho^{(0)}$ is a non-negative constant which can be found at least numerically as the solution of a non-linear equation; (iv) $c_1, \ldots, c_r$ are constants which can be calculated from a recursive algorithm.

In relation (1) we can separate between two types of asymptotics depending on if the absorption time $\mu_0^{(\varepsilon)} \to \infty$ in probability as $\varepsilon \to 0$ or if $\mu_0^{(\varepsilon)}$ are stochastically bounded as $\varepsilon \to 0$. In the former case we get so-called *pseudo-stationary* asymptotics and in the latter case we get so-called *quasi-stationary* asymptotics. The pseudo-stationary asymptotics have a simpler form. In this case, $\rho^{(0)} = 0$ and the constants $\widetilde{\pi}_{ij}^{(0)}$ do not depend on the initial state i and are given by the stationary probabilities of the limiting semi-Markov process.

In order to prove (1) we use the theory of perturbed discrete time renewal equations developed in Gyllenberg and Silvestrov[9], Englund and Silvestrov[7], and Silvestrov and Petersson[18]. For the proofs of some intermediate results, we will refer to Petersson[16] which is an extended report version of the present paper.

Relation (1) is proved for continuous time semi-Markov processes in Gyllenberg and Silvestrov[10,11]. In Gyllenberg and Silvestrov[11] the result is also extended to the case of initial transient states.

Results in the literature related to pseudo-stationary asymptotics are usually concerned with an asymptotic analysis of absorption times or other types of first hitting times in various types of Markov and semi-Markov processes, see for example Keilson[13], Latouche and Louchard[14], Avrachenkov and Haviv[2], and Drozdenko[6].

For quasi-stationary asymptotics, almost all papers in the literature deals with models without perturbations. In particular, a great deal of attention has been given the study of so-called quasi-stationary distributions, see for example Darroch and Seneta[4], Cheong[3], Flaspohler and Holmes[8], and van Doorn and Pollett[5]. For models with perturbations, asymptotic expansions of quasi-stationary distributions are given in Gyllenberg and Silvestrov[11] for continuous time regenerative processes and semi-Markov processes, and in Petersson[15] for discrete time regenerative processes.

One of the most extensively studied models of perturbed stochastic processes is the model of linearly perturbed Markov chains. In particular, asymptotic expansions of stationary distributions have been given for so-called nearly uncoupled Markov chains. For some results and more references related to this line of research we refer to Simon and Ando[19], Schweitzer[17], Stewart[20], Hassin and Haviv[12], Yin and Zhang[21], and Avrachenkov, Filar, and Howlett[1].

More references related to pseudo-stationary and quasi-stationary asymptotics can be found in the extensive bibliography given in Gyllenberg and Silvestrov[11].

Let us finally briefly outline the structure of the paper. Section 2 presents exponential expansions for perturbed discrete time regenerative processes. In Section 3 we define perturbed discrete time semi-Markov processes. Section 4 presents some results for moment generating functions of first hitting times which are essential for our results. Section 5 constructs asymptotic power series expansions for moments of first hitting times. Finally, in Section 6 we give exponential expansions for perturbed discrete time semi-Markov processes.

2 Perturbed Regenerative Processes

In this section we present exponential expansions for perturbed discrete time regenerative processes. These expansions are obtained by applying a corresponding result for discrete time renewal equations given in Silvestrov and Petersson[18].

For every $\varepsilon \geq 0$, let $Z_n^{(\varepsilon)}$, $n = 0, 1, \ldots$, be a regenerative process on a measurable state space $(\mathcal{X}, \Gamma)$ with proper regeneration times $0 = \tau_0^{(\varepsilon)} < \tau_1^{(\varepsilon)} < \cdots$. Furthermore, let $\mu^{(\varepsilon)}$ be a random variable, defined on the same probability space, that takes values in the set $\{0, 1, \ldots, \infty\}$. Assume that for each $A \in \Gamma$, the probabilities $P^{(\varepsilon)}(n, A) = \mathsf{P}\{Z_n^{(\varepsilon)} \in A,\ \mu^{(\varepsilon)} > n\}$ satisfy the renewal equation

$$P^{(\varepsilon)}(n, A) = q^{(\varepsilon)}(n, A) + \sum_{k=0}^{n} P^{(\varepsilon)}(n-k, A) f^{(\varepsilon)}(k),\ n = 0, 1, \ldots,$$

where

$$q^{(\varepsilon)}(n, A) = \mathsf{P}\{Z_n^{(\varepsilon)} \in A,\ \mu^{(\varepsilon)} \wedge \tau_1^{(\varepsilon)} > n\}$$

and

$$f^{(\varepsilon)}(k) = \mathsf{P}\{\tau_1^{(\varepsilon)} = k,\ \mu^{(\varepsilon)} > \tau_1^{(\varepsilon)}\}.$$

Then, we call $\mu^{(\varepsilon)}$ a regenerative stopping time.

Notice that $f^{(\varepsilon)}(n)$ are possibly improper distributions with defect given by $f^{(\varepsilon)} = 1 - \sum_{n=0}^{\infty} f^{(\varepsilon)}(n) = \mathsf{P}\{\mu^{(\varepsilon)} \leq \tau_1^{(\varepsilon)}\}$.

Let us define the following mixed power-exponential moment generating functions:

$$\phi^{(\varepsilon)}(\rho, r) = \sum_{n=0}^{\infty} n^r e^{\rho n} f^{(\varepsilon)}(n),\ \rho \in \mathbb{R},\ r = 0, 1, \ldots$$

We also define $\phi^{(\varepsilon)}(\rho) = \phi^{(\varepsilon)}(\rho, 0)$.

The solution of the following characteristic equation plays a crucial role in what follows:

$$\phi^{(\varepsilon)}(\rho) = 1. \tag{2}$$

Under conditions $\mathbf{A}^*$ and $\mathbf{B}^*$ given below, there exists a unique non-negative solution $\rho^{(\varepsilon)}$ of Equation (2) for sufficiently small ε.

We will assume that the following conditions hold:

A*: **(a)** $f^{(\varepsilon)}(n) \to f^{(0)}(n)$ as $\varepsilon \to 0$, for all $n = 0, 1, \ldots$, where the limiting distribution $f^{(0)}(n)$ is non-periodic and not concentrated at zero.
(b) $f^{(\varepsilon)} \to f^{(0)} \in [0, 1)$ as $\varepsilon \to 0$.

B*: There exists $\delta > 0$ such that (**a**) $\limsup_{0 \le \varepsilon \to 0} \phi^{(\varepsilon)}(\delta) < \infty$; (**b**) $\phi^{(0)}(\delta) > 1$.

C*: $\phi^{(\varepsilon)}(\rho^{(0)}, r) = \phi^{(0)}(\rho^{(0)}, r) + a_{1,r}\varepsilon + \cdots + a_{k-r,r}\varepsilon^{k-r} + o(\varepsilon^{k-r})$, for $r = 0, \ldots, k$, where $|a_{n,r}| < \infty$, $n = 1, \ldots, k-r$, $r = 0, \ldots, k$.

D*: There exists $\gamma > 0$ such that $\limsup_{0 \le \varepsilon \to 0} \sum_{n=0}^{\infty} e^{(\rho^{(0)}+\gamma)n} q^{(\varepsilon)}(n, \mathcal{X}) < \infty$.

For convenience we denote $a_{0,r} = \phi^{(0)}(\rho^{(0)}, r)$, for $r = 0, \ldots, k$.
Furthermore, we define

$$\Gamma_0 = \{A \in \Gamma : q^{(\varepsilon)}(n, A) \to q^{(0)}(n, A) \text{ as } \varepsilon \to 0,\ n = 0, 1, \ldots\}$$

and

$$\widetilde{\pi}^{(0)}(A) = \frac{\sum_{n=0}^{\infty} e^{\rho^{(0)} n} q^{(0)}(n, A)}{\sum_{n=0}^{\infty} n e^{\rho^{(0)} n} f^{(0)}(n)},\ A \in \Gamma.$$

The following result is proved in Silvestrov, Petersson[18] for a general renewal equation under conditions formulated in a slightly different way.

Theorem 1. *Assume that conditions* **A***–**D*** *hold. Then:*

(**i**) *For sufficiently small* ε*, there exists a unique non-negative solution* $\rho^{(\varepsilon)}$ *of the characteristic equation* (2)*. Moreover we have the asymptotic expansion*

$$\rho^{(\varepsilon)} = \rho^{(0)} + c_1\varepsilon + \cdots + c_k\varepsilon^k + o(\varepsilon^k),$$

where $c_1 = -a_{1,0}/a_{0,1}$ *and for* $n = 2, \ldots, k$,

$$c_n = -\frac{1}{a_{0,1}}\left(a_{n,0} + \sum_{q=1}^{n-1} a_{n-q,1}c_q + \sum_{m=2}^{n}\sum_{q=m}^{n} a_{n-q,m} \cdot \sum_{n_1,\ldots,n_{q-1} \in D_{m,q}} \prod_{p=1}^{q-1} \frac{c_p^{n_p}}{n_p!}\right),$$

and $D_{m,q}$ *is the set of all non-negative integer solutions to the system*

$$n_1 + \cdots + n_{q-1} = m, \quad n_1 + \cdots + (q-1)n_{q-1} = q.$$

(**ii**) *For any non-negative integer valued function* $n^{(\varepsilon)} \to \infty$ *as* $\varepsilon \to 0$ *in such a way that* $\varepsilon^r n^{(\varepsilon)} \to \lambda_r \in [0, \infty)$ *for some* $1 \le r \le k$*, we have*

$$\frac{P^{(\varepsilon)}(n^{(\varepsilon)}, A)}{\exp(-(\rho^{(0)} + c_1\varepsilon + \cdots + c_{r-1}\varepsilon^{r-1})n^{(\varepsilon)})} \to \frac{\widetilde{\pi}^{(0)}(A)}{e^{\lambda_r c_r}} \text{ as } \varepsilon \to 0,\ A \in \Gamma_0.$$

3 Perturbed Semi-Markov Processes

In this section we define perturbed discrete time semi-Markov processes.

For every $\varepsilon \geq 0$, let $(\eta_n^{(\varepsilon)}, \kappa_n^{(\varepsilon)})$, $n = 0, 1, \ldots$, be a discrete time Markov chain on the state space $(X, \mathbb{N})$, where $X = \{0, 1, \ldots, N\}$ and $\mathbb{N} = \{1, 2, \ldots\}$. We assume that the Markov chain is homogeneous in time and that the transition probabilities do not depend on the current value of the second component. Thus, the process $(\eta_n^{(\varepsilon)}, \kappa_n^{(\varepsilon)})$ is characterized by an initial distribution $p_i^{(\varepsilon)} = \mathsf{P}\{\eta_0^{(\varepsilon)} = i\}$, $i \in X$, and transition probabilities

$$Q_{ij}^{(\varepsilon)}(k) = \mathsf{P}\{\eta_{n+1}^{(\varepsilon)} = j,\ \kappa_{n+1}^{(\varepsilon)} = k \,|\, \eta_n^{(\varepsilon)} = i\},\ i, j \in X,\ k \in \mathbb{N}.$$

Let $\tau^{(\varepsilon)}(0) = 0$ and $\tau^{(\varepsilon)}(n) = \kappa_1^{(\varepsilon)} + \cdots + \kappa_n^{(\varepsilon)}$ for $n \geq 1$. Furthermore, let $\nu^{(\varepsilon)}(n) = \max\{k \geq 0 : \tau^{(\varepsilon)}(k) \leq n\}$ for $n \geq 0$. The semi-Markov process associated with the Markov chain $(\eta_n^{(\varepsilon)}, \kappa_n^{(\varepsilon)})$ is defined by

$$\xi^{(\varepsilon)}(n) = \eta_{\nu^{(\varepsilon)}(n)}^{(\varepsilon)},\ n = 0, 1, \ldots$$

For the semi-Markov process $\xi^{(\varepsilon)}(n)$, we have that $\kappa_n^{(\varepsilon)}$ are the times between successive moments of jumps, $\tau^{(\varepsilon)}(n)$ are the moments of the jumps, and $\nu^{(\varepsilon)}(n)$ are the number of jumps in the interval $[0, n]$. Furthermore, $\eta_n^{(\varepsilon)}$ is the embedded Markov chain with transition probabilities given by $p_{ij}^{(\varepsilon)} = \sum_{k=1}^{\infty} Q_{ij}^{(\varepsilon)}(k)$, $i, j \in X$.

It is sometimes convenient to write the transition probabilities as $Q_{ij}^{(\varepsilon)}(k) = p_{ij}^{(\varepsilon)} f_{ij}^{(\varepsilon)}(k)$ where

$$f_{ij}^{(\varepsilon)}(k) = \mathsf{P}\{\kappa_{n+1}^{(\varepsilon)} = k \,|\, \eta_n^{(\varepsilon)} = i,\ \eta_{n+1}^{(\varepsilon)} = j\},\ i, j \in X,\ k \in \mathbb{N},$$

are the distributions of transition times.

Let us also define random variables for first hitting times. For $j \in X$, let $\nu_j^{(\varepsilon)} = \min\{n \geq 1 : \eta_n^{(\varepsilon)} = j\}$ and $\mu_j^{(\varepsilon)} = \tau^{(\varepsilon)}(\nu_j^{(\varepsilon)})$. Then, $\nu_j^{(\varepsilon)}$ is the first hitting time of the embedded Markov chain into state j and $\mu_j^{(\varepsilon)}$ is the first hitting time of the semi-Markov process into state j. Note that $\nu_j^{(\varepsilon)}$ and $\mu_j^{(\varepsilon)}$ are both possibly improper random variables taking values in the set $\{1, 2, \ldots, \infty\}$.

Throughout the paper, the following notation will also be used:

$$g_{ij}^{(\varepsilon)}(n) = \mathsf{P}_i\{\mu_j^{(\varepsilon)} = n,\ \nu_0^{(\varepsilon)} > \nu_j^{(\varepsilon)}\},\ i, j \in X,\ n = 0, 1, \ldots,$$

and

$$g_{ij}^{(\varepsilon)} = \mathsf{P}_i\{\nu_0^{(\varepsilon)} > \nu_j^{(\varepsilon)}\},\ i, j \in X.$$

Here, and in what follows, we write $\mathsf{P}_i(A) = \mathsf{P}(A \,|\, \eta_0^{(\varepsilon)} = i)$ for any event A. Corresponding notation for conditional expectations will also be used.

We will assume that state 0 is absorbing, that is, $p_{0j}^{(\varepsilon)} = 0$ for all $j \neq 0$. However, all our results hold also in the case when 0 is not an absorbing state.

The reason for this is that we will only consider events whose probabilities do not depend on transition probabilities from state 0.

In order to consider the process $\xi^{(\varepsilon)}(n)$, for $\varepsilon > 0$, as a perturbation of $\xi^{(0)}(n)$, we will assume that the following continuity condition holds:

A: **(a)** $p_{ij}^{(\varepsilon)} \to p_{ij}^{(0)}$ as $\varepsilon \to 0$, for all $i \neq 0$, $j \in X$.

(b) $f_{ij}^{(\varepsilon)}(n) \to f_{ij}^{(0)}(n)$ as $\varepsilon \to 0$, for all $i \neq 0$, $j \in X$, $n \in \mathbb{N}$.

Furthermore, we will assume that $\{1, \ldots, N\}$ is a communicating class of states for sufficiently small ε. This is implied by condition **A** together with the following condition:

B: $g_{ij}^{(0)} > 0$, for all $i, j \neq 0$.

Transitions to state 0 may, or may not be possible, both for the limiting process and the perturbed process.

4 Moment Generating Functions of First Hitting Times

In this section we present some properties for moment generating functions of first hitting times. The proofs of the results given in this section can be found in Petersson[16]. These proofs are based on techniques which is used in Gyllenberg and Silvestrov[11] for proofs of corresponding results in continuous time.

For $i, j \in X$ we define the following moment generating functions:

$$\phi_{ij}^{(\varepsilon)}(\rho) = \sum_{n=0}^{\infty} e^{\rho n} g_{ij}^{(\varepsilon)}(n), \ \rho \in \mathbb{R}; \quad p_{ij}^{(\varepsilon)}(\rho) = \sum_{n=0}^{\infty} e^{\rho n} Q_{ij}^{(\varepsilon)}(n), \ \rho \in \mathbb{R}.$$

Note that we can write $\phi_{ij}^{(\varepsilon)}(\rho) = \mathsf{E}_i e^{\rho \mu_j^{(\varepsilon)}} \chi(\nu_0^{(\varepsilon)} > \nu_j^{(\varepsilon)})$. By conditioning on $(\eta_1^{(\varepsilon)}, \kappa_1^{(\varepsilon)})$ we get

$$\phi_{ij}^{(\varepsilon)}(\rho) = p_{ij}^{(\varepsilon)}(\rho) + \sum_{l \neq 0, j} p_{il}^{(\varepsilon)}(\rho) \phi_{lj}^{(\varepsilon)}(\rho), \ i, j \neq 0. \tag{3}$$

In what follows, it will sometimes be more convenient to work with matrices. For each $j \neq 0$, we define column vectors

$$\mathbf{\Phi}_j^{(\varepsilon)}(\rho) = \left[\phi_{1j}^{(\varepsilon)}(\rho) \ \phi_{2j}^{(\varepsilon)}(\rho) \ \cdots \ \phi_{Nj}^{(\varepsilon)}(\rho) \right]^T, \tag{4}$$

$$\mathbf{p}_j^{(\varepsilon)}(\rho) = \left[p_{1j}^{(\varepsilon)}(\rho) \ p_{2j}^{(\varepsilon)}(\rho) \ \cdots \ p_{Nj}^{(\varepsilon)}(\rho) \right]^T, \tag{5}$$

and $N \times N$ matrices ${}_j\mathbf{P}^{(\varepsilon)}(\rho) = \| {}_j p_{ik}^{(\varepsilon)}(\rho) \|$ where the elements are given by

$${}_j p_{ik}^{(\varepsilon)}(\rho) = \begin{cases} p_{ik}^{(\varepsilon)}(\rho) & i = 1, \ldots, N, \ k \neq j, \\ 0 & i = 1, \ldots, N, \ k = j. \end{cases} \tag{6}$$

Using (4), (5), and (6), we can write (3) in matrix notation:

$$\mathbf{\Phi}_j^{(\varepsilon)}(\rho) = \mathbf{p}_j^{(\varepsilon)}(\rho) + {}_j\mathbf{P}^{(\varepsilon)}(\rho)\mathbf{\Phi}_j^{(\varepsilon)}(\rho),\ j \neq 0. \tag{7}$$

The following lemma gives a necessary and sufficient condition for $\mathbf{\Phi}_j^{(\varepsilon)}(\rho)$ to be finite.

Lemma 1. *Assume that for some $\varepsilon \geq 0$ we have $g_{ik}^{(\varepsilon)} > 0$, for all $i, k \neq 0$. Then $\mathbf{\Phi}_j^{(\varepsilon)}(\rho) < \infty$ if and only if $\mathbf{p}_j^{(\varepsilon)}(\rho) < \infty$, ${}_j\mathbf{P}^{(\varepsilon)}(\rho) < \infty$, and the inverse matrix $(\mathbf{I} - {}_j\mathbf{P}^{(\varepsilon)}(\rho))^{-1}$ exists.*

We supplement Lemma 1 with a corresponding result for the moment generating functions $\widetilde{\phi}_{ij}^{(\varepsilon)}(\rho) = \mathsf{E}_i e^{\rho\mu_0^{(\varepsilon)}}\chi(\nu_0^{(\varepsilon)} < \nu_j^{(\varepsilon)})$, $\rho \in \mathbb{R}$, $i, j \neq 0$. The vectors $\widetilde{\mathbf{\Phi}}_j^{(\varepsilon)}(\rho)$ and $\mathbf{p}_0^{(\varepsilon)}(\rho)$ used in this lemma are defined in analogue with Equations (4) and (5).

Lemma 2. *Assume that for some $\varepsilon \geq 0$ we have $g_{ik}^{(\varepsilon)} > 0$, for all $i, k \neq 0$. Then $\widetilde{\mathbf{\Phi}}_j^{(\varepsilon)}(\rho) < \infty$ if and only if $\mathbf{p}_0^{(\varepsilon)}(\rho) < \infty$, ${}_j\mathbf{P}^{(\varepsilon)}(\rho) < \infty$, and the inverse matrix $(\mathbf{I} - {}_j\mathbf{P}^{(\varepsilon)}(\rho))^{-1}$ exists.*

We now introduce the following Cramér type condition on moments of transition probabilities:

C: There exists $\beta > 0$ such that:

(a) $\limsup_{0 \leq \varepsilon \to 0} p_{ij}^{(\varepsilon)}(\beta) < \infty$, for all $i \neq 0$, $j \in X$.

(b) $\phi_{ii}^{(0)}(\beta_i) > 1$, for some $i \neq 0$ and $\beta_i \leq \beta$.

We close this section with a lemma that gives some asymptotic solidarity properties for moment generating functions of first hitting times. These properties are essential for the proof of our main result.

Lemma 3. *Assume that conditions* **A**, **B**, *and* **C** *hold. Then there exist $\delta \in (0, \beta]$ and $\varepsilon_0 > 0$ such that the following holds for all $\varepsilon \leq \varepsilon_0$:*

(i) *$\phi_{jj}^{(\varepsilon)}(\delta) > 1$, $j \neq 0$ and $\phi_{kj}^{(\varepsilon)}(\delta) < \infty$, $k, j \neq 0$.*

(ii) *There exists a unique $\rho^{(\varepsilon)} \in [0, \delta)$ such that $\phi_{jj}^{(\varepsilon)}(\rho^{(\varepsilon)}) = 1$ for all $j \neq 0$.*

5 Expansions for Moments of First Hitting Times

In this section it is described how mixed power-exponential moments of first hitting times can be expanded in power series with respect to the perturbation parameter.

Let us introduce the following mixed power-exponential moment generating functions:

$$\phi_{ij}^{(\varepsilon)}(\rho, r) = \sum_{n=0}^{\infty} n^r e^{\rho n} g_{ij}^{(\varepsilon)}(n),\ \rho \in \mathbb{R},\ r = 0, 1, \ldots,\ i, j \in X.$$

$$p_{ij}^{(\varepsilon)}(\rho, r) = \sum_{n=0}^{\infty} n^r e^{\rho n} Q_{ij}^{(\varepsilon)}(n),\ \rho \in \mathbb{R},\ r = 0, 1, \ldots,\ i, j \in X.$$

Notice that $\phi_{ij}^{(\varepsilon)}(\rho, 0) = \phi_{ij}^{(\varepsilon)}(\rho)$ and $p_{ij}^{(\varepsilon)}(\rho, 0) = p_{ij}^{(\varepsilon)}(\rho)$.

It follows from conditions **A**–**C** and Lemma 3 that there exists $\varepsilon_0 > 0$ such that for any $i, j \neq 0$, $\varepsilon \leq \varepsilon_0$, and $\rho < \delta$, the functions $p_{ij}^{(\varepsilon)}(\rho)$ and $\phi_{ij}^{(\varepsilon)}(\rho)$ are arbitrarily many times differentiable with respect to ρ. Moreover, the derivative of order r for $p_{ij}^{(\varepsilon)}(\rho)$ and $\phi_{ij}^{(\varepsilon)}(\rho)$ are given by $p_{ij}^{(\varepsilon)}(\rho, r)$ and $\phi_{ij}^{(\varepsilon)}(\rho, r)$, respectively.

Recall that the moment generating functions of first hitting times satisfy the following relation:

$$\phi_{ij}^{(\varepsilon)}(\rho) = p_{ij}^{(\varepsilon)}(\rho) + \sum_{l \neq 0, j} p_{il}^{(\varepsilon)}(\rho) \phi_{lj}^{(\varepsilon)}(\rho),\ i, j \neq 0. \tag{8}$$

Differentiating both sides of relation (8) gives the following for all $\varepsilon \leq \varepsilon_0$ and $\rho < \delta$:

$$\phi_{ij}^{(\varepsilon)}(\rho, r) = \lambda_{ij}^{(\varepsilon)}(\rho, r) + \sum_{l \neq 0, j} p_{il}^{(\varepsilon)}(\rho) \phi_{lj}^{(\varepsilon)}(\rho, r),\ i, j \neq 0,\ r = 1, 2, \ldots, \tag{9}$$

where

$$\lambda_{ij}^{(\varepsilon)}(\rho, r) = p_{ij}^{(\varepsilon)}(\rho, r) + \sum_{m=1}^{r} \binom{r}{m} \sum_{l \neq 0, j} p_{il}^{(\varepsilon)}(\rho, m) \phi_{lj}^{(\varepsilon)}(\rho, r - m). \tag{10}$$

Let us rewrite relations (8), (9), and (10) in matrix notation. For each $j \neq 0$, we define column vectors

$$\mathbf{\Phi}_j^{(\varepsilon)}(\rho, r) = \left[\phi_{1j}^{(\varepsilon)}(\rho, r)\ \phi_{2j}^{(\varepsilon)}(\rho, r) \cdots\ \phi_{Nj}^{(\varepsilon)}(\rho, r)\right]^T, \tag{11}$$

$$\boldsymbol{\lambda}_j^{(\varepsilon)}(\rho, r) = \left[\lambda_{1j}^{(\varepsilon)}(\rho, r)\ \lambda_{2j}^{(\varepsilon)}(\rho, r) \cdots\ \lambda_{Nj}^{(\varepsilon)}(\rho, r)\right]^T, \tag{12}$$

$$\mathbf{p}_j^{(\varepsilon)}(\rho, r) = \left[p_{1j}^{(\varepsilon)}(\rho, r)\ p_{2j}^{(\varepsilon)}(\rho, r) \cdots\ p_{Nj}^{(\varepsilon)}(\rho, r)\right]^T, \tag{13}$$

and $N \times N$ matrices ${}_j\mathbf{P}^{(\varepsilon)}(\rho, r) = \|{}_j p_{ik}^{(\varepsilon)}(\rho, r)\|$ where the elements are given by

$${}_j p_{ik}^{(\varepsilon)}(\rho, r) = \begin{cases} p_{ik}^{(\varepsilon)}(\rho, r) & i = 1, \ldots, N,\ k \neq j, \\ 0 & i = 1, \ldots, N,\ k = j. \end{cases} \tag{14}$$

With these definitions we have

$$\mathbf{\Phi}_j^{(\varepsilon)}(\rho, 0) = \mathbf{\Phi}_j^{(\varepsilon)}(\rho),\ \mathbf{p}_j^{(\varepsilon)}(\rho, 0) = \mathbf{p}_j^{(\varepsilon)}(\rho),\ {}_j\mathbf{P}^{(\varepsilon)}(\rho, 0) = {}_j\mathbf{P}^{(\varepsilon)}(\rho). \tag{15}$$

Using (8)–(15), we get

$$\mathbf{\Phi}_j^{(\varepsilon)}(\rho) = \mathbf{p}_j^{(\varepsilon)}(\rho) + {}_j\mathbf{P}^{(\varepsilon)}(\rho) \mathbf{\Phi}_j^{(\varepsilon)}(\rho),\ j \neq 0, \tag{16}$$

and for $r = 1, 2, \ldots,$

$$\mathbf{\Phi}_j^{(\varepsilon)}(\rho, r) = \boldsymbol{\lambda}_j^{(\varepsilon)}(\rho, r) + {}_j\mathbf{P}^{(\varepsilon)}(\rho)\mathbf{\Phi}_j^{(\varepsilon)}(\rho, r),\ j \neq 0, \tag{17}$$

where

$$\boldsymbol{\lambda}_j^{(\varepsilon)}(\rho, r) = \mathbf{p}_j^{(\varepsilon)}(\rho, r) + \sum_{m=1}^{r} \binom{r}{m} {}_j\mathbf{P}^{(\varepsilon)}(\rho, m)\mathbf{\Phi}_j^{(\varepsilon)}(\rho, r-m). \tag{18}$$

Relations (16), (17), and (18) allows us to recursively calculate mixed power-exponential moments of first hitting times for a fixed (sufficiently small) value of ε.

In order to construct asymptotic expansions for these moments we will assume that the following perturbation condition holds for some $\rho < \delta$, where δ is the number from Lemma 3:

D′: $p_{ij}^{(\varepsilon)}(\rho, r) = p_{ij}^{(0)}(\rho, r) + p_{ij}[\rho, r, 1]\varepsilon + \cdots + p_{ij}[\rho, r, k-r]\varepsilon^{k-r} + o(\varepsilon^{k-r})$, $r = 0, \ldots, k$, $i, j \neq 0$, where $|p_{ij}[\rho, r, n]| < \infty$, $r = 0, \ldots, k$, $n = 1, \ldots, k-r$, $i, j \neq 0$.

For convenience we denote $p_{ij}[\rho, r, 0] = p_{ij}^{(0)}(\rho, r)$, for $r = 0, \ldots, k$.

To prepare for the next result, note that it follows from condition **D′** that the vectors $\mathbf{p}_j^{(\varepsilon)}(\rho, r)$ and matrices ${}_j\mathbf{P}^{(\varepsilon)}(\rho, r)$, defined by relations (13) and (14), respectively, have asymptotic expansions

$$\mathbf{p}_j^{(\varepsilon)}(\rho, r) = \mathbf{p}_j^{(0)}(\rho, r) + \mathbf{p}_j[\rho, r, 1]\varepsilon + \cdots + \mathbf{p}_j[\rho, r, k-r]\varepsilon^{k-r} + \mathbf{o}(\varepsilon^{k-r}),$$

and

$${}_j\mathbf{P}^{(\varepsilon)}(\rho, r) = {}_j\mathbf{P}^{(0)}(\rho, r) + {}_j\mathbf{P}[\rho, r, 1]\varepsilon + \cdots + {}_j\mathbf{P}[\rho, r, k-r]\varepsilon^{k-r} + \mathbf{o}(\varepsilon^{k-r}),$$

where the vector coefficients $\mathbf{p}_j[\rho, r, n]$ are given by

$$\mathbf{p}_j[\rho, r, n] = \left[p_{1j}[\rho, r, n]\ p_{2j}[\rho, r, n] \cdots\ p_{Nj}[\rho, r, n]\right]^T,$$

and the coefficients ${}_j\mathbf{P}[\rho, r, n] = \|{}_jp_{ik}[\rho, r, n]\|$ are $N \times N$ matrices where the elements are given by

$${}_jp_{ik}[\rho, r, n] = \begin{cases} p_{ik}[\rho, r, n] & i = 1, \ldots, N,\ k \neq j, \\ 0 & i = 1, \ldots, N,\ k = j. \end{cases}$$

The following theorem shows how we can construct asymptotic expansions for the vectors $\mathbf{\Phi}_j^{(\varepsilon)}(\rho, r)$. The proof can be found in Petersson[16] but let us here briefly explain the idea of the proof. First note that it follows from conditions **A**–**C**, Lemma 1, and Lemma 3 that $\mathbf{\Phi}_j^{(\varepsilon)}(\rho)$ is the unique solution of the system of linear equations (16) for sufficiently small ε. Using arithmetic rules for asymptotic matrix expansions it follows from condition **D′** that we can construct an asymptotic expansion of order k for this solution. Then we consider the system (17) for $r = 1$. Now using the coefficients in the expansion of $\mathbf{\Phi}_j^{(\varepsilon)}(\rho)$ and condition **D′** we can build an asymptotic expansion of order $k-1$ for $\mathbf{\Phi}_j^{(\varepsilon)}(\rho, 1)$. Continuing in this way we can successively construct asymptotic expansions for $\mathbf{\Phi}_j^{(\varepsilon)}(\rho, r)$, $r = 0, 1, \ldots, k$.

Theorem 2. *Assume that conditions* **A**, **B**, **C**, *and* **D**′ *hold and fix some* $j \neq 0$. *Then:*

(**i**) *The inverse matrix* ${}_j\mathbf{U}^{(\varepsilon)}(\rho) = (\mathbf{I} - {}_j\mathbf{P}^{(\varepsilon)}(\rho))^{-1}$ *exists for sufficiently small* ε *and has the expansion*

$$ {}_j\mathbf{U}^{(\varepsilon)}(\rho) = {}_j\mathbf{U}[\rho, 0] + {}_j\mathbf{U}[\rho, 1]\varepsilon + \cdots + {}_j\mathbf{U}[\rho, k] + \mathbf{o}(\varepsilon^k), $$

where

$$ {}_j\mathbf{U}[\rho, n] = \begin{cases} (\mathbf{I} - {}_j\mathbf{P}^{(0)}(\rho))^{-1} & n = 0, \\ {}_j\mathbf{U}[\rho, 0] \sum_{q=1}^{n} {}_j\mathbf{P}[\rho, 0, q] {}_j\mathbf{U}[\rho, n-q] & n = 1, \ldots, k. \end{cases} $$

(**ii**) *We have the expansion*

$$ \mathbf{\Phi}_j^{(\varepsilon)}(\rho) = \mathbf{\Phi}_j[\rho, 0, 0] + \mathbf{\Phi}_j[\rho, 0, 1]\varepsilon + \cdots + \mathbf{\Phi}_j[\rho, 0, k]\varepsilon^k + \mathbf{o}(\varepsilon^k), $$

where

$$ \mathbf{\Phi}_j[\rho, 0, n] = \begin{cases} \mathbf{\Phi}_j^{(0)}(\rho) & n = 0, \\ \sum_{q=0}^{n} {}_j\mathbf{U}[\rho, q] \mathbf{p}_j[\rho, 0, n-q] & n = 1, \ldots, k. \end{cases} $$

(**iii**) *For* $r = 1, \ldots, k$, *we have the expansion*

$$ \mathbf{\Phi}_j^{(\varepsilon)}(\rho, r) = \mathbf{\Phi}_j[\rho, r, 0] + \mathbf{\Phi}_j[\rho, r, 1]\varepsilon + \cdots + \mathbf{\Phi}_j[\rho, r, k-r]\varepsilon^{k-r} + \mathbf{o}(\varepsilon^{k-r}), $$

where the coefficients can be calculated recursively by the formulas

$$ \mathbf{\Phi}_j[\rho, r, n] = \begin{cases} \mathbf{\Phi}_j^{(0)}(\rho, r) & n = 0, \\ \sum_{q=0}^{n} {}_j\mathbf{U}[\rho, q] \boldsymbol{\lambda}_j[\rho, r, n-q], & n = 1, \ldots, k-r, \end{cases} $$

where, for $s = 0, \ldots, k-r$,

$$ \boldsymbol{\lambda}_j[\rho, r, s] = \mathbf{p}_j[\rho, r, s] + \sum_{m=1}^{r} \binom{r}{m} \sum_{q=0}^{s} {}_j\mathbf{P}[\rho, m, q] \mathbf{\Phi}_j[\rho, r-m, s-q]. $$

6 Exponential Expansions for Semi-Markov Processes

In this section we give exponential expansions for perturbed discrete time semi-Markov processes with absorption. The results are obtained by applying corresponding results for perturbed regenerative processes given in Section 2.

Our main objective is to give a detailed asymptotic analysis of the probabilities $P_{ij}^{(\varepsilon)}(n) = \mathsf{P}_i\{\xi^{(\varepsilon)}(n) = j,\ \mu_0^{(\varepsilon)} > n\}$, $i, j \neq 0$, as $n \to \infty$ and $\varepsilon \to 0$.

Let us assume that the initial distribution of the semi-Markov process $\xi^{(\varepsilon)}(n)$ is concentrated at some state $i \neq 0$. Then $\xi^{(\varepsilon)}(n)$ is a regenerative process with regeneration times being successive return times to state i. If state 0 is an absorbing state, these regeneration times are possibly improper random variables. In Section 2 it was assumed that the regeneration times

were proper random variables. However, the probabilities $P_{ij}^{(\varepsilon)}(n)$, $i,j \neq 0$, do not depend on the transition probabilities from state 0. This means that we can modify these transition probabilities without affecting the probabilities $P_{ij}^{(\varepsilon)}(n)$, $i,j \neq 0$. For example, if we take $Q_{0j}^{(\varepsilon)}(n) = \chi(n=1)/(N+1)$, $j \in X$, then return times to any fixed initial state $i \neq 0$ can serve as proper regeneration times. We can apply the results of Section 2 to this modified process and then it follows that the results also hold for the process where 0 is an absorbing state.

By using the regenerative property of the semi-Markov process at return times to the initial state, we can for any $i,j \neq 0$ write the following renewal equation:

$$P_{ij}^{(\varepsilon)}(n) = h_{ij}^{(\varepsilon)}(n) + \sum_{k=0}^{n} P_{ij}^{(\varepsilon)}(n-k) g_{ii}^{(\varepsilon)}(k), \ n = 0, 1, \ldots,$$

where $h_{ij}^{(\varepsilon)}(n) = \mathsf{P}_i\{\xi^{(\varepsilon)}(n) = j, \ \mu_0^{(\varepsilon)} \wedge \mu_i^{(\varepsilon)} > n\}$. It follows that $\mu_0^{(\varepsilon)}$, the first hitting time of state 0, is a regenerative stopping time for $\xi^{(\varepsilon)}(n)$.

For the model of perturbed semi-Markov processes, the characteristic equation takes the form

$$\phi_{ii}^{(\varepsilon)}(\rho) = 1. \tag{19}$$

Under conditions **A**–**C**, it follows from Lemma 3 that there exists a unique non-negative solution $\rho^{(\varepsilon)}$ of the characteristic equation (19) for sufficiently small ε which does not depend on the initial state i.

Furthermore, let us define

$$\widetilde{\pi}_{ij}^{(0)} = \frac{\sum_{n=0}^{\infty} e^{\rho^{(0)} n} h_{ij}^{(0)}(n)}{\sum_{n=0}^{\infty} n e^{\rho^{(0)} n} g_{ii}^{(0)}(n)}, \ i,j \neq 0.$$

It can be shown that if $p_{i0}^{(0)} = 0$ for all $i \neq 0$, then the constants $\widetilde{\pi}_{ij}^{(0)}$ do not depend on i and are given by the stationary probabilities of $\xi^{(0)}(n)$.

Let us formulate condition **D′** for $\rho = \rho^{(0)}$:

D: $p_{ij}^{(\varepsilon)}(\rho^{(0)}, r) = p_{ij}^{(0)}(\rho^{(0)}, r) + p_{ij}[\rho^{(0)}, r, 1]\varepsilon + \cdots + p_{ij}[\rho^{(0)}, r, k-r]\varepsilon^{k-r} + o(\varepsilon^{k-r})$, $r = 0, \ldots, k$, $i,j \neq 0$, where $|p_{ij}[\rho^{(0)}, r, n]| < \infty$, $r = 0, \ldots, k$, $n = 1, \ldots, k-r$, $i,j \neq 0$.

Under conditions **A**–**D**, it follows from Theorem 2 that we for each $i \neq 0$ and $r = 0, \ldots, k$ have the asymptotic expansion

$$\phi_{ii}^{(\varepsilon)}(\rho^{(0)}, r) = b_i[r,0] + b_i[r,1]\varepsilon + \cdots + b_i[r,k-r]\varepsilon^{k-r} + o(\varepsilon^{k-r}),$$

where $b_i[r,0] = \phi_{ii}^{(0)}(\rho^{(0)}, r)$, $r = 0, \ldots, k$, $i \neq 0$, and the coefficients $b_i[r,n]$, $r = 0, \ldots, k$, $n = 1, \ldots, k-r$, $i \neq 0$, can be calculated from the recursive formulas given in this theorem.

In order to guarantee non-periodicity of $g_{ii}^{(0)}(n)$, it will be assumed that the following condition holds:

E: $g_{jj}^{(0)}(n)$ is non-periodic for some $j \neq 0$.

We are now ready to formulate our result that gives exponential expansions for the probabilities $P_{ij}^{(\varepsilon)}(n)$.

Theorem 3. *Assume that conditions* **A**–**E** *hold. Then:*

(**i**) *For sufficiently small ε, there exists a unique root $\rho^{(\varepsilon)}$ of the characteristic equation* (19) *which does not depend on the choice of initial state i. Moreover, we have the asymptotic expansion*

$$\rho^{(\varepsilon)} = \rho^{(0)} + c_1\varepsilon + \cdots + c_k\varepsilon^k + o(\varepsilon^k),$$

where $c_1 = -b_i[0,1]/b_i[1,0]$ and for $n = 2, \ldots, k$,

$$c_n = -\frac{1}{b_i[1,0]}\Bigg(b_i[0,n] + \sum_{q=1}^{n-1} b_i[1,n-q]c_q + \sum_{m=2}^{n}\sum_{q=m}^{n} b_i[m,n-q] \cdot \sum_{n_1,\ldots,n_{q-1} \in D_{m,q}} \prod_{p=1}^{q-1} \frac{c_p^{n_p}}{n_p!}\Bigg),$$

and $D_{m,q}$ is the set of all non-negative integer solutions to the system

$$n_1 + \cdots + n_{q-1} = m, \quad n_1 + \cdots + (q-1)n_{q-1} = q.$$

(**ii**) *For any non-negative integer valued function $n^{(\varepsilon)} \to \infty$ as $\varepsilon \to 0$ in such a way that $\varepsilon^r n^{(\varepsilon)} \to \lambda_r \in [0,\infty)$ for some $1 \leq r \leq k$, we have*

$$\frac{\mathsf{P}_i\{\xi^{(\varepsilon)}(n^{(\varepsilon)}) = j,\ \mu_0^{(\varepsilon)} > n^{(\varepsilon)}\}}{\exp(-(\rho^{(0)} + c_1\varepsilon + \cdots + c_{r-1}\varepsilon^{r-1})n^{(\varepsilon)})} \to \frac{\widetilde{\pi}_{ij}^{(0)}}{e^{\lambda_r c_r}} \text{ as } \varepsilon \to 0,\ i,j \neq 0.$$

Proof. Throughout the proof, we let the initial state $i \neq 0$ be fixed. It will be shown that conditions **A**–**E** imply that conditions $\mathbf{A}^*$–$\mathbf{D}^*$ hold for the functions $f^{(\varepsilon)}(n) = g_{ii}^{(\varepsilon)}(n)$ and $q^{(\varepsilon)}(n,A) = \sum_{j\in A} h_{ij}^{(\varepsilon)}(n)$. Then, Theorem 1 can be applied in order to prove Theorem 3.

Recall from Section 4 that the vector of moment generating functions $\mathbf{\Phi}_i^{(\varepsilon)}(\rho)$ satisfies the following system of linear equations:

$$\mathbf{\Phi}_i^{(\varepsilon)}(\rho) = \mathbf{p}_i^{(\varepsilon)}(\rho) + {}_i\mathbf{P}^{(\varepsilon)}(\rho)\mathbf{\Phi}_i^{(\varepsilon)}(\rho). \tag{20}$$

It follows from Lemma 3 that there exist $\varepsilon_0 > 0$ and $\delta > 0$ such that $\mathbf{\Phi}_i^{(\varepsilon)}(\rho) < \infty$ for all $\varepsilon \leq \varepsilon_0$ and $\rho \leq \delta$. Thus, we can use Lemma 1 to conclude that the system (20) has a unique solution for $\varepsilon \leq \varepsilon_0$ and $\rho \leq \delta$ given by

$$\mathbf{\Phi}_i^{(\varepsilon)}(\rho) = (\mathbf{I} - {}_i\mathbf{P}^{(\varepsilon)}(\rho))^{-1}\mathbf{p}_i^{(\varepsilon)}(\rho). \tag{21}$$

Using (21) and condition **A** it follows that $\mathbf{\Phi}_i^{(\varepsilon)}(\rho) \to \mathbf{\Phi}_i^{(0)}(\rho)$ as $\varepsilon \to 0$ for $\rho \leq \delta$ and in particular

$$\phi_{ii}^{(\varepsilon)}(\rho) \to \phi_{ii}^{(0)}(\rho) \text{ as } \varepsilon \to 0,\ \rho \leq \delta. \tag{22}$$

Relation (22) implies that for all $n = 0, 1, \ldots$, we have $g_{ii}^{(\varepsilon)}(n) \to g_{ii}^{(0)}(n)$ as $\varepsilon \to 0$. Since $\phi_{ii}^{(\varepsilon)}(0) = g_{ii}^{(\varepsilon)}$, relation (22) also implies that $g_{ii}^{(\varepsilon)} \to g_{ii}^{(0)}$ as $\varepsilon \to 0$. Furthermore, by condition **B**, the function $g_{ii}^{(0)}(n)$ is not concentrated at zero and under conditions **B** and **E**, we have that $g_{ii}^{(0)}(n)$ is non-periodic. Thus, the function $g_{ii}^{(\varepsilon)}(n)$ satisfies condition $\mathbf{A}^*$.

It follows from Lemma 3 that the moment generating function $\phi^{(\varepsilon)}(\rho) = \phi_{ii}^{(\varepsilon)}(\rho)$ satisfies condition $\mathbf{B}^*$.

It follows from Theorem 2 that condition $\mathbf{C}^*$ holds for

$$\phi^{(\varepsilon)}(\rho^{(0)}, r) = \phi_{ii}^{(\varepsilon)}(\rho^{(0)}, r), \ r = 0, \ldots, k.$$

We now show that the function $q^{(\varepsilon)}(n, X) = \mathsf{P}_i\{\mu_0^{(\varepsilon)} \wedge \mu_i^{(\varepsilon)} > n\}$ satisfies condition $\mathbf{D}^*$. Thus, we show that there exists $\gamma > 0$ such that

$$\limsup_{0 \le \varepsilon \to 0} \sum_{n=0}^{\infty} e^{(\rho^{(0)}+\gamma)n} \mathsf{P}_i\{\mu_0^{(\varepsilon)} \wedge \mu_i^{(\varepsilon)} > n\} < \infty. \tag{23}$$

In order to do this, first note that

$$\sum_{n=0}^{\infty} e^{\rho n} \mathsf{P}_i\{\mu_0^{(\varepsilon)} \wedge \mu_i^{(\varepsilon)} > n\} = \frac{\mathsf{E}_i e^{\rho(\mu_0^{(\varepsilon)} \wedge \mu_i^{(\varepsilon)})} - 1}{e^{\rho} - 1}, \ \rho \neq 0. \tag{24}$$

By Lemma 3 there exist $\delta \in (0, \beta]$ and $\varepsilon_0' > 0$ such that $\Phi_i^{(\varepsilon)}(\delta) < \infty$, for all $\varepsilon \le \varepsilon_0'$. Using this, Lemma 1 implies that for any $\varepsilon \le \varepsilon_0'$, we have ${}_i\mathbf{P}^{(\varepsilon)}(\delta) < \infty$ and the inverse matrix $(\mathbf{I} - {}_i\mathbf{P}^{(\varepsilon)}(\delta))^{-1}$ exists. Moreover, since $\delta \le \beta$, condition **C** gives that there exists $\varepsilon_0'' > 0$ such that $\mathbf{p}_0^{(\varepsilon)}(\delta) < \infty$ for $\varepsilon \le \varepsilon_0''$. By Lemma 2, it can now be concluded that $\widetilde{\Phi}_i^{(\varepsilon)}(\delta) < \infty$ for $\varepsilon \le \min\{\varepsilon_0', \varepsilon_0''\}$. Using this we get

$$\mathsf{E}_i e^{\delta(\mu_0^{(\varepsilon)} \wedge \mu_i^{(\varepsilon)})} = \phi_{ii}^{(\varepsilon)}(\delta) + \widetilde{\phi}_{ii}^{(\varepsilon)}(\delta) < \infty, \ \varepsilon \le \min\{\varepsilon_0', \varepsilon_0''\}. \tag{25}$$

Since $\rho^{(0)} < \delta$, we can choose $\gamma > 0$ such that $\rho^{(0)} + \gamma < \delta$. With this choice of γ, relation (23) now follows from (24) and (25).

Applying Theorem 1 now shows that part (**i**) of Theorem 3 holds and that part (**ii**) of Theorem 3 holds for all $j \neq 0$ for which we have

$$h_{ij}^{(\varepsilon)}(n) \to h_{ij}^{(0)}(n) \text{ as } \varepsilon \to 0, \ n = 0, 1, \ldots \tag{26}$$

However, under condition **A**, relation (26) holds for all $j \neq 0$ since it is possible to write $h_{ij}^{(\varepsilon)}(n)$ as a finite sum where each term in the sum is a continuous function of quantities given in condition **A**. This concludes the proof.

References

1. K.E. Avrachenkov, J.A. Filar and P.G. Howlett. *Analytic perturbation theory and its applications*. SIAM, Philadelphia, 2013.

2. K.E. Avrachenkov and M. Haviv. The first Laurent series coefficients for singularly perturbed stochastic matrices. *Linear Algebra and Its Applications*, **386**, 243–259, 2004.
3. C.K. Cheong. Quasi-stationary distributions in semi-Markov processes. *Journal of Applied Probability*, **7**, 388–399, 1970. (Correction in *Journal of Applied Probability*, **7**, 788.)
4. J.N. Darroch and E. Seneta. On quasi-stationary distributions in absorbing discrete-time finite Markov chains. *Journal of Applied Probability*, **2**, 88–100, 1965.
5. E.A. van Doorn and P.K. Pollett. Quasi-stationary distributions for discrete-state models. *European Journal of Operational Research*, **230**, 1–14, 2013.
6. M. Drozdenko. Weak convergence of first-rare-event times for semi-Markov processes. PhD Thesis, Mälardalen University, School of Education, Culture and Communication, Västerås, 2007.
7. E. Englund and D.S. Silvestrov. Mixed large deviation and ergodic theorems for regenerative processes with discrete time. *Theory of Stochastic Processes*, **3(19)**, no. 1–2, 164–176, 1997.
8. D.C. Flaspohler and P.T. Holmes. Additional quasi-stationary distributions for semi-Markov processes. *Journal of Applied Probability*, **9**, 671–676, 1972.
9. M. Gyllenberg and D.S. Silvestrov. Quasi-stationary distributions of stochastic metapopulation model. *Journal of Mathematical Biology*, **33**, 35–70, 1994.
10. M. Gyllenberg and D.S. Silvestrov. Quasi-stationary phenomena for semi-Markov processes. In: Janssen, J., Limnios, N. (eds) *Semi-Markov Models and Applications*. Kluwer, Dordrecht, 33–60, 1999.
11. M. Gyllenberg and D.S. Silvestrov. *Quasi-stationary phenomena in nonlinearly perturbed stochastic systems*. De Gruyter Expositions in Mathematics, vol. 44. Walter de Gruyter, Berlin, 2008.
12. R. Hassin and M. Haviv. Mean passage times and nearly uncoupled Markov chains. *SIAM Journal on Discrete Mathematics*, **5(3)**, 386–397, 1992.
13. J. Keilson. A limit theorem for passage times in ergodic regenerative processes. *The Annals of Mathematical Statistics*, **37**, 866–870, 1966.
14. G. Latouche and G. Louchard. Return times in nearly-completely decomposable stochastic processes. *Journal of Applied Probability*, **15**, 251–267, 1978.
15. M. Petersson. Quasi-stationary distributions for perturbed discrete time regenerative processes. *Theory of Probability and Mathematical Statistics*, **89**, 153–168, 2014.
16. M. Petersson. Quasi-stationary asymptotics for perturbed semi-Markov processes in discrete time. Report 2015:2, Mathematical Statistics, Stockholm University, 36 pages, 2015.
17. P.J. Schweitzer. Perturbation theory and finite Markov chains. *Journal of Applied Probability*, **5**, 401–413, 1968.
18. D.S. Silvestrov and M. Petersson. Exponential expansions for perturbed discrete time renewal equations. In: Frenkel, I., Karagrigoriou, A., Lisnianski, A., Kleyner A. (eds) *Applied Reliability Engineering and Risk Analysis: Probabilistic Models and Statistical Inference*, Wiley, Chichester, 349–362, 2013.
19. H.A. Simon and A. Ando. Aggregation of variables in dynamic systems. *Econometrica*, **29**, 111–138, 1961.
20. G.W. Stewart. On the sensitivity of nearly uncoupled Markov chains. In: Stewart, W. J. (ed) *Numerical Solution of Markov Chains*. Probability: Pure and Applied, **8**. Marcel Dekker, New York, 105–119, 1991.
21. G. Yin and Q. Zhang. *Continuous-time Markov Chains and applications. A singular perturbation approach.* Applications of Mathematics, **37**, Springer, New York, 1998.

Application of the Stochastic Models in Operational Risk Modelling

Gaida Pettere[1], Darja Stepchenko[2], and Irina Voronova[3]

[1] Department of Engineering Mathematics, Riga Technical University, LV1658, Kaļķu street 1, Riga, Latvia
(E-mail: gaida@latnet.lv)
[2] Department of Innovation and Business Management, Riga Technical University, LV1048, Kalnciema street 6, Riga, Latvia
(E-mail: daria.stepchenko@gmail.com)
[3] Department of Innovation and Business Management, Riga Technical University, LV1048, Kalnciema street 6, Riga, Latvia
(E-mail: irina.voronova@rtu.lv)

Abstract. Operational risk is one of the core risks of every insurance company under the Solvency II framework and can be defined as the financial losses occurred due to incorrectly defined systems or processes; failures in IT system, human mistakes or other external processes. The research is performed in order to assess the capital to cover possible losses due to the occurrence of the operational risk sub-risks and nature of an operational risk. We have shown that operational risks can be modelled by skew *t*-copula and estimated tail dependence in each situation for modelling distributions with heavier tail area. The model is prepared on a non-life insurance company's example and is based on the recorded data from loss database that encompasses historical information of five main operational sub-risks: legal, informational, organizational, human resources and expense risk.
Keywords: Operational risk, skew *t*-copula, *t*-copula, tail dependence, modelling, solvency capital, insurance.

1 Introduction

The fact is that the requirements of the Solvency II Directive are not just about capital of an insurance company but about risk assessment through the implementation and enhancement of risk measurement and risk management. Also, the Solvency II regime requires higher capital compared with the requirements of the Solvency I Directive that should ensure the solvency and financial stability of each insurance company. Moreover, the new requirements of the Solvency II Directive, which will come in force from 1st January 2016, set a lot of challenges to every insurance company in the European Union member states in relation to the establishment of more sensitive and sophisticated risk coverage in order to ensure solvency and the safety of policyholders. Based on the requirements of the Solvency II Directive, the

16th ASMDA Conference Proceedings, 30 June – 4 July 2015, Piraeus, Greece

insurance companies should hold the appropriate amount of capital that could ensure safety of policyholders and beneficiaries. The target of this research is to study the improvement possibilities of the operational risk measurement under the Solvency II regime. The object of this paper is measurement of operational risk. Operational risk is the change in value of capital needed caused by the fact that actual losses, incurred from inadequate or failed internal processes, people and systems, or from external events, including legal risk but excluding strategic and reputational risks Since 2001, when document about operational risks *Sound Practices for the Management and Supervision of Operational Risk* was published by Basel Committee on Banking Supervision [2] operational risk has been in the centre of interest of mathematicians. Because needed capital for different risks in banks is estimated by risk measure *VaR* (what is 99.9% in banks and 99.5% in insurance), it seems natural to use the same measure for operational risk too. But the problem is that *VaR* measure is not a coherent risk measure: $VaR_\alpha(\sum_{i=1}^{n} R_i) \le \sum_{i=1}^{n} VaR_\alpha(R_i)$, where R_i, $i \in \{1,2,...,n\}$ are different risks. Therefore, different bounds for *VaR* of a portfolio of risks can be found in Chavez-Demoulin *et al*. [5] or improved bounds in Embrechts and Puccetti [10]. Further different copulas (Gumbel, Gaussian) were used for analysis of risk across a non-symmetric matrix of loss data in Embrechts and Puccetti [11]. Extreme value theory was used to evaluate operational risks in El-Gamal *et al*. [9], Chavez-Demoulin *et al*. [6]. Our aim in this paper is to show that skew *t*-copula can be used to estimate *VaR* of portfolio of different operational risks including confidence intervals for such as risk measure like *VaR* and finally calculate estimates of tail dependence for risks and for portfolio. We have worked out our methodology using data basis of recorded operational risks during one year in one insurance company of Latvia.

2 Construction of skew *t*-copula

We are going to model the joint distribution of different risks via skew *t*-copula to show advantage of the last one. Usually operational risk data have univariate marginals with skewed distributions of different types. To construct a multivariate model with certain dependence structure and different marginals copula theory has been the only tool at hand so far. But most of the suggested copulas are symmetric. To join skewed marginals into a multivariate distribution it seems more natural to use a skewed multivariate distribution. There exist many different modifications and extensions of the standard multivariate *t*-distribution. An overview of these distributions is given in Kotz and Nadarajah [15], Ch. 5. We have constructed skew *t*-copula based on the multivariate *t*-distribution and skew *t*-distribution introduced in Azzalini and Capitanio [1] and corresponding copulas constructed using these distributions. Notation $t_{p,\nu}$ is used when we talk about density of the p-variate t-distribution with ν degrees

of freedom and notation $g_{p,\nu}$ is used for the density of the p-variate skew t-distribution with ν degrees of freedom. Similar notations are used for the distribution functions.

DEFINITION 1. A p-dimensional random vector $\mathbf{X}=(X_1,...,X_p)^T$ *is said to have p-variate t-distribution with* ν *degrees of freedom, mean vector* $\boldsymbol{\mu}$ *and positive definite matrix* $\boldsymbol{\Sigma}$*, if its density function is given by (*Azzalini and Capitanio [1]*):*

$$t_{p,\nu}(\mathbf{x},\boldsymbol{\mu},\boldsymbol{\Sigma})=\frac{\Gamma\left(\frac{\nu+p}{2}\right)}{(\pi\nu)^{\frac{p}{2}}\Gamma\left(\frac{\nu}{2}\right)|\boldsymbol{\Sigma}|^{\frac{1}{2}}}\left[1+\frac{(\mathbf{x}-\boldsymbol{\mu})^T\boldsymbol{\Sigma}^{-1}(\mathbf{x}-\boldsymbol{\mu})}{\nu}\right]^{-\frac{\nu+p}{2}}. \qquad (1)$$

Next we give the definition of the p-dimensional skew $t_{p,\nu}$-distribution (Azzalini and Capitanio [1]).

DEFINITION 2. A random p-vector $\mathbf{X}=(X_1,...,X_p)^T$ *has p-variate skew* t*-distribution with parameters* $\boldsymbol{\mu}$*,* $\boldsymbol{\alpha}$ *and* $\boldsymbol{\Sigma}$*, if its density function is of the form*

$$g_{p,\nu}(\mathbf{x};\boldsymbol{\mu},\boldsymbol{\Sigma},\boldsymbol{\alpha})=2\cdot t_{p,\nu}(\mathbf{x};\boldsymbol{\mu},\boldsymbol{\Sigma})\cdot T_{1,\nu+p}\left[\boldsymbol{\alpha}^T\mathbf{W}^{-1}(\mathbf{x}-\boldsymbol{\mu})\left(\frac{\nu+p}{Q+\nu}\right)^{\frac{1}{2}}\right], \qquad (2)$$

where Q *denotes the quadratic form*

$$Q=(\mathbf{x}-\boldsymbol{\mu})^T\boldsymbol{\Sigma}^{-1}(\mathbf{x}-\boldsymbol{\mu})$$

and $\mathbf{W}$ *is the* $p\times p$ *diagonal matrix* $\mathbf{W}=(\delta_{ij}\sqrt{\sigma_{ij}})$*,* $i,j=1,...,p$*, where* δ_{ij} *is the Kronecker delta.* $T_{1,\nu+p}(\cdot)$ *denotes the distribution function of the central univariate* t*- distribution with* $\nu+p$ *degrees of freedom.*

The skew t-copula is introduced in Kollo and Pettere [13]. As marginal distributions of the business lines are skewed, a skewed copula will be a natural model to give a good fit with the data.

DEFINITION 3. A copula $C_{p,\nu}$ *is called skew* $t_{p,\nu}$*-copula with parameters* $\boldsymbol{\mu}$*,* $\boldsymbol{\Sigma}$*,* $\boldsymbol{\alpha}$*, if*

$$C_{p,\nu}(u_1,...,u_p:\boldsymbol{\mu},\boldsymbol{\Sigma},\boldsymbol{\alpha})=G_{p,\nu}(G^{-1}_{p,\nu}(u_1;\mu_1,\sigma_{11},\alpha_1),...,G^{-1}_{p,\nu}(u_p;\mu_p,\sigma_{pp},\alpha_p),\boldsymbol{\mu},\boldsymbol{\Sigma},\boldsymbol{\alpha})$$

where $G^{-1}_{p,\nu}(u_i;\mu_i,\sigma_{ii},\alpha_i)$*,* $i\in\{1,2,...,p\}$ denotes the inverse of the univariate skew $t_{p,\nu}$*-distribution function and* $G_{p,\nu}$ *is the distribution function of p-variate skew* $t_{p,\nu}$*-distribution with density (2).*

The corresponding copula density function is

$$c_{p,\nu}(\mathbf{u};\boldsymbol{\mu},\boldsymbol{\Sigma},\boldsymbol{\alpha}) = \frac{g_{p,\nu}[\{G_{1,\nu}^{-1}(u_1;0,\sigma_{11},\alpha_1),...,G_{1,\nu}^{-1}(u_p;0,\sigma_{pp},\alpha_p)\};\boldsymbol{\mu},\boldsymbol{\Sigma},\boldsymbol{\alpha}]}{\prod_{i=1}^{p} g_{1,\nu}[G_{1,\nu}^{-1}(u_i;\mu_i,\sigma_{ii},\alpha_i);\mu_i,\sigma_{ii},\alpha_i]}$$

where the density function $g_{p,\nu}(\cdot;\boldsymbol{\mu},\boldsymbol{\Sigma},\boldsymbol{\alpha}) : R^p \to R$ *is defined by (2) and function* $G_{1,\nu}^{-1}(u_i;\mu_i,\sigma_{ii},\alpha_i)$ *is as in Definition 3.*

We are going to apply the skew *t*-copula in a special case when the shift parameter $\boldsymbol{\mu} = \mathbf{0}$. To find a model for our data we have to estimate the parameters $\boldsymbol{\Sigma}$ and $\boldsymbol{\alpha}$. For that, we shall apply the method of moments. Parameters $\boldsymbol{\Sigma}$ and $\boldsymbol{\alpha}$ are estimated from the first two sample moments (Kollo and Pettere [13]). Let $\bar{\mathbf{X}}$ and $\mathbf{S}_{\mathbf{X}}$ denote the sample mean and the sample covariance matrix, respectively. Then the estimates are

$$\hat{\boldsymbol{\Sigma}} = \frac{\nu-2}{\nu}(\mathbf{S}_{\mathbf{X}} + \bar{\mathbf{X}}\bar{\mathbf{X}}^T) \tag{3}$$

$$\hat{\boldsymbol{\alpha}} = \frac{b(\nu)\cdot\boldsymbol{\beta}}{\sqrt{b^2(\nu) - \bar{\mathbf{X}}^T\hat{\boldsymbol{\Sigma}}^{-1}\bar{\mathbf{X}}}}\ , \tag{4}$$

where

$$\boldsymbol{\beta} = \frac{1}{b(\nu)}\hat{\mathbf{W}}\hat{\boldsymbol{\Sigma}}^{-1}\bar{\mathbf{X}}, \tag{5}$$

with $\hat{\mathbf{W}} = (\delta_{ij}\sqrt{\hat{\sigma}_{ij}})$, $i, j = 1,...,p$, *where* δ_{ij} *is the Kronecker delta and*

$$b(\nu) = \left[\frac{\nu}{\pi}\right]^{\frac{1}{2}} \cdot \frac{\Gamma(\frac{\nu-1}{2})}{\Gamma(\frac{\nu}{2})}.$$

We have to assume in formula (4) that $\nu > 2$.

Variable ν is possible to estimate between every two variables using formula from Kotz and Nadarajah [15]:

$$3\nu^2 - (\nu-2)(\nu-4)(m_4(X_1) + m_4(X_2)) = 0 \tag{6}$$

where $m_4(X_i)$ denotes the sample estimate of the fourth order moments of random variable X_i , $i \in \{1,2\}$. The estimates are closest integers to the solution of equation (6) and can be found for $\nu > 4$.

3 Tail dependence for skew *t*–distribution

Let us assume that (X_1, X_2) is a two-dimensional vector with univariate marginal distributions functions $F_1(x)$ and $F_2(x)$. Then the upper tail dependence coefficient is

$$\lambda_U = \lim_{u \to 1} \lambda_U(u)$$

where $\lambda_U(u) = P(F_1(x) > u / F_2(x) > u)$.

Similarly is defined the lower tail dependence coefficient

$$\lambda_L = \lim_{u \to 1} \lambda_L(u)$$

where $\lambda_L(u) = P(F_1(x) < u / F_2(x) < u)$.

For symmetric elliptical distributions $\lambda_U = \lambda_L = \lambda$, for normal distributions λ equals zero. For two-dimensional *t*-distribution with ν degrees of freedom

$$\lambda = 2T_{1,\nu}\left(-\sqrt{\frac{(\nu+1)\cdot(1-\rho)}{(\rho+1)}}\right) \tag{7}$$

where $T_{1,\nu}(.)$ is the distribution function of standard *t*-distribution with ν degrees of freedom (see Demarta and McNeil [7])

It is proved in Bortot [3] that it is sufficient to study the upper tail dependence as the lower tail dependence coefficient is determined by the upper one. To follow Bortot [3] let us denote by

$$\alpha_1^* = \frac{\alpha_1 + \alpha_2 \cdot \rho}{\sqrt{1+\alpha_2^2 \cdot (1-\rho^2)}} \quad \text{and} \quad \alpha_2^* = \frac{\alpha_2 + \alpha_1 \cdot \rho}{\sqrt{1+\alpha_1^2 \cdot (1-\rho^2)}} \tag{8}$$

Assume that $\alpha_1^* \le \alpha_2^*$. Then

$$\begin{aligned}
\lambda_U &= \lim_{u \to 1} \frac{P(F_1(x) > u, F_2(x) > u)}{P(F_2(x) > u)} = \lim_{x \to \infty} \frac{P(F_1(x) > F_2(x), X_2 > x)}{P(X_2 > x)} \\
&\ge \lim_{x \to \infty} \frac{P(X_1 > x, X_2 > x)}{P(X_2 > x)} \\
&= \lim_{x \to \infty} \frac{2 \cdot P(Y_1 > x, Y_2 > x) \cdot T_{1,\nu+2}\left((\alpha_1 + \alpha_2) \cdot \sqrt{\frac{(\nu+2)\cdot(\rho+1)}{2}}\right)}{2 \cdot T_{1,\nu+1}(\alpha_2^* \cdot \sqrt{\nu+1}) \cdot (1 - T_{1,\nu}(x))}
\end{aligned}$$

or

$$\lambda_U \geq \lambda \cdot \frac{T_{1,\nu+2}\left((\alpha_1+\alpha_2)\cdot\sqrt{\frac{(\nu+2)\cdot(\rho+1)}{2}}\right)}{T_{1,\nu+1}(\alpha_2^*\cdot\sqrt{\nu+1})}. \quad (9)$$

In the case of $\alpha_1 = \alpha_2 = \alpha$ the tail dependence coefficient can be calculated using formula:

$$\lambda_U = \lambda \cdot \frac{T_{1,\nu+2}\left(2\cdot\alpha\cdot\sqrt{\frac{(\nu+2)\cdot(\rho+1)}{2}}\right)}{T_{1,\nu+1}(\alpha^*\cdot\sqrt{\nu+1})}$$

where $\alpha^* = \frac{\alpha\cdot(1+\rho)}{\sqrt{1+\alpha^2\cdot(1-\rho^2)}}$.

The fact is that the difference of tail dependencies between *t*-distribution and skew *t*-distribution is determined by the ratio of univariate distribution functions of the *t*-distribution. It is shown in Bortot [3] that for the equal values of α the difference in tail dependence is not large.

4 Description of the model and data

The simulation model performed during the case study is based on five risks, but it can be used for any number of risks. The model includes the following operational sub-risks:

- Legal risk (LR) means the possibility that lawsuits, adverse judgments from courts, or contracts that turn out to be unenforceable, disrupt or adversely affect the operations or condition of an insurer. The result may lead to unplanned additional payments to policyholders or that contracts are settled on an unfavorable basis, e.g. unrecoverable reinsurance.
- Organizational risk (OR) means possible losses due to unclear organizational structure (unclear processes, unclear responsibilities split between units etc.).
- Informational risk (IR) means possible losses due to failures in the IT system.
- Human Resources risk (HRR) means losses due to changes or loss of personnel, deterioration of morale, inadequate development of human resources, inappropriate working schedule, inappropriate working and safety environment, inequality or inequity in human resource management or discriminatory conduct.
- Expense risk (ER). The risk of a change in value caused by the fact that the timing and/or the amount of expenses incurred differs from those expected, e.g. assumed for pricing basis.

The historical data is based on recorded data in relation to the five risk sub-risks of operational risk from the annual loss database. The loss database introduces

all incurred operational risk events with details about losses during a particular period and is important aspect of the understanding of interconnectivity of different operational sub-risks; thus is a prerequisite to controlling problems and assessing practices.
Basically, the model is based on several main steps:

1) data collection,
2) determination of a marginal distribution of each operational sub-risk,
3) simulation of 10 000 values of each risk using skew *t*-copula,
4) calculating *VaR* of each marginal,
5) finding *VaR* for total portfolio of operational risk,
6) repeating 30 times steps 3 to 5 and calculating descriptive statistics.

Descriptive statistics of the marginal distributions of the above-mentioned risks are presented in Table 1.

Table 1. Descriptive statistics of used data.

Risks	**LR**	**OR**	**IR**	**HRR**	**ER**
Sample size	12	12	12	12	12
Mean	7 564	45 618	5 425	1 747	2 308
Median	3 700	1 610	960	18	0
Standard deviation	11 151	143 207	9 342	4 490	6 655
Largest value	41 278	500 010	31 010	15 001	43 000
Skewness	2.92	3.45	2.21	2.82	3.24

All operational risks are skewed, but the largest maximum value has organizational risk. Risk with so large maximal value was chosen specially to check does model fit in such case too. Before fitting marginal distributions, the data were standardised and only then, the marginal distributions were approximated by exponential, gamma and normal distributions.
The testing results are shown in Table 2.

Table 2. Results of testing.

Risks	**Distribution used**	**Parameters**		**Test value**
LR	Exponential	λ	1.474	0.164
OR	Gamma	α	0.101	0.169
		β	3.139	
IR	Gamma	α	0.227	0.096
		β	2.098	
HRR	Gamma	α	0.152	0.338
		β	2.569	
ER	Normal	μ	3.352	0.079
		σ	1.000	

Correlation matrix between risks (order of risks from left to right and from up to down is LR, OR, IR, HRR and ER) is the following:

$$R = \begin{pmatrix} 1 & -0.143 & 0.357 & 0.183 & 0.071 \\ -0.143 & 1 & -0.118 & -0.135 & -0.085 \\ 0.357 & -0.118 & 1 & -0.086 & -0.132 \\ 0.183 & -0.135 & -0.086 & 1 & -0.063 \\ 0.071 & -0.085 & -0.132 & -0.063 & 1 \end{pmatrix}$$

One can see that smallest correlations are between LR and ER (0.071) and HRR and ER (-0.063).

Estimations of parameters were started by estimating degrees of freedom ν between each two pairs of variables by using formula (6) (see Table 3.)

Table 3. Estimated values of ν by formula (6).

i	**OR**	**IR**	**HRR**	**Ex**
LR	1.839313	1.816586	1.820098	1.833699
OR		1.831101	1.834072	1.845673
IR			1.809678	1.824871
HRR				1.828069

Nearest possible integer in all cases are 2. Formula (6) is right only if $\nu > 4$ and skew *t*-copula is possible to use from $\nu > 2$. In our case formula (4) is possible to use only with $\nu = 5$ and therefore we have chosen $\nu = 5$.

Further parameters for copula were estimated using formulas (3), (4) and (5). The obtained $\hat{\boldsymbol{\Sigma}}$ matrix is:

$$\hat{\boldsymbol{\Sigma}} = \begin{pmatrix} 0.876 & 0.044 & 0.408 & 0.268 & 0.186 \\ 0.044 & 0.661 & 0.020 & -0.007 & 0.016 \\ 0.408 & 0.020 & 0.736 & 0.060 & 0.022 \\ 0.268 & -0.007 & 0.060 & 0.691 & 0.044 \\ 0.186 & 0.016 & 0.022 & 0.044 & 0.674 \end{pmatrix}$$

Estimated values of vector $\boldsymbol{\alpha}$ are

$$\boldsymbol{\alpha}^T = (1.675 \;\; 1.657 \;\; 1.518 \;\; 1.394 \;\; 1.408) .$$

The simulation is based on the simulation rule for the skew $t_{p,\nu}$-distribution (Kollo and Pettere [13]):

1. Find the Cholesky decomposition $\mathbf{A}$ of $\mathbf{S}_\mathbf{X}$, ($\mathbf{A}\mathbf{A}^T = \mathbf{S}_\mathbf{X}$).
2. Simulate *p* independent values from *N(0,1)* and form *p*-vector $\mathbf{z}$.
3. Set vector $\mathbf{x} = \mathbf{A} \cdot \mathbf{z}$.
4. Simulate value w from *N(0,1).*

5. Get realization of the skew normal vector $\mathbf{y}$ putting

$$\mathbf{y} = \begin{cases} \mathbf{x} & if \quad \boldsymbol{\alpha}^T \mathbf{x} > w \\ -\mathbf{x} & if \quad \boldsymbol{\alpha}^T \mathbf{x} \leq w \end{cases} .$$

6. Simulate $h \sim \chi^2_\nu$.
7. Find vector $\mathbf{t} = \frac{\mathbf{y}}{\sqrt{h/\nu}}$.
8. Set vector $\mathbf{u}$ so that every coordinate $u_i = G_{1,\nu}(t_i; 0, \sigma_{ii}, \alpha_i)$, $i \in [1, ..., p]$.
9. Set vector $\mathbf{x} = (F_1^{-1}(u_1), ..., F_p^{-1}(u_p))$ where $F_i(\cdot)$ is the marginal distribution function of the initial random variable X_i.
10. Repeat previous steps 10 000 times.

5 Results

Based on the performed simulations, it is possible to conclude that the obtained portfolio *VaR* by simulations is smaller than sum of *VaR* for different risks and it means that the necessary capital to cover these risks is less by 10.3%. The main findings and results of simulation are in Table 4 and Table 5. In order to understand the information presented in Table 4, the explanation of some values are provided:

- The first line presents the 99.5% *VaR* for each sub-risk using inverse marginal distributions.
- The next lines present characteristics of 99.5% *VaR* for each sub-risk and portfolio obtained from simulations.

Table 4. 99.5% *VaR* of separate risks obtained using simulations and its characteristics.

Risks	**LR**	**OR**	**IR**	**HRR**	**ER**
99.5% VaR from distributions	40 078	947 292	55 567	28 530	19 450
Mean of *99.5% VaR*	39 980	882 287	53 803	27 247	18 936
Median	39 891	875 210	53 560	27 414	18 992
Standard deviation	908	50 990	1 700	1 395	224
Skewness	0.426	0.923	0.591	-0.023	-0.921
Coefficient of variation (%)	2.27	5.78	3.15	5.12	1.18

The same characteristics for portfolio of risks as for each risk in Table 4 are shown in Table 5.

Table 5. 99.5% *VaR* of portfolio obtained using simulations and its characteristics.

	Sum of *VaR*	**Portfolio *VaR***
99.5% VaR from distributions	1 090 917	
Mean of *99.5% VaR*	1 022 333	916 576
Median	1 015 070	910 795
Standard deviation	50569	44 408
Skewness	0.938	0.937
Coefficient of variation (%)	4.95	4.84

Results in Table 4 and in Table 5 show us that simulation results from the skew *t*-copula are stable. Medians are close to means, skewness coefficients and variation coefficients are not large. Therefore, it is possible to assume approximate normal distribution of simulated mean and to calculate confidence intervals for portfolio *VaR*. Estimated confidence intervals for portfolio *VaR* are shown in Table 6.
Additionally it is possible to see from Table 5 that gain of using copula approach is EUR 105 757 or 10% decreasing in capital needed.

Table 6. Confidence interval of portfolio *VaR*.

Confidence probability	Portfolio *VaR*	Lower limit	Upper limit
99.5%	916 576	895 693	937 459

Calculated limits of confidence intervals show us that even upper limit for 99.5 % confidence is lower than portfolio *VaR* obtained simply by adding different risk *VaR*. The tail dependence coefficient calculations for given risks using formulas (7), (8) and (9) are presented in Table 7 and in Table 8. Like it is possible to see from Table 7 and Table 8, tail dependence coefficients are not large but tail dependence exists.

Table 7. Tail dependence coefficients between LR and other risks.

Risks	**LR – OR**	**LR – IR**	**LR – HRR**	**LR – ER**
λ	0.0183	0.0762	0.0486	0.0357
α_1^*	0.7489	1.2772	1.1372	1.0294
α_2^*	0.7324	1.1389	0.8822	0.7841
$T_{1,\nu+2}$	0,9996	0.9998	0.9997	0.9997
$T_{1,\nu+1}$	0.9385	0.9385	0.9385	0.9385
λ_U	**0.0196**	**0.0812**	**0.0518**	**0.0380**

Table 8. Tail dependence coefficients between other risks.

Risks	**OR – IR**	**OR – HRR**	**OR – ER**
λ_U	0.0215	0.0213	0.0241
Risks		**IR – HRR**	**IR – ER**
λ_U		0.0238	0.0206
Risks			**HRR – ER**
λ_U			0.0252

There is no possibility to calculate in direct way tail dependence for skew *t*-distribution because in formula (9) is not the equality sign. Unique what is possible to do is to estimate tail dependence coefficients between each two risks using formula (9) and to have in mind that in reality it can be slightly larger. It is shown in Kollo *et al*. [14] that the upper tail dependence coefficient for skew *t*-copula differs not much when skewness parameters have the same sign and when one of them has positive and another negative value, then skew *t*-copula can have much bigger tail dependence coefficient than the corresponding *t*-copula. Because skewness parameters, which are presented by vector, $\boldsymbol{\alpha}$ are with same sign and close to each other, we can conclude that at least in this case tail dependence does not differ much from the calculated values.

Conclusions

Risk dynamic nature in the changing market conditions sets a lot of challenges to every company. Thus, it is necessary to implement new approaches to follow the nature of risks with the aim to understand their possible impact on financial stability and further development. Under Solvency II regime insurance companies like banks will need to evaluate necessary capital to cover different risks. The largest problem can be to evaluate operational risks because of lack of data. For that reason, many different methods are created to evaluate operational risks. Many methods are based on expert evaluations (see, for example, Durfee and Tselykh [8], Jonek-Kowalska [12] and Stepcenko and Voronova [17]). However, from another side it is very natural to evaluate operational risks by using statistical methods like all other insurance and banking risks. For that is necessary to record very carefully losses in each company. If such data basis exists, we have shown that needed capital for operational risks can be evaluated by different statistical methods. Many new books have appeared in latest years about evaluation of operational risks. Latest books, for example, are Cavestany *et al*. [4] and McConnell [16]. Privilege of that paper is using skew *t*-copula modelling necessary capital to cover operational risks.
Advantages of the proposed method are:

- the skew *t*-copula has a very simple simulation rule,
- by choosing degrees of freedom is possible to find appropriate skewness of copula for simulation,

- possibility to calculate average measure of necessary characterstics,
- possibility to estimate sensitivity of calculated measure,
- possibility to calculate confidence interval of portfolio value at risk,
- tail dependence can be evaluated between risks.

References

1. A. Azzalini and A. Capitanio. Distributions generated by perturbation of symmetry with emphasis on a multivariate skew *t*-distribution. J R Stat Soc Ser B Stat Methodol, 65, 367{389, 2003.

2. Basel Committee on Banking Supervision. Sound Practices for the management and supervision of operational risk. BIS, Basel, Switzerland, 2001.

3. P. Bortot. Tail dependence in bivariate skew-Normal and skew-t distributions. http://www2.stat.unibo.it/bort, 15 pages, 2012.

4. R. Cavestany, B. Boultwood and L. F. Escardero. Operational Risk Capital Models. www.riskbooks.com/operational-risk-capital-models, 2015

5. V. Chavez-Demoulin, P. Embrechts and J. Neželova, Quantitative models for operational risk: extremes, dependence and aggregation. Journal of Banking and Finance, 30, 10, 2635{2658, 2006.

6. V. Chavez-Demoulin, P. Embrechts and M. Hofert, An extreme value approach for modelling Operational Risk losses depending on covariates. https://people.math.ethz.ch/~embrecht/papers.html, 41 pages, 2014.

7. S. Demarta and A. J. McNeil. The T Copula and Related Copulas. International Statistical Review, 73, 1, 111{129, 2005.

8. A. Durfee and A. Tselykh. Evaluating Operational Risk Exposures Using Fuzzy umber Approach to Scenario Analysis. http://www.atlantis-press.com/php/download_paper.php, 1045{1051, 2011.

9. M. El-Gamal, H. Inanoglu and M. Stengel. Multivariate estimation for operational risk with judicious use of extreme value theory. Journal of Operational Risk, 2, 1, 21{54, 2007.

10. P. Embrechts and G. Puccetti. Aggregating risk capital, with an application to operational risks. The Geneva Risk and Insurance Review, 31, 2, 71{90, 2006.

11. P. Embrechts and G. Puccetti. Aggregating risks across matrix structured loss data: the case of operational risk. Journal of Operational Risk, 3, 2, 29{44, 2008.

12. I. Jonek-Kowalska. The Concept of Operational Risk Identification and Evaluation in a Sector Depiction. American International Journal of Contemporary Research 2, 8, 38{48, 2012.

13. T. Kollo and G. Pettere. Parameter Estimation and Application of the Multivariate Skew t-Copula. Copula Theory and Its Applications. Springer-Verlag, Berlin, 289{298, 2010.

14. T. Kollo, G. Pettere and M. Valge. Tail Dependence of Skew t Copulas. Communications in Statistics - Simulation and Computation, accepted, 14 pages, 2015.

15. S. Kotz and S. Nadarajah. Multivariate t Distributions and Their Applications. Cambridge University Press. Cambridge, 2004.

16. P. McConnell. Systemic Operational Risk: Theory, case studies and Regulations. www.Riskbooks.com/systemic-operational-risk-theory-case-studies-regulations, 2015

17. D. Stepcenko and I. Voronova. Insurance Company's Performance: risk Evaluation. Tecnologies of Computer Control. Computer and systems software. RTU izdevniecība, 115{122, 2014.

Probabilistic modelling of the effect of new gas infrastructure to security of supply

Pavel Praks, Vytis Kopustinskas

European Commission, Joint Research Centre, Institute for Energy and Transport,
E. Fermi 2749, TP230, I-21027, Ispra (VA), Italy
(E-mail: pavel.praks@jrc.ec.europa.eu, vytis.kopustinskas@jrc.ec.europa.eu)

Abstract. The aim of our research work is to develop a European gas transmission system probabilistic model to analyse in a single computer model, the reliability and capacity constraints of a gas transmission network. The probabilistic prototype software ProGasNet, which is under our development, is based on generalization of the maximum flow problem for a stochastic-flow network model in which network elements can randomly fail with known failure probabilities. Concerning security of supply, network elements, for example gas storages and compressor stations, are expressed by a multi-state system. To analyse the vulnerability of the gas network, various what-if supply disruption scenarios is necessary to analyse. However, the situation becomes more complex, when the gas network is large and when effects of various gas infrastructure project proposals (for example new LNG terminals) should be evaluated and compared. We present our experience with a statistical approach based on a risk ratio, which can help users with analysing of large number of probabilistic results.
Keywords: energy security; network reliability; network resilience; gas transmission network modelling; Monte-Carlo methods

1. Introduction

Recent crisis (Russia, Ukraine, Libya) challenged security of gas supply to Europe and this stimulated to look at this issue from political, technological and research perspectives. The EU Regulation 994/2010 [1] highlights importance of security of gas supply in Europe and proposes a number of measures to improve the situation.

From research point of view, reliability modelling of large networks became a popular subject for a number of researchers. A detailed review of network reliability methods is provided in [2]. The document deeply analyses properties of exact and simulation-based algorithms for key reliability modelling tasks.

Reliability analysis of networks have been analysed from different perspectives. Reliability analysis of ternary networks by so called ternary spectrum is analysed in [3]. Ternary spectrum is a network combinatorial invariant, and if it is known that all components are statistically independent and identical, system failure probability can be computed by a formula. Authors also analyse a system of two or more interacting networks. A simulation-based framework for interconnected electricity and gas systems is presented in [9]. The book [5] presents a comprehensive, up-to-date description of multi-state system reliability as a natural extension of classical binary-state reliability. The graph theory approach for flow networks is described, for example, in [4], [6], [7] and [8]. This is far from a complete list of references in the field, but it represents diversity and complexity of the approaches and problems to be solved.

16th ASMDA Conference Proceedings, 30 June – 4 July 2015, Piraeus, Greece

In this paper, probabilistic gas availability computations are performed by using a Monte Carlo simulation technique based on a distance-based approach of a stochastic network gas flow model [12], [13], [14]. The model assumes that priority in gas supply is given to the consumer nodes that are closer to the source nodes. This supply pattern is typical in gas transmission pipeline networks; however it can be changed by applying different demand measures in case of real crisis. The model works in such a way that in each Monte-Carlo simulation step, firstly component failures are sampled according to empirical probabilistic law assumed. In order to estimate the maximum of transmitted flow from source nodes to sink nodes under reliability and capacity constraints given by the stochastically imperfect elements, the maximum flow algorithm with multiple sources and multiple sinks is applied. Having collected large sample of network configurations and available flows, statistical estimations of available gas at demand nodes are provided.

2. Monte-Carlo simulation technique for stochastic network model

The reliability and capacity constraints of gas networks are analysed and discussed, for example, in [10] and [11]. The ProGasNet software, which is under our development, runs modified maximum flow algorithm [8] for each network configuration to distribute available gas from supplying nodes to consuming nodes taking into account both reliability and capacity constraints of network elements. The model is not running hydraulic gas flow computations, but uses results of hydraulic computations as a set of rules to define flow limitations.

The ProGasNet simulates network facility failures (pipeline ruptures, failures of compressor stations, unavailability of LNG terminals and storages) by Monte Carlo method and each different network configuration is evaluated by modified maximum flow algorithm to evaluate available gas for each network consuming node. During the network supply analysis, the algorithm distributes the available gas to all demand nodes. In case the total network demand cannot be met by available supply sources, the nodes closer by distance to the supplying source are served first. Finally, the statistical results are obtained from at least 1 million of Monte-Carlo runs.

The paper presents further development of the Monte-Carlo approach and provides a region wide benchmark analysis for probabilistic quantification of gas supply effects of a new LNG terminal. The presented gas network represents a real gas transmission network in Europe, but due to confidentiality, the geographical data is not provided.

3. Modelling of gas transmission network components

3. 1. Probabilistic model of a pipeline

The pipeline failure is modelled by the reduction of the pipeline capacity to zero. According to the EGIG report [10], the average failure frequency of a

European gas transmission pipeline is 3.5×10^{-4} per kilometer-year. Let us assume that 10% of the reported failures cause complete rupture of a pipeline. As a result, we set pipeline failure probability as $p_f = 3.5 \times 10^{-5}$ per kilometer-year. In accordance to the GTE [11], a relationship between the pipeline capacity and the pipeline diameter can be approximated for gas transmission pipelines. Moreover, this model prediction can be tuned if prior information is available. For example, the maximum pipeline capacity at the cross border connection point together with the pipeline diameter can be taken from a transmission system operator (TSO) reports.

3.2. Probabilistic model of a compressor station

It is assumed that a compressor station failure causes the reduction of the capacity of the surrounding pipelines. More precisely, a compressor station failure reduces the inlet pipeline and also the outlet pipeline capacity by 20%. This estimate is based on empirical estimations from known operational cases [14], but physical model simulations could serve as a confirmation for each specific situation.
It is assumed that the annual failure probability of a compressor station is 0.25. This is a conservative estimation obtained by a reliability database from network operators. The compressor station are Nodes 11 and 12 in our model (see Figure 1).

3.3. Probabilistic model of gas storage

In case of a gas storage failure, it is assumed that the capacity of the pipeline connected to the gas storage is reduced to zero [13]. According to expert knowledge [15], we set the annual failure probability of the gas storage to 0.10. Gas storage is Node 19 in our model (Figure 1).

3.4. Probabilistic model of LNG terminal

The LNG terminal is modelled as a special of the gas storage: the LNG terminal is modelled as a gas source that can randomly fail. In case of a LNG component failure, it is assumed that the capacity of the pipeline connected to the LNG terminal is reduced to zero. According to literature indications (e.g.[16]), we set the annual failure probability of the LNG terminal to 0.15. Node 10 is a LNG terminal.

4. Definition of the case-study network

4. 1. Model inputs

Figure 1 shows the network topology of the test gas transmission network model used in our study. The test case is based on the real gas transmission network of three countries. The presented supply/demand data sets are realistic; however, its geographical topology is not disclosed. The network contains the following elements: pipelines, compressor stations and the LNG terminal (Node 10).
Node 1 is a virtual gas source. In total, there are 3 supply nodes: 2, 10 and 19 (see Table 1). All numbers are expressed in million of cubic meter per day (mcm/d).

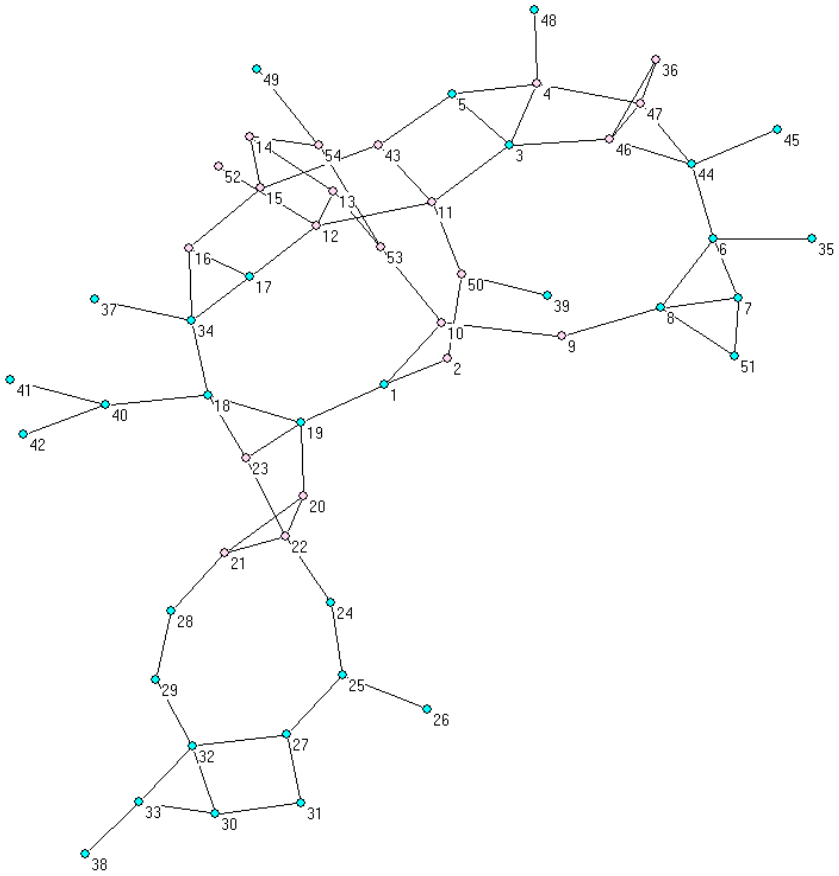

Figure 1: Anonymized topology of the test gas transmission network.

Table 1: Properties of the gas sources of the gas network. The physical limits (column limit) of gas sources are expressed in mcm/d.

from	To	limit
1	2	31
1	10	10.5
1	19	25

Pipeline diameters and their lengths were obtained from the gas operators. Consequently, the respective capacities have been estimated from pipelines diameters according to the GTE report [11], as discussed in Section 2. Moreover, the estimation of the transmission pipeline capacities has been independently verified by the authors and is consistent with results published at

reference [17]. All the properties of the transmission gas pipelines are summarized in Table 2. As the capacity matrix and the length matrix are symmetric in our benchmark, only non-zero elements of the upper triangular matrices are shown in Table 2.
Finally, Table 3 illustrates the properties of the demand nodes of the gas network. Node 55 is a virtual sink node. Node demands have been estimated according to partial information obtained from the gas operators. The 'last mile' is not modelled, as only transmission pipelines are represented in the model.
As our benchmark aims at studying the reliability of the gas network, the demands at the nodes are deterministic. In order to simplify Figure 1, the virtual sink node with the relative connections is not shown.

Table 2: Properties of connected elements of the gas network. Capacities are expressed in mcm/d; lengths are expressed in km.

from	to	capacity	length	from	to	capacity	length
2	50	31	23	18	23	49.16	43
3	4	49.16	0.01	18	34	2.83	43
3	5	12.11	32	18	40	5.05	148
3	11	12.11	29	19	20	12.11	60
3	46	17.13	22	19	23	12.11	0.01
4	5	12.11	32	20	21	49.16	90
4	47	2	22	20	22	12.11	0.01
4	48	12.11	2	21	22	12.11	90
5	43	5.05	5	21	28	12.11	86
6	7	12.11	80	22	23	7	60
6	8	5.05	80	22	24	12.11	86
6	35	5.05	30	24	25	0.83	86
6	44	5.05	11.6	25	26	12.11	46
7	8	49.16	0.01	25	27	49.16	100
7	51	12.11	200	27	31	5.05	0.01
8	9	2.83	25	27	32	5.05	70
8	51	12.11	200	28	29	49.16	50
9	10	2.83	162	29	32	49.16	195
10	53	1.34	144	30	31	5.05	70
10	54	5.05	144	30	32	0.47	0.01
11	12	2	103	30	33	0.47	60
11	43	12.11	34	32	33	2	60
11	50	49.16	31	33	38	5.05	60

12	13	49.16	85	34	37	2.83	200
12	17	49.16	62	36	46	5.05	24
12	52	12.11	10	36	47	5.05	24
13	14	30.6	0.01	39	50	1.34	106
13	53	2	30	40	41	5.05	32
14	15	5.05	85	40	42	12.11	63
14	54	5.05	30	44	45	5.05	1
15	16	12.11	62	44	46	17.13	23
15	43	12.11	132	44	47	2	23
16	17	25	0.01	46	47	49.16	0.01
16	34	4	24	49	54	0.83	40
17	34	12.11	24	53	54	49.16	0.01
18	19	12.11	43				

Table 3: Properties of demand nodes of the gas network. Node demands are expressed by mcm/d; lengths are expressed in km.

from	to	demand	from	to	demand
5	55	3.43	33	55	0.4
6	55	0.57	34	55	1
7	55	0.66	36	55	1.74
10	55	2.02	37	55	1.3
13	55	1.03	39	55	1
17	55	0.46	41	55	0.4
18	55	8.4	42	55	0.5
21	55	0.54	43	55	1.06
25	55	0.6	44	55	2.82
26	55	0.8	47	55	0.68
27	55	3.5	48	55	1.17
28	55	6	51	55	7
30	55	0.4	52	55	0.98

Length data are used for the calculation of the distance from source nodes, in order to model the priority of supply. The demand nodes close to the source are served first. Moreover, length data sets are used for computing pipeline failure probability.
Moreover, the physical limits of gas sources, capacities of connected elements and node demands are used as constrains for the Maximum flow algorithm.

5. Disruption case studies

In order to simulate the network reaction to LNG gas supply disruptions, the following scenarios are studied:

- Case 1: No external disruption; i.e. input nodes 2 and 19 are supplied as contracted. The pipeline between Node 10 (LNG) and Node 53 is not considered in the model. There is no LNG at Node 10.
- Case 2: LNG at Node 10 has upper limit 10.5 mcm/d. No external disruption, i.e. input nodes 2 and 19 are supplied as contracted.

In these scenarios, we assume that the network components (pipelines, compressor stations and LNG terminal) might fail according to the probabilistic estimates discussed above.
For each scenario, 1 million Monte-Carlo simulations were run. The analysis calculated the steady state of supply/demand estimated by the Maximum flow algorithm. The network component failures were simulated on a monthly basis.

6. Results of Monte-Carlo simulations

In order to the test reliability of the gas network, selected gas supply strategies were simulated with the Monte-Carlo approach. The results of simulations are statistically evaluated, in order to estimate reliability of gas supply for consuming nodes. This probabilistic quantification can be used as a tool for comparing, scoring and ranking different gas infrastructure projects.

5.1. Quantification of probabilistic effects of a new gas infrastructure: a case of LNG terminal

Let us analyse in more detail the probabilistic results of Cases 1 and 2, see Table 4 and Table 5. The tables include the list of demand quantities (column D) and probabilities that the supply at node X will be zero, expressed by the symbol P(X=0), or less than 20%, 50%, 80% or 100% of the node demand.
Both analysed cases represent a scenario without external disruption, i.e. input nodes 2 and 19 are supplied as contracted. Moreover, in Case 2, LNG is added at Node 10 with upper limit 10.5 mcm/d. Node 56 represents a virtual node (summary of supply). Adding the LNG source produces a decrease in P(X<D) from 1.24E-02 to 1.17E-02.
Moreover, results of one million of Monte-Carlo simulations indicate that adding the LNG as redundant supply will diminish the gas delivery uncertainty for Nodes 13, 17, 34, 43 - see Table 5.
However, the quantification of the effects of the addition of redundant LNG by direct comparison of the probabilities in Table 4 and Table 5 is not self-evident, due to size of the tables. For this reason, we created another table, which automatically highlights dissimilarities between Table 4 and Table 5: see Table 6.
In our approach, the quantification of security of gas supply of the LNG gas infrastructure for node *i* of the gas network is provided by a risk ratio [18]. The

risk ratio is easy to interpret: the risk ratio (also called 'relative risk') for a 'not enough gas event' at Node *i* is the probability of having 'not enough gas' at Node *i* without the LNG infrastructure divided by the probability of having 'not enough gas' at Node i with the LNG:

$$risk\_ratio = \frac{P(not\ enough\ gas\ at\ Node\ i|\ no\ LNG)}{P(not\ enough\ gas\ at\ Node\ i\ |\ LNG\ is\ connected)}$$

For example, if the risk ratio equals 5, it is 500 percent more likely to occur a 'not enough gas event' at Node *i* when no LNG is assumed than in cases with the connected LNG, holding all other variables constant. On the contrary, a relative risk of one at Node *i* means that the LNG infrastructure has no effect on the Node *i*.

5.2. Discussions of results

As shown in Table 6, if we compare simulations with and without LNG, the risk ratio (expressed by the symbol "*rr*") of having less than 80 % of the demand at Node 6 is, approximately, 97. Naturally, the largest effect of having the LNG infrastructure is directly visible at Node 10. Moreover, the positive effect of LNG is evident also for Nodes 5-7, 44, 47 and, partially, also for Node 36. The results appear to be realistic: As expected, the nodes showing positively effects are those geographically close to the LNG.
Finally, the nodes with relative risk equal to one are not affected by the LNG. For Node 52, and, partially, for Node 36, the relative risk is close to 0.9, considering the inherent numerical approximation of the Monte-Carlo method. But it is not a supply gas problem, as the estimated non-delivery probabilities at these two nodes are very close to zero.

Table 4: Results of Case 1: List of nodes with non-zero demands (D, mcm/d) and probabilities that the node supply will be zero or less than 20%, 50%, 80% or 100% of the node demand.

Node	D	P(X=0)	P(X<0.2D)	P(X<0.5D)	P(X<0.8D)	P(X<D)
5	3.43	2.00E-06	2.00E-06	1.39E-04	1.39E-04	1.39E-04
6	0.57	3.05E-04	3.05E-04	3.90E-04	3.90E-04	3.90E-04
7	0.66	3.90E-04	3.90E-04	3.90E-04	3.90E-04	3.90E-04
10	2.02	2.27E-04	2.27E-04	2.27E-04	9.35E-04	9.35E-04
13	1.03	2.00E-06	2.00E-06	2.00E-06	2.00E-06	2.00E-06
17	0.46	2.00E-06	2.00E-06	2.00E-06	2.00E-06	2.00E-06
18	8.4	5.00E-06	6.00E-06	7.00E-06	8.46E-03	8.46E-03
21	0.54	8.46E-03	8.46E-03	8.46E-03	8.46E-03	8.46E-03
25	0.6	8.46E-03	8.46E-03	8.46E-03	8.46E-03	8.46E-03
26	0.8	8.58E-03	9.10E-03	9.10E-03	9.10E-03	9.10E-03

27	3.5	8.60E-03	8.60E-03	8.60E-03	8.60E-03	8.60E-03
28	6	8.46E-03	8.46E-03	8.68E-03	8.68E-03	8.68E-03
30	0.4	8.60E-03	8.60E-03	8.60E-03	8.60E-03	8.60E-03
33	0.4	8.60E-03	8.60E-03	8.60E-03	8.93E-03	8.93E-03
34	1	2.00E-06	2.00E-06	2.00E-06	2.00E-06	2.00E-06
36	1.74	2.13E-04	2.13E-04	2.13E-04	2.14E-04	2.15E-04
37	1.3	9.04E-03	9.04E-03	9.04E-03	9.04E-03	9.04E-03
39	1	3.61E-04	3.61E-04	3.61E-04	3.61E-04	3.61E-04
41	0.4	8.99E-03	8.99E-03	8.99E-03	8.99E-03	8.99E-03
42	0.5	9.08E-03	9.08E-03	9.08E-03	9.08E-03	9.08E-03
43	1.06	2.00E-06	2.00E-06	2.00E-06	2.00E-06	2.00E-06
44	2.82	1.39E-04	1.39E-04	2.13E-04	2.76E-04	2.76E-04
47	0.68	1.39E-04	1.39E-04	1.39E-04	1.39E-04	1.39E-04
48	1.17	7.00E-06	7.00E-06	7.00E-06	7.00E-06	7.00E-06
51	7	3.90E-04	3.90E-04	3.90E-04	6.18E-04	6.18E-04
52	0.98	3.20E-05	3.20E-05	3.20E-05	3.40E-05	3.40E-05
56	48.46	2.00E-06	2.00E-06	3.00E-06	8.82E-03	1.24E-02

Table 5: Results of Case 2: List of nodes with non-zero demands (D, mcm/d) and probabilities that the node supply will be zero or less than 20%, 50%, 80% or 100% of the node demand.

Node	D	P(X=0)	P(X<0.2D)	P(X<0.5D)	P(X<0.8D)	P(X<D)
5	3.43	0.00E+00	0.00E+00	3.00E-06	3.00E-06	3.00E-06
6	0.57	3.00E-06	3.00E-06	4.00E-06	4.00E-06	4.00E-06
7	0.66	7.40E-05	7.40E-05	7.40E-05	7.40E-05	7.40E-05
10	2.02	4.00E-06	4.00E-06	4.00E-06	4.00E-06	4.00E-06
13	1.03	0.00E+00	0.00E+00	0.00E+00	0.00E+00	0.00E+00
17	0.46	0.00E+00	0.00E+00	0.00E+00	0.00E+00	0.00E+00
18	8.4	0.00E+00	0.00E+00	0.00E+00	8.48E-03	8.48E-03
21	0.54	8.48E-03	8.48E-03	8.48E-03	8.48E-03	8.48E-03
25	0.6	8.49E-03	8.49E-03	8.49E-03	8.49E-03	8.49E-03
26	0.8	8.64E-03	9.14E-03	9.14E-03	9.14E-03	9.14E-03
27	3.5	8.64E-03	8.64E-03	8.64E-03	8.64E-03	8.64E-03
28	6	8.49E-03	8.49E-03	8.75E-03	8.75E-03	8.75E-03
30	0.4	8.64E-03	8.64E-03	8.64E-03	8.64E-03	8.64E-03

33	0.4	8.64E-03	8.64E-03	8.64E-03	8.99E-03	8.99E-03
34	1	0.00E+00	0.00E+00	0.00E+00	0.00E+00	0.00E+00
36	1.74	3.00E-06	3.00E-06	7.30E-05	2.26E-04	2.27E-04
37	1.3	9.10E-03	9.10E-03	9.10E-03	9.10E-03	9.10E-03
39	1	3.47E-04	3.47E-04	3.47E-04	3.47E-04	3.47E-04
41	0.4	8.98E-03	8.98E-03	8.98E-03	8.98E-03	8.98E-03
42	0.5	9.04E-03	9.04E-03	9.04E-03	9.04E-03	9.04E-03
43	1.06	0.00E+00	0.00E+00	0.00E+00	0.00E+00	0.00E+00
44	2.82	3.00E-06	3.00E-06	3.00E-06	3.00E-06	3.00E-06
47	0.68	3.00E-06	3.00E-06	3.00E-06	3.00E-06	3.00E-06
48	1.17	6.00E-06	6.00E-06	6.00E-06	6.00E-06	6.00E-06
51	7	2.28E-04	2.86E-04	3.21E-04	3.99E-04	3.99E-04
52	0.98	3.50E-05	3.50E-05	3.50E-05	3.50E-05	3.50E-05
56	48.46	0.00E+00	0.00E+00	1.00E-06	8.64E-03	1.17E-02

Table 6: Quantifications of probabilistic effects of an 10.5 mln/d LNG source. Positively affected demand nodes highlighted.

Node	D	rr(X=0)	rr(X<0.2D)	rr(X<0.5D)	rr(X<0.8D)	rr(X<D)
5	3.43	-	-	46.3	46.3	46.3
6	0.57	101.7	101.7	97.5	97.5	97.5
7	0.66	5.3	5.3	5.3	5.3	5.3
10	2.02	56.8	56.8	56.8	233.8	233.8
13	1.03	-	-	-	-	-
17	0.46	-	-	-	-	-
18	8.4	-	-	-	1.0	1.0
21	0.54	1.0	1.0	1.0	1.0	1.0
25	0.6	1.0	1.0	1.0	1.0	1.0
26	0.8	1.0	1.0	1.0	1.0	1.0
27	3.5	1.0	1.0	1.0	1.0	1.0
28	6	1.0	1.0	1.0	1.0	1.0
30	0.4	1.0	1.0	1.0	1.0	1.0
33	0.4	1.0	1.0	1.0	1.0	1.0
34	1	-	-	-	-	-
36	1.74	71.0	71.0	2.9	0.9	0.9
37	1.3	1.0	1.0	1.0	1.0	1.0

39	1	1.0	1.0	1.0	1.0	1.0
41	0.4	1.0	1.0	1.0	1.0	1.0
42	0.5	1.0	1.0	1.0	1.0	1.0
43	1.06	-	-	-	-	-
44	2.82	46.3	46.3	71.0	92.0	92.0
47	0.68	46.3	46.3	46.3	46.3	46.3
48	1.17	1.2	1.2	1.2	1.2	1.2
51	7	1.7	1.4	1.2	1.5	1.5
52	0.98	0.9	0.9	0.9	1.0	1.0
56	48.46	-	-	3.0	1.0	1.1

7. Conclusions and future work

The ProGasNet tool provides probabilistic results of the gas network ability to meet its demand and such results can be used either as absolute values to compare among different networks or in qualitative terms to choose between better or worse options. The ProGasNet has been applied to test cases based on the real gas transmission network of selected EU countries. The results obtained indicate the benefits that might derive from the insertion of a new infrastructure (LNG terminal) to an existing network, and in particular to certain nodes. It is important to note that security of supply also depends on redundancy of supply sources, and that this can be quantified by the model proposed.
The model will be expanded and improved in many directions in the future, in particular by integrating more results from physical flow models (important for larger networks containing many compressor stations) and optimizing the algorithm to handle more Monte-Carlo runs.

References

[1] Regulation (EU) No. 994/2010 of the European Parliament and of the Council of 20 October 2010 concerning measures to safeguard security of gas supply and repealing Council Directive 2004/67/EC. Official Journal of the European Union, 2010.

[2] M. O. Ball, C. J. Colbourn, J.S. Provan, Network Reliability, University of Maryland, 1992.

[3] I. Gertsbakh, Y. Shpungin, R. Vaisman, Ternary networks: reliability and Monte Carlo. Heidelberg, Berlin, Springer 2014. On-line copy: http://gnedenko-forum.org/library/Gertsbakh/Ternary+Networks+Brief.pdf

[4] N. Deo, Graph Theory with Applications to Engineering with Computer Science. Prentice Hall, 2008

[5] A. Lisnianski, I. Frenkel, Y. Ding, Multi-state System Reliability Analysis and Optimization for Engineers and Industrial Managers. London: Springer.
[6] R.K. Ahuja, T.L. Magnanti, J.B. Orlin, Network flows, in G.L. Nemhauser, A.H.G. Rinnooy Kan, M.J. Todd (Eds.), Optimization, Elsevier North-Holland Inc., New York, 1989, pp. 211-369.
[7] M.S. Bazaraa, J.J. Jarvis, H.D. Sherali, Linear Programming and Network Flows, John Wiley & Sons, New York, 2010.
[8] N. Deo, Graph Theory with Applications to Engineering with Computer Science. Prentice Hall, 2008.
[9] B. Cakir Erdener, K. A. Pambour, R. Bolado Lavin, B. Dengiz, An integrated simulation model for analysing electricity and gas systems, Electrical Power and Energy Systems 61 (2014) 410-420
[10] EGIG report, 8th Report of the European Gas Pipeline Incident Data Group. Groningen, 2011
[11] Definition of available capacities at interconnection points in liberalized market. Gas Transmission Europe, July 2, 2004; Ref.: 04CA041-final.
[12] V.Kopustinskas, P.Praks, Development of gas network reliability model, JRC technical report JRC78151, European Commission, Luxembourg, 2012.
[13] V. Kopustinskas, P. Praks: Time dependent gas transmission network probabilistic simulator: focus on storage discharge modeling. European Safety and Reliability Conference ESREL 2014. 14th-18th Sept. 2014. Wroclaw, Poland (Safety and Reliability: Methodology and Applications – Nowakowski et al. (Eds) © 2015 Taylor & Francis Group, London; pg. 2069-2075; ISBN 978-1-138-02681-0
[14] P. Praks, V. Kopustinskas, Monte-Carlo based reliability modelling of a gas network using graph theory approach. Proceedings - 9th International Conference on Availability, Reliability and Security, ARES 2014. University of Fribourg; Switzerland; http://dx.doi.org/10.1109/ARES.2014.57
[15] M. Ouyang, Review on modeling and simulation of interdependent critical infrastructure systems, Reliab. Eng. Syst. Saf. 121 (2014) 43-60
[16] MJ Jung, JH Cho, W. Ryu, LNG terminal design feedback from operator's practical improvements. In: the 22nd World Gas Congress. Tokyo, Japan; 2003
[17] C. Pelletier, J.C. Wortmann, A risk analysis for gas transport network planning expansion under regulatory uncertainty in Western Europe, Energy Policy, 37(2), 2009, 721-732
[18] EC Norton, H Wang, C Ai: Computing interaction effects and standard errors in logit and probit models. The Stata Journal (2004) 4, Number 2, pp. 154-167

On ordered categorical modelling for complex skill development

Natalya Pya[1] and Arman Kussainov[2]

[1] Department of Mathematical Sciences, School of Science and Technology, Nazarbayev University, Astana, Kazakhstan
(E-mail: natalya.pya@nu.edu.kz)
[2] Physics and Technology Department, al-Farabi Kazakh National University, Almaty, Kazakhstan
(E-mail: arman.kussainov@gmail.com)

Abstract. In cognitive science there has been considerable interest in the understanding of expertise development. Models for exploring human complex skill development are often based on comparisons between experts and novices, and use measurements of performance at different levels of skills as predictors. In this paper we study the development of expertise by analysing video game telemetry data collected from a real-time strategy game. Data that relate to cognitive-motor abilities, attentional and perceptual processes were collected from StarCraft 2 game players from seven levels of expertise. We develop an extended generalized additive model for ordered categorical data to investigate the effects of predictors on skill development.
Keywords: ordered categorical, cognitive science, generalized additive models, skill learning.

1 Introduction

Thompson *et al.*[18] conducted a study exploring human complex skill development. Their aim was to identify potential predictors of expertise in real-time strategy (RTS) video games using the telemetric data collected from RTS StarCraft 2 game players. StarCraft 2 is a popular video game which has millions of players worldwide. Thompson *et al.*[18] examined measures that relate to cognitive-motor abilities, attentional and perceptual processes. Using random forest classifiers, they disproved the assumption that importance of variables across skill levels remains static. Moreover, they argue that telemetric data can become a standard tool for studying human cognition and learning. As different expert areas such as, e.g. chess, basketball, surgery, are expected to show sufficient consistency in development of expertise, many studies have been devoted to exploring skill development in strategy games (Chase and Simon[8], Charness[9], Ericsson and Charness[10]).

This paper proposes to investigate development of expertise using additive regression modelling. The paper develops an extended generalized additive model for ordered categorical data (Wood *et al.*[19]) to study the effects of predictors on skill learning. Modelling categorical responses using smooth functions of predictors allows us to confirm Thompson *et al.*[18] findings and to further investigate the effects of predictors on skill development.

16^{th}*ASMDA Conference Proceedings, 30 June – 4 July 2015, Piraeus, Greece*

2 Video game data

The telemetric data collected from 3,360 RTS StarCraft 2 game players from 7 levels of expertise. The dataset is public available at UCI Machine Learning Repository (Bache and Lichman[5]). For each player, the level of expertise measured by the league in which they contend, serves as an ordered response Y_i. Y_i takes a value from $r = 1, 2, \ldots, 7$, indicating Bronze, Silver, Gold, Platinum, Diamond, Master, and Professional leagues. There are eighteen predictor variables available including measures of attentional control, perceptual process and cognitive-motor speed. The examination of the data and preliminary modelling revealed 13 variables relevant to skill development. Table 1 summarizes the predictors under study. The time at which values of the predictors is recorded is in terms of timestamps in the StarCraft 2 replay file. `GapBwPACs`, `ActionLatency`, `NumberOfPACs`, and `ActionsInPAC` are four variables that refer to a certain period of time during which a player performs at a specific location. Perception action cycle (PAC) was defined by Thompson *et al.*[18] as screen fixations with one or more actions. For the complete information about the variables used in the study, see Thompson *et al.*[18].

Table 1. Telemetric data characteristics

Name	Description	Min	Max
APM	Action per minute	22.06	389.83
SelectByHotkeys	Number of unit or building selections made using hotkeys per timestamp	0	0.043
AssignToHotkeys	Number of units or buildings assigned to hotkeys per timestamp	0	$1.75 \cdot 10^{-3}$
UniqueHotkeys	Number of unique hotkeys used per timestamp	0	10
MinimapAttacks	Number of attack actions on minimap per timestamp	0	$3.02 \cdot 10^{-3}$
NumberOfPACs	Number of perception action cycles (PAC) per timestamp	$6.79 \cdot 10^{-4}$	$7.97 \cdot 10^{-3}$
GapBwPACs	Mean duration in milliseconds between PACs	6.667	237.143
ActionLatency	Mean latency from the onset of PACs to their first action in milliseconds	24.09	176.37
ActionsInPAC	Mean number of actions within each PAC	2.039	18.558
TotalMapExplored	The number of 24x24 game coordinate grids viewed by the player per timestamp	5	58
WorkersMade	Number of SCVs, drones, and probes trained per timestamp	$7.7 \cdot 10^{-5}$	$5.15 \cdot 10^{-3}$
UniqueUnitsMade	Unique unites made per timestamp	2	13
ComplexAbilUsed	Abilities requiring specific targeting instructions used per timestamp	0	$3.08 \cdot 10^{-3}$

3 Modelling approach

Many models have been proposed to analyze ordered categorical data which became well-known by virtue of Cox[7] and Plackett[16]. The most appealing regression models for ordered categories are cumulative logit (proportional-odds version of the cumulative logit) models expressed in terms of a latent usually unobservable continuous variable proposed by McCullagh[15], Anderson and Philips[4], Hastie and Tibshirani[13]. McCullagh[15] and Anderson and Philips[4] introduced parametric regression models with ordered categorical responses, whereas Hastie and Tibshirani[13] extended this to a non-parametric version. The parameter estimation for those models is based on maximizing likelihood assuming independent multinomial observations using Fisher scoring algorithm. The cumulative logit models were also discussed in Anderson[3], Agresti[1], Agresti[2], Goodman[12]. Fahrmeir and Lang[11], Kneib and Fahrmeir[14] developed a general class of semi-parametric additive regression models for categorical responses from a Bayesian perspective.

Extended generalized additive model

The model proposed in this paper is within a new general framework to generalized additive modelling for non-exponential family responses introduced by Wood *et al.*[19]. The framework of Wood *et al.*[19] proposes two methods for the generalized additive models (GAM) generalization: an extended GAM fitting for the cases with a single linear predictor and a log likelihood expressed as a sum over the log likelihood for each response datum; and a general model estimation when log likelihood depends non-linearly on smooth functions of predictors. The first method includes such distributions outside the exponential family as beta, zero inflated Poisson, negative binomial, Tweedie, scaled t distribution and ordered categorical data. The GAM fitting method is extended for these models. The second extension requires different approach for model fitting and general and reliable smoothing parameter estimation. It covers such models as Cox proportional hazard (Cox[6]) and Cox process models, generalized additive models for location scale and shape proposed by Rigby and Stasinopoulos[17] and multivariate additive models (Yee and Wild[21]). Below is a brief description of modelling with ordered categorical responses within a new extended GAM.

Consider independent response observations, y_i, that take values from $r = 1, \ldots, R$, where r is ordered category label. A latent variable $u_i = \mu_i + \epsilon_i$ is introduced with the c.d.f. of ϵ_i being F. Then, given $-\infty = \alpha_0 < \alpha_1 < \ldots < \alpha_R = \infty$, $y_i = r$ if a latent variable u_i is such that $\alpha_{r-1} < u_i \leq \alpha_r$,

$$P(Y_i = r) = F(\alpha_r - \mu_i) - F(\alpha_{r-1} - \mu_i).$$

The usual choice for the c.d.f. of ϵ is the standard logistic or normal. For identifiability reasons $\alpha_1 = -1$, so there are $R - 2$ extra unknown parameters. To impose increasing ordering on the cutting points, α_r are set as

$$\alpha_r = \alpha_1 + \sum_{j=1}^{r-1} \exp(\theta_j), \quad 1 < r < R,$$

so θ_j are parameters to be estimated. The mean value of the latent variable depends on the predictor variable in the following way,

$$\mu_i = \mathbf{A}_i\boldsymbol{\gamma} + \sum_j f_j(x_{ji}),$$

where $\mathbf{A}$ is a model matrix for the strictly parametric terms, $\boldsymbol{\gamma}$ is a vector of unknown parameters, f_j is an unknown smooth function of the predictor variable x_j, where x_j can be vector valued. Each smooth term is represented by reduced rank spline smoothers $f_j(x_j) = \sum_k \beta_{kj} b_{kj}(x_j)$, where b_{kj} are known spline basis functions, β_{kj} unknown coefficients. Then, the mean of the latent variable can be expressed as $\boldsymbol{\mu} = \mathbf{X}\boldsymbol{\beta}$, with the model matrix $\mathbf{X}$ combining $\mathbf{A}$ and matrix of spline basis, and $\boldsymbol{\gamma}$ being a part of $\boldsymbol{\beta}$.

The log likelihood of the model can be written as

$$l = \sum_{i=1}^{n} l_i(y_i, \mu_i, \boldsymbol{\theta}),$$

where l_i is the log likelihood for each observation, $\boldsymbol{\theta}$ is a $(R-2)-$vector of the extra parameters, θ_j, that control the thresholds. Then, the deviance corresponding to the observation y_i is defined in the standard way as $D_i = 2(\tilde{l}_i - l_i)$, where $l_i = \max_{\mu_i} l_i(y_i, \mu_i, \boldsymbol{\theta})$ is the saturated log likelihood. Given $\boldsymbol{\theta}$, the parameters $\boldsymbol{\beta}$ are estimated by minimization of the penalized deviance

$$\mathcal{D}(\boldsymbol{\beta}, \boldsymbol{\theta}) = \sum_i D_i(\boldsymbol{\beta}, \boldsymbol{\theta}) + \sum_j \lambda_j \boldsymbol{\beta}^T \mathbf{S}^j \boldsymbol{\beta},$$

where a quadratic penalty term $\boldsymbol{\beta}^T \mathbf{S}^j \boldsymbol{\beta}$ measuring function smoothness is associated with each smooth f_j and λ_j being a smoothing parameter. Penalized iteratively re-weighted least squares (PIRLS) is applied for $\boldsymbol{\beta}$ estimation. Estimation of $\boldsymbol{\theta}$ is achieved by minimization of the negative Laplace approximate marginal likelihood (LAML),

$$\mathcal{V} = \frac{\mathcal{D}(\hat{\boldsymbol{\beta}}, \boldsymbol{\theta})}{2} - \tilde{l}(\boldsymbol{\theta}) + \frac{\log|\mathbf{X}^T\mathbf{W}\mathbf{X} + \mathbf{S}^\lambda| - \log|\mathbf{S}^\lambda|_+}{2} - \frac{M_p}{2}\log(2\pi),$$

where $\mathbf{S}^\lambda = \sum_j \lambda_j \mathbf{S}^j$ and $|\mathbf{S}^\lambda|_+$ is the product of the positive eigenvalues of $\mathbf{S}^\lambda$, M_p is the number of zero eigenvalues of $\mathbf{S}^\lambda$. Newton's or a quasi-Newton's method is used for $\mathcal{V}$ minimization. Several issues with numerical instability have to be taken into account to make the optimization procedure efficient and reliable. This is fully covered in Wood *et al.*[19]. Generalized additive modelling with ordered categorical data as well as other extensions are implemented in an R package `mgcv` available at CRAN (Wood[20]).

Additive model for video game data

The preliminary backward selection, first in the framework of a generalized linear model and then in the framework of an extended GAM, revealed thirteen covariates

relevant to skill development (see section 2). The extended GAM for ordered categorical data with $R = 7$ was fitted with the selected set of predictors using smooth terms. We first consider a model with all selected predictors having non-linear effects on the mean of the ordered categorical latent variable.

Model 1:

$$\begin{aligned}\mu_i = f_1(\texttt{NumberOfPACs}_i) + f_2(\texttt{UniqueHotkeys}_i) + f_3(\texttt{WorkersMade}_i)\\ + f_4(\texttt{GapBwPACs}_i) + f_5(\texttt{ActionLatency}_i) + f_6(\texttt{AssignToHotkeys}_i)\\ + f_7(\texttt{MinimapAttacks}_i) + f_8(\texttt{APM}_i) + f_9(\texttt{SelectByHotkeys}_i)\\ + f_{10}(\texttt{ActionsInPAC}_i) + f_{11}(\texttt{TotalMapExplored}_i)\\ + f_{12}(\texttt{UniqueUnitsMade}_i) + f_{13}(\texttt{ComplexAbilUsed}_i),\end{aligned}$$

where the model terms $f_1 - f_{13}$ are unknown smooth functions of the corresponding predictors. Thin plate regression splines are used for their representations. The predictor values were preprocessed using square root or log transformation in order to avoid gaps with very small amount of data that account for the Professional league. There was a significant linear dependence of `NumberOfPACs`, `UniqueHotkeys` and `WorkersMade` on the mean of the latent variable, so that it was sufficient to add strictly parametric structure for these three predictors. The resulted model has the following structure.

Model 2:

$$\begin{aligned}\mu_i = \beta_1 \cdot \texttt{NumberOfPACs}_i + \beta_2 \cdot \texttt{UniqueHotkeys}_i + \beta_3 \cdot \texttt{WorkersMade}_i\\ + f_1(\texttt{GapBwPACs}_i) + f_2(\texttt{ActionLatency}_i) + f_3(\texttt{AssignToHotkeys}_i)\\ + f_4(\texttt{MinimapAttacks}_i) + f_5(\texttt{APM}_i) + f_6(\texttt{SelectByHotkeys}_i)\\ + f_7(\texttt{ActionsInPAC}_i) + f_8(\texttt{TotalMapExplored}_i)\\ + f_9(\texttt{UniqueUnitsMade}_i) + f_{10}(\texttt{ComplexAbilUsed}_i),\end{aligned}$$

where β_1, β_2 and β_3 are unknown parameters.

Including the bivariate smooth of the `APM` and the second most important variable, `SelectByHotkeys`, gives better model in comparison with the model with univariate effect of the `APM`. Moreover, constructing a tensor product interaction of `GapBwPACs` and `ActionLatency`, with their main effects being included separately further improves the model fit. The following additive structure for the mean value of the ordered categorical latent variable was considered as the third model.

Model 3:

$$\begin{aligned}\mu_i = \beta_1 \cdot \texttt{NumberOfPACs}_i + \beta_2 \cdot \texttt{UniqueHotkeys}_i + \beta_3 \cdot \texttt{WorkersMade}_i\\ + f_1(\texttt{GapBwPACs}_i) + f_2(\texttt{ActionLatency}_i)\\ + f_3(\texttt{GapBwPACs}_i, \texttt{ActionLatency}_i) + f_4(\texttt{AssignToHotkeys}_i)\\ + f_5(\texttt{MinimapAttacks}_i) + f_6(\texttt{APM}_i, \texttt{SelectByHotkeys}_i)\\ + f_7(\texttt{ActionsInPAC}_i) + f_8(\texttt{TotalMapExplored}_i)\\ + f_9(\texttt{UniqueUnitsMade}_i) + f_{10}(\texttt{ComplexAbilUsed}_i),\end{aligned}$$

where all the predictors except for the first three have nonparametric smooth effects. A tensor product interaction of `GapBwPACs` and `ActionLatency`, is used for representing f_3 with the main effects comprised in f_1 and f_2. .

4 Results and discussion

In addition to the above mentioned models, we fitted submodels with certain terms omitted. The model selection procedure showed that the best model in terms of the Akaike information criterion is the full model 3. Other model performance measures such as generalized cross validation score, adjusted r^2 and percentage deviance explained were also better for model 3 than for other considered models.

Figure 1 illustrates the estimated effects of the two bivariate smooths of model 3. `APM` variable is used as a measure of cognitive speed. This variable is shown to have the highest rank of the predictive importance Thompson *et al.*([18]) in distinguishing Bronze-Professional classifier. The first decreasing trend of the `APM` (figure 1, right panel) is due to the high correlation between the `APM` and `SelectByHotkeys` variables (higher values of the covariate effect correspond to higher league level). Both predictors have increasing trends when considered separately as smooths of a single variable.

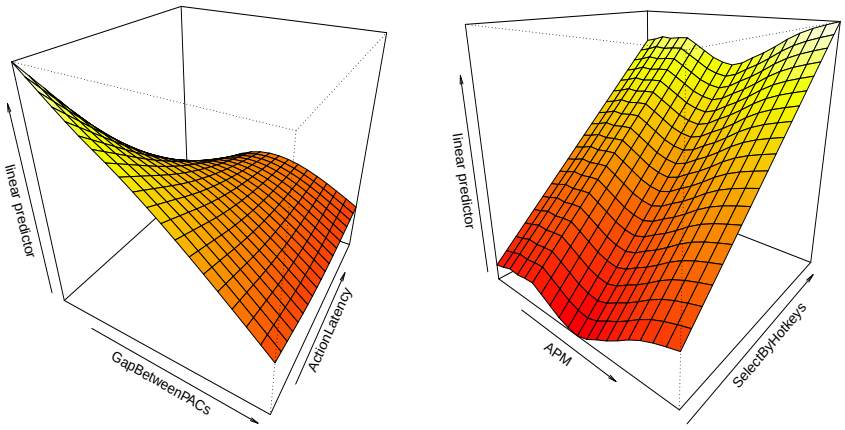

Fig. 1. Video game data: the estimated interactions between Gap Between PACs and Action Latency variables, and between APM and Select By Hotkeys.

The estimates of the univariate effects are shown in figure 2. As expected, the main effects of the two characteristics of the PACs, `GapBwPACs` and `ActionLatency`, are decreasing with increase in the skill level (panels (a) and (b)), while the other two have increasing trends (panel (e) and the positive parametric effect of `NumberOfPACs`). An adaptive smoother was used to estimate the effect of the `ActionsInPAC`, that allowed the degree of smoothing to vary along the range of the predictor values.

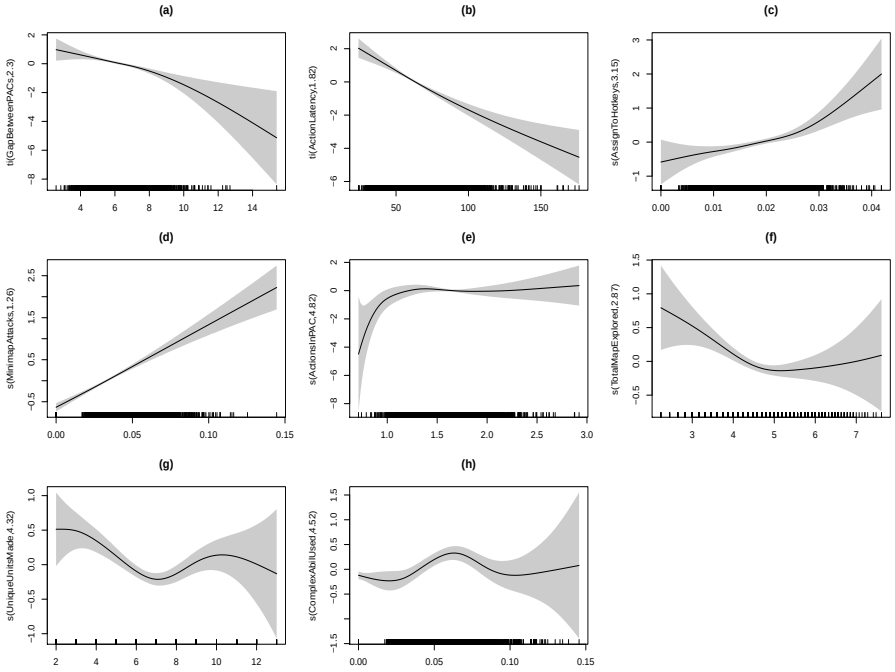

Fig. 2. Video game data: the estimated univariate smooth effects.

The strong increasing effect of the `MinimapAttacks` (fig. 2, panel (d)) which is used as a measure of the attentional control, supports the hypothesis of Thompson *et al.*[18] that more skillful players act on minimap more often. On the contrary the `TotalMapExplored` has a decreasing trend (panel (f)), more skillful players view the total map less often. Usage of hotkeys allows players to build and control game units in more efficient way, so that the higher values of the `AssignToHotkeys` variable would correspond to higher level of expertise (panel (c)). The estimated effects of the last two predictors do not have such monotonic features as for the other smooths. Players in the highest leagues seem to use moderately abilities that require particular targeting instructions (panel (h)), and keeping from the production of the Unique Units (panel (g)). Whereas, the lowest league players make medium number of units while avoiding complex abilities. The estimated monotone increasing trend of the `WorkersMade` shows that to progress players must produce more workers. How-

ever, the importance of this variable diminishes for the highest league (Thompson *et al.*[18]), which is explained by possible automatization of the worker production skill. Moreover, to advance in skills, players are required to put more effort on managing their learning and increasing cognitive demand, which is reflected by the positive linear trend of the `UniqueHotKeys` predictor.

This study supports Thompson's *et al.* [18] proposition that telemetric data can be used as a standard tool for studying human cognition and learning. Moreover, the proposed model confirms the previous findings that the assumption that importance of predictors across skill levels remains static is not correct. We showed that constructing non-isotropic tensor product splines used to model smooth interactions improves prediction of skill development. Modelling categorical responses using smooth functions of predictors allows to capture skill learning in a continuous fashion.

References

1. A. Agresti. *Categorical data analysis*, volume 359. John Wiley and Sons, 2002.
2. A. Agresti.*Analysis of ordinal categorical data*, volume 656. Wiley, 2010.
3. J.A. Anderson, J. A. Regression and ordered categorical variables. *Journal of the Royal Statistical Society. Series B*, 1–30, 1984.
4. J. Anderson and P. Philips. Regression, discrimination and measurement models for ordered categorical variables. *Applied Statistics*, 22–31, 1981.
5. K. Bache and M. Lichman. UCI machine learning repository, 2013.
6. D.D.R. Cox. Regression models and life tables. *Journal of the Royal Statistical Society. Series B*, 34(2), 187–220, 1972.
7. D.D.R. Cox. *The analysis of binary data*. volume 32, CRC Press, 1989.
8. W.G. Chase and H.A. Simon. Perception in chess. *Cognitive Psychology*, 4, 55–81, 1973.
9. N. Charness. Age, skill, and bridge bidding: A chronometric analysis, *Journal of Verbal Learning and Verbal Behavior*, 22(4), 406–416, 1983.
10. K.A. Ericsson, N. Charness. Expert performance. *American Psychologist*, 49(8), 725–747, 1994
11. L. Fahrmeir and S. Lang. Bayesian semiparametric regression analysis of multicategorical time-space data. *Annals of the institute of Statistical Mathematics*, 53(1), 11–30, 2001.
12. L.A. Goodman. The analysis of dependence in cross-classifications having ordered categories, using log-linear models for frequencies and log-linear models for odds. *Biometrics*, 149–160, 1983.
13. T. Hastie and R. Tibshirani. Non-parametric logistic and proportional odds regression. *Applied statistics*, 260–276, 1987.
14. T. Kneib and L. Fahrmeir. Structured additive regression for categorical spacetime data: A mixed model approach. *Biometrics*, 62(1), 109–118, 2006.
15. P. McCullagh. Regression models for ordinal data. *Journal of the Royal Statistical Society. Series B*, 109–142, 1980
16. RL. Plackett. *The Analysis of Categorical Data*. Griffin, London, 1981.
17. R. Rigby and D.M. Stasinopoulos. Generalized additive models for location, scale and shape. *Journal of the Royal Statistical Society. Series C*, 54(3), 507–554, 2005
18. J.J. Thompson, M.R. Blair, L. Chen, and A.J. Henrey. Video game telemetry as a critical tool in the study of complex skill learning. *PloS One*, 8, 9, e75129, 2013.
19. S. Wood, N. Pya, and B. Säfken. On doubly generalized additive models. (submitted)
20. S. Wood. mgcv: Mixed GAM Computation Vehicle with GCV/AIC/REML smoothness estimation. R package version 1.8-6, 2015.
21. T.W. Yee and C. Wild. Vector generalized additive models. *Journal of the Royal Statistical Society. Series B*, 481–493, 1996

Incorporating shape constraints in generalized additive modelling of the height-diameter relationship for Norway spruce

Natalya Pya[1] and Matthias Schmidt[2]

[1] Department of Mathematical Sciences, School of Science and Technology, Nazarbayev University, Astana, Kazakhstan
(E-mail: natalya.pya@nu.edu.kz)
[2] The Northwest German Forest Research Station, Department of Forest Growth, Grätzelstr. 2, 37079 Göttingen, Germany
(E-mail: matthias.schmidt@nw-fva.de)

Abstract. Measurements of tree heights and diameters are essential in forest assessment and modelling. Tree heights are used for estimating timber volume, site index and other important variables related to forest growth and yield, succession and carbon budget models. However, the diameter at breast height (dbh) can be more accurately obtained and at lower cost, than total tree height. Hence, models are needed that predict tree height from dbh, age and other covariates. In this paper we develop unconstrained generalized additive models (GAM) and shape constrained generalized additive models (SCAM) for investigating the possible effects of tree-specific parameters such as tree age, relative diameter at breast height, and site-specific parameters such as altitude, index of aridity and sum of daily mean temperature during vegetation period, on the height-diameter relationship for the current status of forests in Lower Saxony, Germany. We use causal site parameters such as index of aridity to enhance the generality and causality of the models and to enable predictions under projected changeable climatic conditions. We demonstrate that the SCAM approach allows optimal regression modelling flexibility similar to the standard GAM but with the additional possibility of defining specific constraints for the model effects.
Keywords: height-diameter curve, Norway spruce, shape constrained additive models, impact of climate change, varying coefficient models.

1 Introduction

Two of the main questions of forest management planning concern the current status of forests and how forests will develop in future. To estimate forest stock and assortment from sample forest inventories, for example, in forest districts or federal states, single tree volumes have to be predicted and then summed up to get timber volume estimates for a considered forest area. A tree volume estimate is usually based on three parameters: tree species, tree diameter and tree height. Since measuring tree diameter at breast height (1.3 m) (dbh), is relatively cheap, but measuring tree height is cost intensive, it is desirable to model tree height as a function of tree species, tree diameter, tree age and other possible stand- and site-specific parameters. An important feature of the height-diameter (h-d) relationship is that it develops over time and varies from

16^{th}*ASMDA post conference publication in book, 30 June – 4 July 2015, Piraeus, Greece*

stand to stand (Curtis[5], Lappi[20], Mehtätalo[22]). In Mehtätalo[23] it is noted that trees reach maturity at different ages depending on site conditions. Hence, asymptotic height and the height that is reached at any particular age differ significantly among sites. The poorer the site conditions are, the lower the tree height will be for a certain age and dbh, with the dbh itself depending on age, stand and site conditions, but also on silvicultural treatments.

In this paper we develop site-sensitive longitudinal h-d models for forests in Lower Saxony, Germany, with the main focus on modelling fixed effects via unconstrained (GAM) and shape constrained generalized additive models (SCAM). Since climate change has already affected forests in Central Europe and much heavier impact is anticipated in the future, the models should be applicable for prediction of future tree height development and able to quantify the impact of climate change. Therefore, to achieve the necessary higher causality we use a combination of causal and proxy site parameters as predictors.

In this study a general underlying modelling approach of a reparameterized version of the Korf-function, that was developed by Lappi[20] is used as the principal model. The reason for using this model is that the model parameters considered there are less correlated and have biological meaning. Moreover, a heuristic fixation of the 'non-linear' parameters applied in this case linearizes the model, which makes the generalized additive model approach reasonable to use for the estimation of the covariate effects on the original parameters. The model is then extended to include some tree-specific and site-specific variables. As some of the covariate effects are supposed to be monotone, a shape constrained additive modelling (SCAM) approach (Pya and Wood[25]) is applied to account for influence of such variables as tree age, relative diameter at breast height and altitude among others, and also of site variables that will partially alter with expected climate change.

2 Data

The data analyzed here are observations from 23 145 sample plots of 29 324 Norway spruce trees [*Picea abies (L.) Karst.*] and some site-specific variables from the first cycle of the state forest enterprise inventories (district sample plot inventories) conducted by the Lower Saxony forest planning agency (Tab.1). Lower Saxony is the second largest federal state of Germany and is located in the north-western part. Every year two or three state owned forest districts are inventoried. The data come from inventories in the time interval 1996 – 2008. There are almost no consecutive inventories during this period (no longitudinal data), but all forest districts are inventoried, with the exception of a small area of the "Nationalpark Harz".

Two types of covariates are considered: tree-specific and stand- and site-specific. The tree-specific variables are tree diameter at breast height (`dbh`), tree age (`age`) and relative diameter at breast height (`rel.dbh`). The relative diameter at breast height is calculated as $\texttt{rel.dbh} = \texttt{dbh}/\texttt{mqd}$, where `mqd` is the mean quadratic diameter of a sample plot. The `rel.dbh` is a measure of the rank of a tree within all trees in a stand. A similar covariate is used by Eerikäinen[7] who used the tree's `dbh` in relation to the `dbh` of a stand's dominant tree as predictor.

The second type of covariates, site-specific, can be differentiated into causal and proxy site variables (Tab. 1). The proxy variables include altitude (`alt`), topex in-

dex (`topex.sw`), and geographic location, easting (`east`) and northing (`north`) in Gauß-Krüger coordinates referring to the 3rd meridian. The topex index describes topographic exposure and terrain morphology in the South-West direction. It is calculated as a sum of topographic exposure indices in the directions to the West, South-West and South using a distance limit of 250 meters (see, e.g., Scott and Mitchell[28]). A digital terrain model (DTM) with a resolution of 90 meters by 90 meters was used for topex calculation. A tree located on a summit is highly exposed resulting in a negative topex index. Positive topex indices belong to sites such as depressed areas or valleys rectangular-orientated in the direction of the topographic exposure. Topex indices of trees growing along the flat areas would be near zero. Since exposure to the South-West might result in drought stress, the topex index is used as a proxy for drought stress. Moreover, extra exposed sites will usually show a lower capacity of available soil water due to higher percentage of rocks and lower depth to parent rock.

The additional causal site (climate) explanatory variables are temperature sum of daily mean temperature during vegetation period (growing season) (`temp.veg`), and De Martonne's aridity index (`ari`). The aridity index is a fraction of annual precipitation in millimetres over mean annual temperature in degrees Centigrade plus ten (P/(T+10)) (De Martonne[6], Thornthwaite[32]). The aridity index is calculated for the entire year, since the precipitation during winter (non-growing season) could be partially stored by the soil. `Temp.veg` and `ari` are retrospective simulation means (Spekat *et al.*[31]) of the normal climate period 1961-1990 that were regionalized from weather stations of the German weather service (DWD) using GAM with model effects for the geographic location and altitude.

Table 1. Characteristics of Norway spruce trees and site parameters from the first cycle of all state forest enterprise inventories in Lower Saxony. 29 324 Norway spruce trees from 23 145 sample plots were observed.

	Min	25%qu.	Median	75%qu.	Max
Tree height [m]	3.7	14.6	21.8	27	47.3
dbh [cm]	7	16.8	30.5	37.9	104
Tree age [years]	20	41	54	77	199
Altitude [m]	0	90	307	475.2	947
Sum of topographic exposure indices [°x1000]					
(DTM 90mx90m resolution)	-84 560	-3108	1489	8135	89 208
Temperature sum during vegetation period [°C]	833.6	1716.4	1996.6	2196.5	2456.8
Aridity index	24.8	37	44.8	54.6	87.5

3 Modelling approach

3.1 Additive model for tree height

A difficulty with the h-d relationship is that it is not constant but rather varies from stand to stand and develops over time (Lappi[20], Mehtätalo[22]). In this paper we use an approach to modelling the longitudinal h-d relationship proposed by Schmidt[26]

that combines the principal h-d-model of Lappi[20] with (unconstrained) generalized additive model technology as a starting point. The development of the h-d model consists of three steps: 1) initial specification of the h-d relationship as a log-linear mixed model with random stand effects, 2) 'a priori' determination of non-linear model parameters, and 3) developing unconstrained and shape constrained generalized additive models for investigating potential tree and site specific effects on the original parameters of the modified Korf function (Lappi[20]).

The initial steps, 1) and 2), of the model development are briefly described in Appendix A, as the main focus of this paper is on modelling fixed effects of causal and proxy variables via shape constrained generalized additive models. One of the model requirements is to predict actual and future tree heights of a forest stand. Since every stand has different characteristics, effects of site and stand variables should be incorporated into the h-d model in combination with an age effect that describes the developmental stage of the trees within a stand. Since the proportion of structured and multi-aged stands in Lower-Saxony is constantly increasing we use single tree age as a covariate. The additional tree- and site-specific effects on the original parameters A and B of the Korf function (see appendix A) that are partially sensitive to climate change, are assumed to be non-linear. Then, based on the principal h-d model

$$\log(\mu_{ki}) = \eta_{ki} = A - B \times x_{ki}, \tag{1}$$

where $\mu_{ki} = \mathrm{E}(H_{ki})$ and H_{ki} is the height of tree i on sample plot k, the mean tree height can be modelled as a function of tree age and additional tree and site parameters using GAM (Hastie and Tibshirani[9], Wood[36])

Model h1: unconstrained additive model

$$\begin{aligned}\log(\mu_{ki}) = {} & f_{1a}(\mathtt{age}_{ki}) + f_{2a}(\mathtt{rel.dbh}_{ki}) + f_{3a}(\mathtt{topex.sw}_{k}) \\ & + f_{4a}(\mathtt{temp.veg}_{k}) + f_{5a}(\mathtt{ari}_{k}) + f_{6a}(\mathtt{east}_{k}, \mathtt{north}_{k}) \\ & + p_{0b} \times x_{ki} + p_{1b} \times \mathtt{age}_{ki} \times x_{ki} + p_{2b} \times \mathtt{alt}_{k} \times x_{ki},\end{aligned} \tag{2}$$

where x_{ki} is the re-parameterized $\mathtt{dbh}$ of tree i on sample plot k introduced at the initial step of the h-d model development (appendix A). H_{ki} is assumed to follow a Gaussian distribution. The preliminary modelling showed that Gaussian models with the log link function performed better in terms of the Akaike information criterion (AIC) than Gamma models. The model terms $f_{1a}()$–$f_{5a}()$ are unknown smooth functions of the corresponding predictor variables. We also added a spatial smooth function $f_{6a}(\mathtt{east}, \mathtt{north})$ of easting and northing, since there is a spatial correlation in the residuals. This unconstrained model assumes a linear combination of the covariate effects and due to the log-link, the effects act multiplicative exponentially on tree height. In the above mentioned case the effects of age and altitude on the slope B of the h-d curve were assumed to be linear. Now, suppose that both predictors have non-linear effects on B. Then the following model may be considered:

Model h2: GAM with varying coefficients

$$\begin{aligned}\log(\mu_{ki}) = {} & f_{1a}(\mathtt{age}_{ki}) + f_{2a}(\mathtt{rel.dbh}_{ki}) + f_{3a}(\mathtt{topex.sw}_{k}) \\ & + f_{4a}(\mathtt{temp.veg}_{k}) + f_{5a}(\mathtt{ari}_{k}) + f_{6a}(\mathtt{east}_{k}, \mathtt{north}_{k}) \\ & + p_{0b} \times x_{ki} + f_{1b}(\mathtt{age}_{ki}) \times x_{ki} + f_{2b}(\mathtt{alt}_{k}) \times x_{ki},\end{aligned} \tag{3}$$

where the non-linear effects of age and altitude are represented by the smooth functions $f_{1b}(\texttt{age})$ and $f_{2b}(\texttt{alt})$. Model h2 is referred to as a 'variable coefficient model' (Hastie and Tibshirani[10], Wood[36]).

The drawback of modelling with GAM is that it may result in insufficiently smooth effects of the covariates. Moreover, it is biologically plausible to expect that the effects of such covariates as `age`, `rel.dbh`, `topex.sw`, `temp.veg` and `ari` on the original parameter A will be monotone, which is not guaranteed for the GAM fit. Therefore, we propose to impose additional constraints on the univariate smooth terms by applying a SCAM approach (Pya and Wood[25]) described in the next subsection.

3.2 Modelling non-linear effects using SCAM

The first shape constrained model (model h3) considered is simply h1 as given in (2) with monotonicity restrictions described below on univariate smooth components,

Model h3: shape constrained additive model

$$\begin{aligned}\log(\mu_{ki}) = {} & m_{1a}(\texttt{age}_{ki}) + m_{2a}(\texttt{rel.dbh}_{ki}) + m_{3a}(\texttt{topex.sw}_k) \\ & + m_{4a}(\texttt{temp.veg}_k) + m_{5a}(\texttt{ari}_k) + f_{6a}(\texttt{east}_k, \texttt{north}_k) \\ & + p_{0b} \times x_{ki} + p_{1b} \times \texttt{age}_{ki} \times x_{ki} + p_{2b} \times \texttt{alt}_k \times x_{ki}.\end{aligned} \tag{4}$$

To distinguish from unconstrained smooths, smooth terms under monotonicity constraints are denoted by m_{ja}. The effect of `age` on the original parameter A in (1) is supposed to be increasing, since for any constant vector of model predictors, the level of the h-d curve, that is the expected $\log(H_{ki})$ of a tree with $\texttt{dbh} = 30$ cm (see Appendix A), is assumed to be increasing with increasing age. The effect of `rel.dbh` on the original parameter A is expected to be monotone decreasing, since lower values of the `rel.dbh` correspond to a lower rank of a tree within a stand. Within the same stand a tree with a lower rank has on average a greater competition pressure compared to a tree with a higher rank. While struggling for the light, suppressed trees have to invest more into height than diameter growth. Hence, trees will be taller with the value of `rel.dbh` decreasing given fixed values of `dbh`, `age` and the additional covariates. Trees with high values of `rel.dbh` are dominant trees that are usually more exposed to the wind and consequently, they have to invest more into diameter than height growth for stability reason. The effect of `topex.sw` on the original parameter A should be monotone increasing, since an exposure to the South West might result in drought stress as it was explained in section 1.1. We assume a monotone increasing netto assimilation with increasing `temp.veg` under the climatic conditions of Lower Saxony (if not limited by the deficit of other resources). The lower site indices of Norway spruce, that are partially observed on warmer sites of Lower Saxony, are, for instance, assumed to result from limited water and lower nutrient supply. The effect of `temp.veg` must not be confused with optimum curves that are observed under varying temperature values in experiments. The effect of `ari` on the original parameter A is expected to increase with increasing humidity. The lower site indices of Norway spruce that are partially observed on very humid sites in higher altitudes of the uplands, are assumed to be a result of limited temperature sums. Next, we consider the shape constrained version of the variable coefficient model h2 as model h4.

Model h4: SCAM with varying coefficients

$$\begin{aligned}\log(\mu_{ki}) = {} & m_{1a}(\texttt{age}_{ki}) + m_{2a}(\texttt{rel.dbh}_{ki}) + m_{3a}(\texttt{topex.sw}_k) \\ & + m_{4a}(\texttt{temp.veg}_k) + m_{5a}(\texttt{ari}_k) + f_{6a}(\texttt{east}_k, \texttt{north}_k) \\ & + p_{0b} \times x_{ki} + m_{1b}(\texttt{age}_{ki}) \times x_{ki} + m_{2b}(\texttt{alt}_k) \times x_{ki},\end{aligned} \tag{5}$$

where the non-linear effects of age and alt on the slope B are represented by the smooth functions $m_{1b}(\texttt{age})$ and $m_{2b}(\texttt{alt})$. Increasing effects of both $m_{1b}(\texttt{age})$ and $m_{2b}(\texttt{alt})$ on the h-d relationship are assumed in this model. It is well known that the slope of the h-d relationship increases with the developmental stage of a stand (e.g., Mehtäatalo[22]). In our investigation age serves as a covariate that describes the developmental stage of a stand. Therefore, when fitting a varying coefficient model for the age effect on B, it should be monotone increasing. However, the gradient of the actual tree heights that are predicted in applications is also affected by the dbh values that are used to initialize the model. The direction of the monotonicity of effect $m_{2b}(\texttt{alt})$ remains unspecified at this point and will be defined later based on the results of the unconstrained model variant. Moreover, for all the monotonicity constraints a validation of the assumptions will be conducted based on the corresponding unconstrained model effects.

When fitting model with monotonicity constraints on the effects of temp.veg and of ari, we noticed some possibly artificial sharp changes in the corresponding estimated smooths (see sec. 4.2). To avoid these limitations the shape constrained model is enhanced by concavity constraints on the smooth terms of temp.veg and of ari. We propose model h5 as a variable coefficient model since the performance of model h4 was shown to be better than of model h3 in terms of AIC and GCV scores.

Model h5: SCAM with concavity constraints

$$\begin{aligned}\log(\mu_{ki}) = {} & m_{1a}(\texttt{age}_{ki}) + m_{2a}(\texttt{rel.dbh}_{ki}) + m_{3a}(\texttt{topex.sw}_k) \\ & + mc_{4a}(\texttt{temp.veg}_k) + mc_{5a}(\texttt{ari}_k) + f_{6a}(\texttt{east}_k, \texttt{north}_k) \\ & + p_{0b} \times x_{ki} + m_{1b}(\texttt{age}_{ki}) \times x_{ki} + m_{2b}(\texttt{alt}_k) \times x_{ki},\end{aligned} \tag{6}$$

where now mc_{4a}, mc_{5a} are subject to both monotone increasing and concavity constraint. The following basic initial model with only age effect on the original parameters A and B was used as a reference model which all the considered models were compared with.

Model h.ref:

$$\log(\mu_{ki}) = f_{1a}(\texttt{age}_{ki}) + p_{0b} \times x_{ki} + p_{1b} \times \texttt{age}_{ki} \times x_{ki}. \tag{7}$$

3.3 Model estimation

To estimate the SCAM models (4), (5) and (6) we employ the penalized regression spline approach which can be split into two stages: representation of smooth model terms via penalized unconstrained and constrained regression splines along with specification of the smoothness/wiggliness penalty followed by model coefficients estimation by penalized log likelihood maximization along with smoothness parameter selection by minimization of a prediction error criterion such as AIC or GCV. Shape

COnstrained P-splines (SCOP-splines) (Pya and Wood[25]) were used for representation of the shape constrained smooth model terms. Since the bivariate function $f_{6a}(\texttt{east},\texttt{north})$ is a function of geographic coordinates, it was represented by a thin plate regression spline (Wood[36]). Combining the model matrices of each smooth column-wise into one model matrix and absorbing identifiability constraints result in the expression of the SCAM model as $\log(\mu_{ki}) = \mathbf{X}_{ki}\boldsymbol{\beta}$, where $\mathbf{X}$ is the combined model matrix of strictly parametric model components and smooth basis functions and $\boldsymbol{\beta}$ is a vector of unknown coefficients.

After setting the penalties on each smooth model term which are expressed as quadratic forms of the full coefficient vector, $\boldsymbol{\beta}$, the penalized log likelihood maximization can be written as $l_p(\boldsymbol{\beta}) = l(\boldsymbol{\beta}) - \boldsymbol{\beta}^T\mathbf{S}\boldsymbol{\beta}/2$, where $l(\boldsymbol{\beta})$ is the log likelihood of the model, $\mathbf{S} = \sum_k \lambda_k \mathbf{S}_k$, and $\mathbf{S}_k$ are the smooth penalty matrices enlarged by zeros to be expressed in terms of the full vector of the model coefficients, λ_k are smoothing parameters. The model coefficients, $\boldsymbol{\beta}$, are estimated by $l_p(\boldsymbol{\beta})$ maximization given the values of the vector of smoothing parameters, $\boldsymbol{\lambda}$. Optimization of the $l_p(\boldsymbol{\beta})$ is achieved by a Newton method which shares several features with a penalized iteratively re-weighted least squares scheme standard for GLM estimation. The smoothing parameter vector $\boldsymbol{\lambda}$ is estimated by minimizing the generalized cross validation score (GCV), $\mathcal{V}_g = nD(\hat{\boldsymbol{\beta}})/(n-\tau)^2$, where $D(\hat{\boldsymbol{\beta}}) = 2\left\{l_{\max} - l(\hat{\boldsymbol{\beta}})\right\}\sigma^2$ is the model deviance, $l_{\max}$ is the saturated log likelihood, and τ is the effective degrees of freedom. Confidence intervals for the model smooth terms are obtained through the distributional results for $\hat{\boldsymbol{\beta}}$. The Bayesian approach to interval estimates for the smoothing spline models proposed by Wahba[33] and Silverman[30] was extended to generalized additive models by Lin and Zhang[21] and Wood[35]. SCAM adopts this approach with an addition for establishing the approximate distribution of the exponentiated $\boldsymbol{\beta}$, resulting in the normal distribution $\tilde{\boldsymbol{\beta}}|\mathbf{y} \sim N(\hat{\tilde{\boldsymbol{\beta}}}, \mathbf{V}_{\tilde{\boldsymbol{\beta}}})$, where the expression for the covariance matrix $\mathbf{V}_{\tilde{\boldsymbol{\beta}}}$ as well as all tedious details of the model parameters estimation can be found in [25]. The SCAM approach is implemented in an R package `scam` available at http://CRAN.R-project.org/.

To fit the unconstrained models h1 and h2 we use the penalized regression spline approach (Wood[36]). The univariate functions f_{2a}–f_{5a} of (2) and (3) and also the unconstrained effects f_{1b} and f_{2b} of model h2 (3) are represented by P-splines (Eilers and Marx[8]) whereas an isotropic two dimensional thin plate regression spline (Wood[36]) was used for representation of f_{6a}. The standard penalized iteratively re-weighted least squares (PIRLS) scheme is applied for the model parameter estimation. The multiple smoothing parameter is selected by minimizing the GCV score in outer iterations. The Newton method is used for optimizing the GCV to update the smoothing parameter. The interval estimates for the component smooth functions of models h1 and h2 are obtained using the Bayesian approach to uncertainty estimation (Wahba[33], Silverman[30], Wood[37]).

4 Results

4.1 Model selection

All covariates considered in the h-d models revealed their relevance to the tree height modelling. In addition we estimated possible submodels, where one at a time smooth

effect were dropped (Tab. 2). The adjusted r^2, the percentage deviance explained and GCV scores are included into the table. The last columns of the table show the percentage of improvement in the Akaike information criterion (AIC.diff) in comparison with the reference model, h.ref, calculated as follows

$$\text{AIC.diff} = \frac{\text{AIC}_{h.ref} - \text{AIC}_{h_i}}{\text{AIC}_{h.ref}} \times 100,$$

where $\text{AIC}_{h.ref}$ is the AIC of the reference model and AIC_{h_j} of the model under consideration.

Table 2. Comparison of statistics for different height-diameter-models including the unconstrained additive model (h1), unconstrained additive model with varying coefficients (h2), shape constrained additive model (h3), shape constrained additive model with varying coefficients (h4), additive model with concavity constraints (h5) and base model with only age effects (h.ref). For all models the result of dropping single model effects on different model statistics are presented.

Model	adj r^2	Dev.expl.	GCV	AIC.diff	Model	adj r^2	Dev.expl.	GCV	AIC.diff
h1	.909	90.9	5.798	4.79	h3	.909	90.9	5.805	4.77
h1$-f_{2a}$	.907	90.8	5.883	4.49	h3$-m_{2a}$	.907	90.8	5.887	4.48
h1$-f_{3a}$	.908	90.8	5.846	4.63	h3$-m_{3a}$	.908	90.8	5.851	4.61
h1$-f_{4a}$	.908	90.8	5.842	4.64	h3$-m_{4a}$	.901	90.1	6.290	3.11
h1$-f_{5a}$	.908	90.8	5.848	4.62	h3$-m_{5a}$	.908	90.8	5.866	4.55
h1$-f_{6a}$	.900	90.0	6.324	2.99	h3$-f_{6a}$	.901	90.1	6.316	3.02
h2	.909	90.9	5.784	4.85	h4	.909	90.9	5.778	4.87
h2$-f_{2a}$	.908	90.8	5.87	4.54	h4$-m_{2a}$	.908	90.8	5.867	4.55
h2$-f_{3a}$	.908	90.8	5.832	4.68	h4$-m_{3a}$	.909	90.9	5.812	4.75
h2$-f_{4a}$	.908	90.8	5.83	4.68	h4$-m_{4a}$	.902	90.2	6.2582	3.21
h2$-f_{5a}$	.908	90.8	5.837	4.66	h4$-m_{5a}$	.908	90.8	5.838	4.66
h2$-f_{6a}$	.901	90.1	6.311	3.04	h4$-f_{6a}$	.899	89.9	6.382	2.81
h2$-f_{1b}$	.907	90.7	5.916	4.38	h4$-m_{1b}$	.907	90.8	5.895	4.45
h2$-f_{2b}$	.909	90.9	5.811	4.75	h4$-m_{2b}$	.907	90.7	5.914	4.39
h5	.907	90.7	5.877	4.52	h5$-f_{6a}$	.900	90.0	6.406	2.73
h5$-m_{2a}$	.906	90.6	5.93	4.33	h5$-m_{1b}$	.906	90.6	5.96	4.22
h5$-m_{3a}$	.907	90.7	5.865	4.56	h5$-m_{2b}$	.908	90.7	5.86	4.58
h5$-mc_{4a}$	.901	90.1	6.302	3.07					
h5$-mc_{5a}$	.907	90.7	5.860	4.58	h.ref	.885	88.5	7.309	0

The best selected model in terms of the AIC is the shape constrained varying coefficients model h4 with all initial smooth effects included. The measures of the model performance of the model h2 are only slightly worse than those of h4. Adding the variable coefficients proposed in the GAM model h2 improves the unconstrained model h1, although to a lesser extent that it does in case of the SCAMs. Dropping either of the effects from any of the five considered models increases the AIC. The other measures of the model performance also give worse results than those of the full models h1-h5, when dropping any single effects. The spatial effect improves the model significantly: e.g., the models without spatial effect result in much higher GCV than the corresponding full model (about 24% difference in the GCV in case of h2).

Introducing stricter concavity constraints in model h5 leads to a slight increase in AIC, GCV and model deviance, and correspondingly to a poorer model fit. It should be noted that there are only marginal differences in the performance criteria between the unconstrained GAM models h1 and h2, and their constrained counterparts, SCAM models h3-h5.

4.2 Interpretation of unconstrained effects and validation of their monotone counterparts

Overall, the monotonicity constraints on the univariate smooth terms result in less wiggly pattern compared to the unconstrained effects (see Fig. 2 versus Fig. 1). It should be noticed that the estimated effects of the shape constrained smooths are not centered as they are in the case of the unconstrained GAM, as different identifiability constraints were applied.

The estimated unconstrained effect of `age` on the original parameter A of model h1 is increasing with a decreasing gradient for almost the whole data range (Fig.1a). However, for high ages, above 150 years, the effect is implausibly decreasing. This pattern probably occurred due to an unbalanced data structure for the combination of site index and age. It is typical for forests and especially managed forests that 'old stands grow on poor sites', since trees need longer production periods to reach merchantable timber dimensions. The proposed h-d models cover some site factors, e.g. `temp.veg`. However, a certain proportion of the variability in site quality probably remains unquantified, which presumably leads to the implausible decreasing effect for high ages. The effect of `age` of model h3 is assumed to be monotone increasing, so that at high ages the estimated smooth tends to a constant guaranteeing a plausible pattern over the whole data range (Fig. 2a).

The estimated unconstrained effect of `rel.dbh` of model h1 (Fig.1b) supports the imposition of a monotone decreasing constraint on the function $f_{2a}(\texttt{rel.dbh})$ when constructing model h3. The confidence intervals of f_{2a} near both boundaries of the data range are very wide which suggest that the minor deviates of the estimated smooth from monotonicity are not significant. The monotone effect of `rel.dbh` of model h3 is linear with a negative slope which fulfills the imposed monotone decreasing constraint (Fig. 2b). The effect of `topex.sw` on the original parameter A is not very strong, which might be because the digital terrain model used for the topex calculation has a low resolution of 90m x 90m (Fig. 1c). At the upper boundary of the range of `topex.sw` the estimated smooth is considerably decreasing, but has a wide confidence interval. Hence, the assumption of a monotone increasing effect made in model h3 need not to be rejected (Fig. 2c).

The unconstrained effects of `temp.veg` and `ari` of model h1 (Fig. 1d, e) are both increasing over almost the whole data ranges except for the boundaries with not many data available. The corresponding constrained effect of `temp.veg` of model h3 (Fig. 2d) is monotone increasing with a weak effect below $\texttt{temp.veg} = 1400$, a stronger effect above 1500 and with a slight tendency of a decreasing gradient. The constrained effect of `ari` (Fig. 2e) is approximately linear with a steep slope below the value of `ari` around 70 and nearly constant above that value, indicating almost no further impact of increasing humidity. Compared to the other shape constrained effects the constraint effects for `temp.veg` and `ari` might be thought as still implausible to

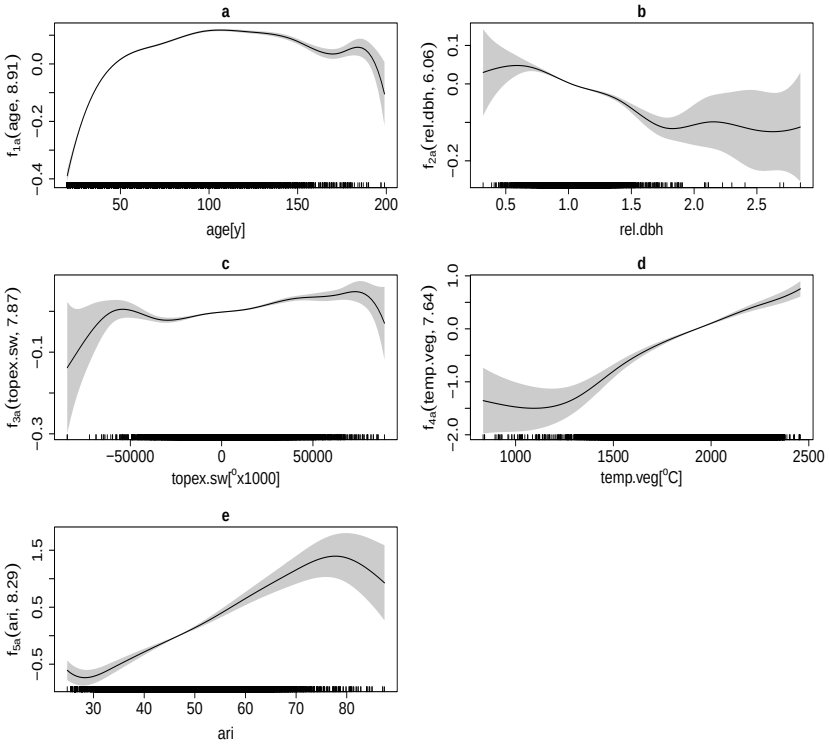

Fig. 1. The estimated smooth terms of the unconstrained model without varying coefficients, h1. The labels of the vertical axes for the univariate smooths denote the smooth model components with the corresponding covariate and estimated degrees of freedom (edf) given in brackets.

a certain extent. The weak effect of `temp.veg` at its small values can be considered as implausible, since the marginal utility of a unit increase of the temperature sum should be high especially under the condition of low temperature. Furthermore, the sharp change in the gradient of $m_{4a}(\texttt{temp.veg})$ at around 1400 seems to be artificial. The plateau part of the estimated effect of `ari` (Fig. 2e) is observed at very humid site conditions only which also could be validated as implausible. Additionally, the sharp change in the gradient seems to be spurious. Fig. 3 shows the estimated effects of the two terms with both monotone increasing and concavity constraints, mc_{4a} and mc_{5a}. This figure reveals now more convincing and reasonable smooth curves of the sum of daily mean temperature during vegetation period and aridity index. The other smooth terms of model h5 have similar effect to those of model h3.

The estimated varying coefficients smooths of the unconstrained h2 and shape constrained h4 models, are illustrated in Fig. 4 and Fig. 5 correspondingly. From an expert view the unconstrained non-linear structure of the effects of age and altitude on the original parameter B is too flexible (Fig. 4). The unconstrained effect of `age` supports the assumption of an increasing slope of the h-d curve with increasing developmental stage, since generally the effect of `age` on B is increasing. Only for high ages the effect is decreasing. The unconstrained effect of altitude, $f_{2b}(\texttt{alt})$,

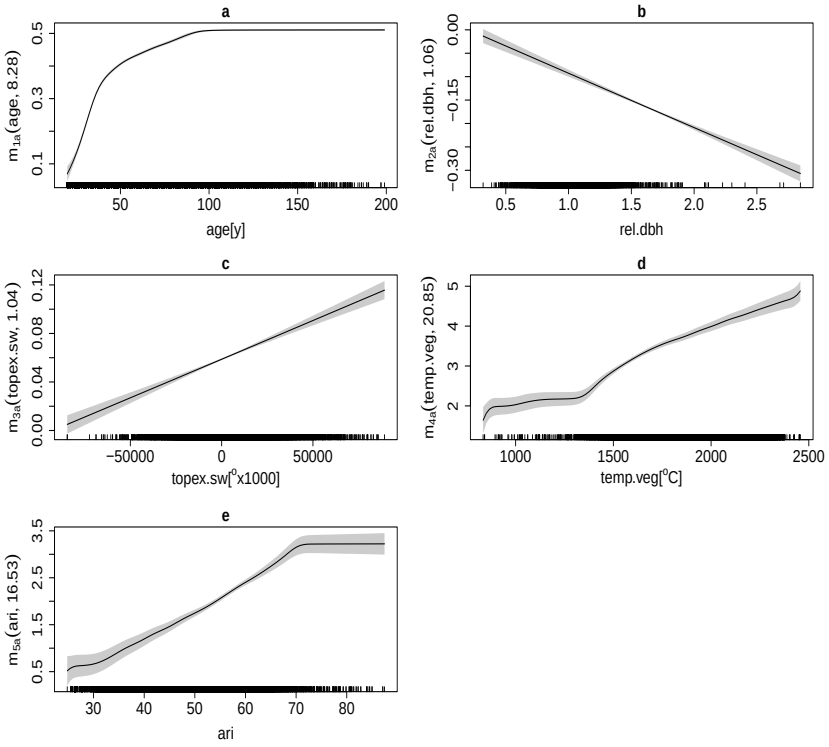

Fig. 2. The estimated shape constrained univariate smooths of model h3. The labels of the vertical axes denote the smooth terms with the corresponding covariate and edf given in brackets.

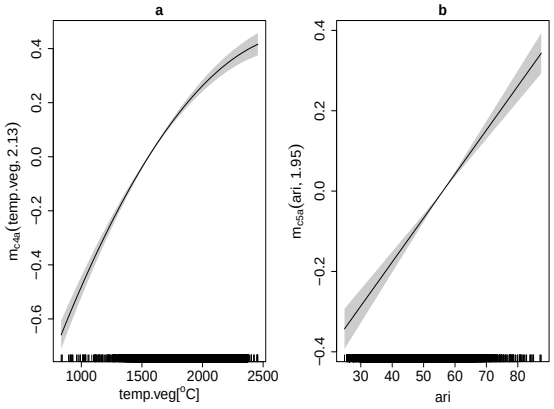

Fig. 3. Model h5: the estimated smooth terms with both monotonicity and concavity constraints.

shows a weak increasing tendency, and the overall amplitude of the effect is small in comparison with the age effect. The corresponding confidence intervals are very large.

However, the two plots of the constrained version (Fig. 5) show the plausible monotone effects of age and altitude, although the non-linear structure of $m_{2b}(\texttt{alt})$

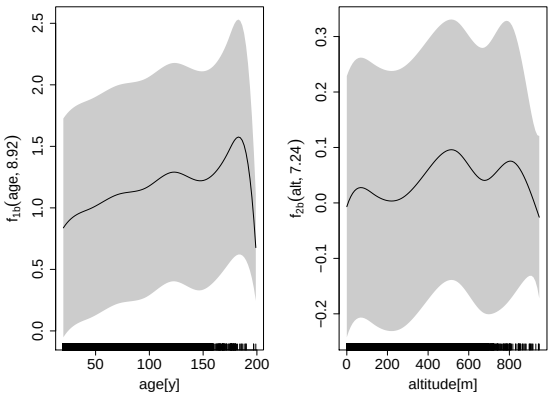

Fig. 4. The estimated varying coefficients effects of the unconstrained model h2. Left panel: estimate of $f_{1b}(\texttt{age})$; right panel: of $f_{2b}(\texttt{alt})$. The labels of the vertical axes denote the smooth terms with the corresponding covariate and edf given in brackets.

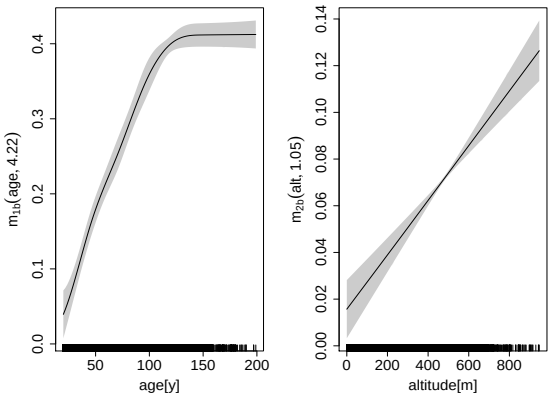

Fig. 5. The estimated shape constrained varying coefficients effects of model h4. Left panel: estimate of $m_{1b}(\texttt{age})$; right panel: of $m_{2b}(\texttt{alt})$. The labels of the vertical axes denote the smooth terms with the corresponding covariate and edf given in brackets.

is not very strong. Additional information about monotonicity of the effects narrowed the confidence intervals. The variability of the smooth estimates decreased as our beliefs in the shape of the effects were appended to the h-d relationship.

Fig. 6 shows the spatial effect of the model h5. The effect was similar for the other considered models. The spatial smooth can be interpreted as a proxy of additional predictors such as available water capacity of the soil, nutrient supply of the soil, etc., which were not at our disposal. The southern medium mountain area has better soil condition, therefore the trees are taller and slender in this part (light grey), compared to the worser conditions in the flat lands (silver) which have mainly glacial (sandy) type of soil. The conditions are even worse in terms of height growth near the North Sea coast (dark grey) due to the higher wind speed.

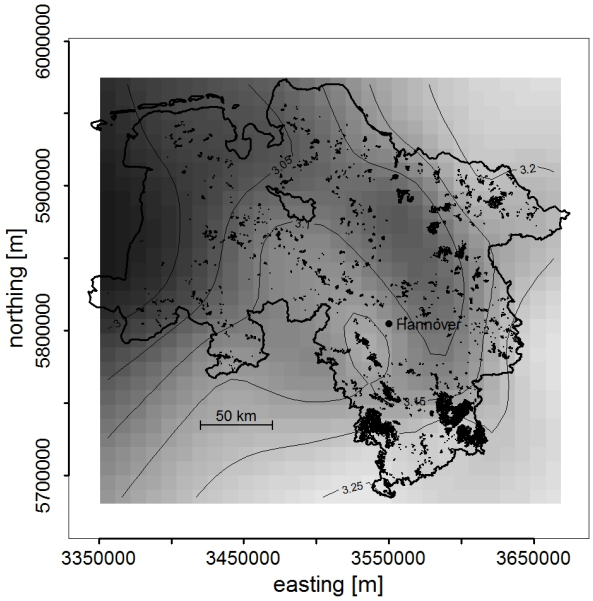

Fig. 6. An illustration of the non-linear effect of the spatial smooth $f_{6a}(\texttt{east},\texttt{north})$ of model h5, all other covariates were set to their mean values. The coordinates are Gauß-Krüger coordinates referring to the 3rd Meridian. The black dots mark the locations of inventory plots and give an impression of the state owned forest area. Light grey indicates high values of $\log(E(H_{ki}))$, silver medium, and dark grey small values.

5 Discussion

The presented framework and software allow the inclusion of a combination of shape constrained and unconstrained smooth terms of one or more covariates as well as inclusion of strictly parametric model components and varying coefficient terms. The smoothing parameter selection is integrated with the SCAM parameter estimation procedure which is a great advantage. The model estimation scheme also provides interval estimates of the smooth terms which does not incur any additional simulations.

The previous approach that was used as a starting model (Schmidt[26]) used unconstrained GAM for modelling fixed effects on tree height development which resulted in some non-monotonic effects that are scientifically implausible. Based on the foregoing justification for the monotonicity of such model components, it is claimed that the observed non-monotonicity is a result of unmeasured and unknown covariates and insufficient observations and collinearity of covariates. Not only does this limit the interpretability and usage of the scientific model, but it also leads to underestimating the variation associated with prediction of tree height. The specification of appropriate monotonicity constraints allows for an optimal combination of flexibility and expert knowledge to guarantee for a more robust modelling. This is especially useful in models using causal covariates applied to the prediction of future forest status.

The properties of the finally selected model (h5) can be summarized as follows:
1) The model comprises significant non-linear effects of covariates.
2) The plausibility of non-linear effects of covariates is enforced by the integration of

monotonicity constraints.
3) The plausibility of some non-linear effects of covariates is enforced by the additional integration of concavity constraints.
4) The implementation of expert knowledge via constraints is enabled because the original parameters of the principal h-d model have a biological meaning.
5) The present autocorrelation in the large scale data base is covered by a 2-dimensional surface fitting as a function of coordinates.
6) The causality and generality of the model for prediction purposes is improved by use of causal site variables like sum of daily mean temperature during vegetation period and index of aridity.

None of the height-diameter-models referenced in the introduction chapter cover all these aspects simultaneously. Most models assume linear effects of covariates (e.g., Lappi[20], Eerikäinen[7], Calama and Montero[3], Mehtätalo[22]). However, sometimes transformations of covariates are employed to achieve approximately linear effects (Eerikäinen[7]). At least in our case the estimated effects are significantly non-linear. Moreover, there is a qualified need for constraining the non-linear effects because particularly at the boundaries of data ranges effect pattern resulted that conflict with expert knowledge. Hofner *et al.*[11] presented a structured additive regression model for ordered categorical data of the breeding distribution of Red Kite that employs monotonic penalized splines. As in our application they emphasize the optimal combination of flexibility and expert knowledge that is enabled by use of the monotone P-Splines. Schmidt *et al.*[27] modelled non-linear effects of covariates via penalized regression splines but monotonicity resulted directly from the model fit without specifying constraints. Moreover, since the original parameters of their principal height-diameter model ("Näslund function", see e.g. Kangas and Maltamo[17]) have no clear biological meaning, there would not be biological expert knowledge that could be included in the model selection as in our case. Data from large scale forest inventories typically show spatial autocorrelation of residuals that could not be related to fixed effects when conducting regression analyses. In h-d-modelling often a mixed model approach is used to assess between-plot covariance structures (Jayaraman and Lappi[15], Mehtäatalo[22]). However, in this approach it is disregarded that random effects of sample plots are usually not spatially independent themselves, but show some similarity due to effects of unobserved covariates like soil properties. As a solution to the problem Brezger and Lang[2] separate the overall spatial trend into a spatially correlated (structured) and an uncorrelated (unstructured) effect. The latter one accounts for local correlation, in the case of h-d modelling of trees of the same sample plot or stand. Only the unstructured spatial effect should be modelled by uncorrelated random effects. Structured spatial effects can be modelled via a Gaussian Markov random field, i.e. spatially correlated random effects are estimated for discrete spatial units (Kammann and Wand[16]) or via 2-dimensional surface fitting by applying specific generalized additive models based on e.g. penalized regression splines with thin plate basis (Wahba[34], Wood[36]). We use the latter approach since our observations are exactly localized via coordinates. More simple approaches for describing structured spatial effects in h-d-models are dummy variables for territorial units (Huang *et al.*[13], Jayaraman and Lappi[15], Calama and Montero[3]) or univariate linear effects of coordinates (Hökkä[12], Mehtäatalo[22]). However, these approaches disregard either the large scale autocorrelation between units or would as-

sume at least in our case unrealistically simple pattern of the structured spatial effect (Fig. 6). A more detailed analysis is presented by Nanos *et al.*[24], who fitted ordinary mixed models but applied Kriging methods to the estimated random effects to account for spatial correlation. Hence, a structured spatial effect is modeled but in a 2 step procedure. We did not model random effects on plot level to account for local, hence unstructured spatial effects because for most sample plots only one height was measured (Table 1). Causal site variables have not been widely used as predictors in h-d modelling. Many approaches use no site variables at all or only proxy site variables like altitude or coordinates (Hökkä[12]). Huang *et al.*[13] use ecoregions as a proxy for large scale site conditions. Mehtäatalo[22] combined causal variables like a longtime mean cumulative temperature sum and a soil type classification with proxy site variables as we did. For this specific application of modelling the height-diameter relationship of Norway spruce, we have shown that the implementation of shape constrained smooths ensures a robust biologically meaningful interpretation with only marginal loss of prediction accuracy and no increase in prediction bias.

Acknowledgements

The forest data were provided by the Lower Saxony forest planning agency. NP has been partly funded by the EPSRC grant EP/K005251/1.

References

1. A. Agresti. *Categorical data analysis*, volume 359. John Wiley and Sons, 2002.
2. A. Brezger and S. Lang. Generalized structured additive regression based on Bayesian P-splines. *Computational Statistics & Data Analysis*, 50(4), 967–991, 2006.
3. R. Calama and G. Montero. Interregional nonlinear height-diameter model with random coefficients for stone pine in Spain. *Can. J. For. Res.*, 34, 150–163, 2004.
4. F. Castedo-Dorado, U. Diéguez-Aranda, M. Barrio Anta, M. Sánchez Rodríguez, and von Gadow K. A generalized height-diameter model including random components for radiata pine plantations in northwestern Spain. *Forest Ecology and Management*, 229(1-3), 202–213, 2006.
5. R.O. Curtis. Height-diameter and height-diameter-age equations for second-growth Douglas-fir. *Forest Science*, 13(4), 365–375, 1967.
6. E. De Martonne. Une nouvelle fonction climatologique: l'indice d'aridité. *La Météorologie*, 2, 1926.
7. K. Eerikäinen. Predicting the height-diameter pattern of planted Pinus kesiya stands in Zambia and Zimbabwe. *Forest Ecology and Management*, 175, 355–366, 2003.
8. P.H. Eilers and B.D. Marx. Flexible smoothing with B-splines and penalties. *Statistical Science*, 11, 89–121, 1996.
9. T. Hastie and R. Tibshirani. *Generalized Additive Models*. Chapman & Hall, 1990.
10. T. Hastie and R. Tibshirani. Varying-coefficient models. *Journal of the Royal Statistical Society: Series B*. 55(4), 757–796, 1993.
11. B. Hofner, J. Müller and T. Hothorn. Monotonicity-constrained species distribution models. *Ecology*. 92(10), 1895–1901, 2011.
12. H. Hökkä. Height-diameter curves with random intercepts and slopes for trees growing on drained peatlands. *Forest Ecology and Management*, 97, 63–72, 1997.
13. S. Huang, D. Price and S.J. Titus. Development of ecoregion-based height-diameter models for white spruce in boreal forests. *Forest Ecology and Management*, 129, 125–141, 2000.

14. S. Huang, S.J. Titus and D.P. Wiens. Comparison of nonlinear height-diameter functions for major Alberta tree species. *Can. J. For. Res.*, 22, 1297–1304, 1992.
15. K. Jayaraman and J. Lappi. Estimation of height-diameter curves through multilevel models with special reference to even-aged teak stands. *Forest Ecology and Management*, 142, 155–162, 2001.
16. E.E. Kammann and M.P. Wand. Geoadditive models. *Journal of the Royal Statistical Society: Series C*,52, 1–18, 2003.
17. A. Kangas and M. Maltamo. Anticipating the variance of predicted stand volume and timber assortments with respect to stand characteristics and field measurements. *Silva Fennica*, 36(4), 799–811, 2002.
18. E. Kublin, J. Breidenbach and G. Kändler. A flexible stem taper and volume prediction method based on mixed-effects B-spline regression. *European Journal of Forest Research*, 132(5-6), 983–997, 2013.
19. J. Laasasenaho. Taper curve and volume functions for pine, spruce and birch. *Communicationes Instituti Forestalis Fenniae*, 108(74), 1982.
20. J. Lappi. A longitudinal analysis of height/diameter curves. *Forest science*, 43(4), 555–570, 1997.
21. X. Lin and D. Zhang. Inference in generalized additive mixed models by using smoothing splines. *Journal of the Royal Statistical Society: Series B*, 61381–400, 1999.
22. L. Mehtätalo. A longitudinal height diameter model for Norway spruce in Finland. *Can. J. For. Res.*, 34(1), 131–140, 2004.
23. L. Mehtätalo. Height-diameter models for Scots pine and birch in Finland. *Silva Fennica*, 39(1), 55–66, 2005.
24. N. Nanos, R. Calama, G. Montero, and L. Gil. Geostatistical prediction of height/diameter models. *Forest Ecology and Management*, 195(1-2), 221–235, 2004.
25. N. Pya and S.N. Wood. Shape constrained additive models. *Statistics and Computing*, 25(3), 543–559, 2015.
26. M. Schmidt. Ein standortsensitives, longitudinales Höhen-Durchmesser-Modell als eine Lösung für das Standort-Leistungs-Problem in Deutschland. Available from $http$: $//sektionertragskunde.fvabw.de/and2010/Tag2010\_14.pdf$, 2010.
27. M. Schmidt, A. Kiviste, and K. Gadow. A spatially explicit height-diameter model for Scots pine in Estonia. *European Journal of Forest Research*, 130, 303–315, 2011.
28. R. Scott and S. Mitchell. Empirical modelling of windthrow risk in partially harvested stands using tree neighbourhood and stand attributes. *Forest Ecology and Management*, 218, 193–209, 2005.
29. M. Sharma and J. Parton. Height-diameter equations for boreal tree species in Ontario using a mixed-effects modeling approach. *Forest Ecology and Management*, 249, 187–198, 2007.
30. B.W. Silverman. Some aspects of the spline smoothing approach to nonparametric regression curve fitting. *Journal of the Royal Statistical Society: Series B*, 47, 1–52, 1985.
31. A. Spekat, W. Enke, and F. Kreienkamp. Neuentwicklung von regional hoch aufgelösten Wetterlagen für Deutschland und Bereitstellung regionaler Klimaszenarios auf der Basis von globalen Klimasimulationen mit dem Regionalisierungsmodell WETTREG auf der Basis von globalen Klimasimulationen mit ECHAM5/MPI-OM T63L31 2010 bis 2100 fr die SRES-Szenarios B1, A1B und A2, 2007.
32. C.W. Thornthwaite. The climates of North America: according to a new classification. *Geographical Review*, 21(4), 633–655, 1931.
33. G. Wahba. Bayesian confidence intervals for the cross validated smoothing spline. *Journal of the Royal Statistical Society: Series B*, 45, 133–150, 1983.
34. G. Wahba. *Spline models for observational data*. Philadelphia: SIAM, 1990.
35. S.N. Wood. Modelling and smoothing parameter estimation with multiple quadratic penalties. *Journal of the Royal Statistical Society: Series B*, 62, 413–428, 2000.

36. S.N.Wood. *Generalized Additive Models. An Introduction with R*. Chapman & Hall, 2006.
37. S.N.Wood. On confidence intervals for generalized additive models based on penalized regression splines. *Australian and New Zealand Journal of Statistics*, 48(4), 445–464, 2006.

A Initial model development

The following briefly describes the initial steps of the h-d model development proposed by Schmidt[26]. A data base for the whole of Germany was applied for this 'a priori' estimation of specific model parameters. As a starting point, the following height-diameter model known as the Korf function is used for the description of the relationship between tree height and diameter (Lappi[20]):

$$\log(H_{ki}) = A_k - B_k \left(\mathtt{dbh}_{ki} + \lambda\right)^{-C} + \epsilon_{ki}, \tag{8}$$

where H_{ki} is a height of tree i on sample plot k, $\mathtt{dbh}_{ki}$ is the diameter at breast height of tree i on sample plot k; ϵ_{ki} are Gaussian errors; A_k, B_k, λ, and C are parameters of the model. Height-diameter curves differ for different plots and for different points of time, however, the measurement occasion effect was not included in the considered model. The reason behind it was the lack of computer memory as the whole data base contains several thousands of sample plots with on average only very few height measurements per measurement occasion. Therefore, the model parameters vary only over plots. Since parameters A_k and B_k are highly correlated, it is suggested to reparameterize $\mathtt{dbh}$ as follows (Lappi[20]):

$$x_{ki} = \frac{(\mathtt{dbh}_{ki} + \lambda)^{-C} - (30 + \lambda)^{-C}}{(10 + \lambda)^{-C} - (30 + \lambda)^{-C}}.$$

The model (8) can now be written as

$$\log(H_{ki}) = A_k - B_k x_{ki} + \epsilon_{ki}, \tag{9}$$

where A_k and B_k are not highly correlated and have biological meanings. A_k is the expected value of the log height of trees with $\mathtt{dbh} = 30$ cm for sample plot k; and B_k is the expected value of the difference in the $\log(H_{ki})$ between trees of $\mathtt{dbh} = 30$ cm and 10 cm for sample plot k. These interpretations are important since the parameters will be described as functions of additional tree, stand and site-level covariates in the second step of the model development.

The model (9) is linear with respect to A_k and B_k. Taking into consideration the random stand effect, these parameters can be represented at the first stage as $A_k = A + \alpha_k$, $B_k = B + \beta_k$, where A and B represent fixed effects which have to be estimated; α_k and β_k are random stand level effects with zero means and constant variance. It may be noted that (9) is overparameterized. Moreover, a model of that specification cannot be linearized with respect to the parameters λ and C. Therefore, it is suggested firstly to estimate λ and C. These parameters were selected by testing a variety of combinations of λ and C when fitting a linear mixed model

$$\log(H_{ki}) = A - Bx_{ki} + \alpha_k + \beta_k x_{ki} + \epsilon_{ki},$$

The combination of the parameters with the lowest error variance was $\lambda = 7$ and $C = 1.225$. There were no clear trends found in λ and C over different mean stand age and the models were not very sensitive to the value C.

Methods for estimating the number of older high-risk drug users

Clive Richardson[1] and Argyro Antaraki[2]

[1] Department of Economicc and Regional Development, Panteion University of Social and Political Sciences, Athens, Greece
(E-mail: crichard@panteion.gr)
[2] Greek REITOX Focal Point, University Mental Health Research Unit, University of Athens Medical School
(E-mail: aandaraki@ektepn.gr)

Abstract. It is important to know the size of the population of high-risk drug users (HRDU), for whom services must be provided. As direct ascertainment (e.g. by a general population survey) is impossible, indirect methods of estimation are employed, notably capture-recapture methods. These are based on identifying individual users in one or more sources of data (such as treatment services or records of arrests by the police). The data take the form of an incomplete contingency table. We examine issues in applying indirect methods to the particular problem of estimating the number of older HRDU, who are now becoming an important segment of the population for which special provision must be made by planners. Capture-recapture analysis by fitting Poisson log-linear models based on the analysis of incomplete contingency tables may face difficulty because of relatively sparse data, especially when separate estimates are required for specific subgroups. For older drug users in Greece, this is overcome in the present analysis by fitting a single model to data for each year from 2004 onwards and both age groups (50-59 years and 60+). We also examine the application of single-source methods (fitting truncated Poisson distributions), multiplier methods and multiple indicator methods.
Keywords: incomplete contingency tables; capture-recapture method; Poisson regression; truncated Poisson distribution; multiple indicator methods

1 Background

Because of the importance of the problem of drug use, the European Union maintains the European Monitoring Centre for Drugs and Drug Addiction (EMCDDA: www.emcdda.europa.eu) to report on trends and developments in the drug situation across the EU. One of the five Key Indicators on which its reporting is based is the High-Risk Drug Use Indicator, which aims to provide numerical estimates of how many high-risk drug users (HRDU) there were in

16th ASMDA Conference Proceedings, 30 June – 4 July 2015, Piraeus, Greece

each Member State in a given year. 'High-risk' use is defined by the EMCDDA as 'recurrent drug use that is causing actual harms (negative consequences) to the person (including dependence, but also other health, psychological or social problems), or is placing the person at a high probability/risk of suffering such harms'. It is important to have good estimates of the prevalence of HRDU in order to monitor the drug-use problem and plan the appropriate provision of treatment and other services.

Western societies are not used to seeing many old drug users. However, not many people succeed in stopping drug use, which means that rapidly increasing numbers of older HRDU are appearing now, as the people who started drug use as adolescents or young adults in the 1970s and 1980s are now over 50 or 60 years old. After many years of drug use, these people tend to have multiple severe health problems. They place heavy demands on health care services which may be different from the needs of younger adults. It is therefore becoming increasingly important to have separate estimates of the size of the population of HRDU in older age groups, whereas the EMCDDA continues to place the emphasis on younger users by reporting estimates in the age ranges 15-24, 25-34 and 35-64 years.

The size of a hard-to-reach population such as HRDU cannot be ascertained directly (e.g. by a general population survey). Indirect methods must be employed. In particular, capture-recapture methods are often used, as described in the following section.

2 Estimation by capture-recapture methods

Capture-recapture or multiple records methods are based on analyzing the "captures" of individual drug users in one or more sources of data, usually within one calendar year. Examples are attending a treatment service or being arrested by the police. It is necessary to be able to identify the individual and this is usually done by employing an anonymized identification code. Given k sources, let an individual capture history be denoted by the k-vector $\boldsymbol{x}$ where x_i takes the value 1 if the individual was recorded in source i, 0 otherwise. The data on all recorded individuals form an incomplete 2^k -1 contingency table $\boldsymbol{C}$. An individual who has been recorded in at least one source within the reference year appears in one of the cells of this table. Members of the population of drug users who were not recorded in that year, corresponding to $\boldsymbol{x} = (0,0\ldots0)$, make up the cell that is missing from the full 2^k table. An estimate of this "hidden population" can be extrapolated from a model fitted to the observed cells of the table $\boldsymbol{C}$.

Model fitting is simplified because of the well-known equivalence between multinomial and Poisson log-linear models - see, for example, Lang [1]. A standard package can be used to fit a Poisson regression model to the observed

cell counts, where the linear predictor will include main effect terms for presence (capture) in the separate sources as well as possible interaction terms between sources. Let the fitted mean for cell *J* corresponding to capture history $\boldsymbol{x}_J$ be

$$\ln \hat{\mu}_J = \hat{\beta}' z_J$$

where the vector $\boldsymbol{z}$ denotes $\boldsymbol{x}$ augmented by any necessary interaction terms. Then, because all the elements of $\mathbf{z}_K$ are zero in the missing cell *K*, an estimate of the hidden population is obtained as

$$\hat{\mu}_K = e^{\hat{\beta}_0}$$

where $\hat{\beta}_0$ is the estimated constant term in the linear predictor. Frequentist confidence intervals may be obtained using the usual standard error or alternatively by a profile likelihood method (Regal and Hook [2]). Modelling and estimation by a Bayesian approach can be carried out very conveniently using an R package provided by Overstall and King [3].

The essential idea of capture-recapture modelling is to exploit the information that is provided by the overlaps between data sources: that is, the numbers of individuals who appear in more than one source. If the overlaps are very small, capture-recapture modelling will be unsuccessful. Inspection of the data from the three sources that are employed in Greece to obtain annual HRDU estimates showed a severe problem for the older age groups that are the focus of interest here. In the 50-59 years age group, the total number of individuals who appeared in more than one source in the same year was never more than four until 2010 and never exceeded ten. In the 60+ age group, the total of the overlaps was zero or one in every year. Consequently, separate estimation in each year was impossible.

To resolve this problem, the five-way contingency table with dimensions 2 x 2 x 2 x 2 x 10 was constructed, corresponding to the three sources (present/absent), age (50-59 and 60+) and year (2004 up to 2013). Twenty cells are missing, corresponding to the hidden population in each age group in each year. Initial examination of values of the deviance, AIC and parameter estimates suggested the model

Main effects + S2.S3 + S1.Year + Year.Age

which contains, in addition to the five main effects, the 2-way interactions between Sources 2 and 3 (this interaction is consistently found in the separate fits to annual data for younger age groups), between Source 1 and Year, and between Year and Age. Values of the deviance from fitting selected Poisson log-linear models to test the significance of the remaining interaction terms are shown in Table 1. Although the contingency table is sparse, it is generally accepted that the chi-squared approximation holds for changes in deviance between nested models. Consequently, the S2 by S3 and S1 by Year interactions should definitely be included in the model, but the case for Year by Age is

marginal (P = 0.03). The Bayesian analysis (Overstall and King [3]) attached highest posterior probability to the model without this interaction (0.29 compared to 0.21 for the model that included it). Its inclusion makes very little difference to fitted values and their confidence intervals. Subsequent results are shown from the model that includes it.

Table 1. Changes in deviance on omitting interaction terms from the basic model identified for the five-way incomplete contingency table.

Basic model	Term omitted	Deviance	d.f.	Change in deviance*	d.f.
Main + S2.S3 +S1.Year + Year.Age		101.4	107		
	-S2.S3	118.9	108	17.5	1
	-S1.Year	143.1	116	41.7	9
	-Year.Age	119.9	116	18.4	9

*from basic model

Table 2 shows annual estimates of the total population of HDRU in the two age groups. As might be expected given the generally low frequencies, the confidence intervals are wide, with the upper limit typically twice as large as the lower. The hidden population is much greater than the observed number of individuals; using the point estimates, the ratio of hidden to observed is about 6:1 after the first two years, increasing to 9:1 in 2013. In separate annual estimates for all age groups, the corresponding ratio is about 4:1.

Table 2. Estimated total HDRU population sizes (observed plus hidden) by age group and year, with 95% confidence intervals in parentheses.

	50-59		60+	
Year	Observed	Total	Observed	Total
2004	50	123 (72 - 287)	9	22 (12 - 58)
2005	48	180 (100 - 385)	4	15 (7 – 45)
2006	78	462 (291 - 772)	15	89 (50 - 171)
2007	70	521 (326 – 866)	10	74 (39 - 154)
2008	72	559 (355 - 910)	17	132 (75 - 245)
2009	137	1312 (899 - 1948)	20	191 (115 - 330)
2010	178	1402 (974 - 2058)	22	173 (107 - 292)
2011	228	1641 (1157 - 2376)	17	122 (74 - 213)
2012	254	1582 (1123 - 2283)	20	125 (78 - 210)
2013	220	2253 (1596 - 3221)	28	287 (182 - 464)

3 Single source methods

The capture-recapture method as presented above does not use information on repeated captures of an individual in the same source, such as repeated arrests within the same year. If only one source exists, however, it may be possible to use this information to estimate population size. An obvious approach is to assume that the number of captures of an individual follows a Poisson distribution. Let f_i be the frequency of individuals captured exactly *i* times. The zero class, with frequency f_0, is unobservable – the hidden population. Let the unknown total population size be *N* and $n = f_1 + f_2 + \ldots$ the number of individuals observed. Then a Horvitz-Thompson estimator of *N* is in general

$$\hat{N} = \frac{n}{1 - p_0} \tag{1}$$

where p_0 is the probability of no captures, which is $e^{-\mu}$ for the Poisson distribution. An estimate of μ could be obtained by fitting the zero-truncated Poisson distribution to the counts $\{f_i : i = 1, 2\ldots\}$ but an alternative is usually adopted. Writing $Po(i \mid \mu)$ for the Poisson probability of exactly *i* captures, observe that

$$Po(i+1 \mid \mu) / Po(i \mid \mu) = \mu / (i+1)$$

This suggests the simple estimator $(i+1) f_{i+1} / f_i$ of μ for suitable *i*. In particular, taking $i = 1$ and substituting in equation (1) gives Zelterman's estimator

$$\hat{N}_Z = \frac{n}{1 - \exp(-2 f_2 / f_1)}$$

of the population size *N* (Zelterman [4]). The advantage of this estimator is robustness against heterogeneity in the distribution of the number of captures. Bohning & van der Heijden [5] show how covariates can be introduced into the estimation.

Table 3 gives estimates obtained using Zelterman's estimator for the year 2013. The numbers of individuals aged over 45 years with more than one capture were too small to allow separate estimation. Point estimates are a little higher than the corresponding estimates obtained from the three-sample capture-recapture analysis that is usually applied in order to obtain the annual estimates for Greece. For example, the capture-recapture estimate of the total population is 17415 (15316 – 19883). The confidence intervals of the single-source estimates are much wider than those derived from the capture-recapture analysis.

Because of the wide confidence intervals, there is no reason to use the single-source estimates in place of the capture-recapture ones in general. However, there is interest in using them in cases where reasonable capture-recapture estimates have not been obtained. As noted above, this is particularly liable to

happen when the overlaps between sources are low. For this reason, it has not been possible so far to obtain separate annual estimates of population sizes for older HRDU. However, the same problem arose with the single source estimates: only five out of 280 people aged 45 years and above were recorded more than once.

Table 3. Estimated numbers $\hat{N}_Z$ of HRDU (users of any opioids) in Greece in 2013, obtained by Zelterman's method, with 95% confidence intervals. (Data: Greek Reitox Focal Point.)

Population	n	f_1	f_2	$\hat{N}_Z$	95% c.i.
Total	1737	1649	82	18348	14392 – 22304
Gender					
Male	1453	1382	66	15951	12116 – 19785
Female	284	267	16	2514	1286 – 3740
Age*					
15-24	98	86	12	402	181 – 624
25-34	770	718	46	6386	4552 – 8220
35-44	591	570	19	9164	5051 – 13277
Place					
Athens	690	668	21	11323	6488 – 16158
Thessaloniki	361	331	27	2378	1490- 3267
Other	686	650	34	6886	4581 - 9191

*For age groups for which estimates could be obtained

4 Other methods of estimation

Consider a two-source capture-recapture analysis. Let n_1 be the number of individuals captured by the first source and n_2 the number captured by the second, while n_{12} denotes the number captured by both. Then, the fraction of the total population N that has been captured in the first source is of course n_1/N. Similarly the proportion of the individuals from the second source who have also been captured in the first is n_{12}/n_2. Under the assumption of independence of the two sources, these two proportions can be equated, giving the Petersen estimator of population size

$$\hat{N}_P = \frac{n_1 n_2}{n_{12}}$$

in which the size of Source 1 has been multiplied up the factor n_2/n_{12} in order to estimate N. This estimator is rarely applied to the estimation of the numbers of drug users because the independence assumption, which cannot be checked, is

unlikely to hold true. However, it connects to a range of other *multiplier methods* which are sometimes used (EMCDDA [6]).

For example, suppose that Source 1 comprises the HRDU who died in the reference year: let this number be *D*. Thus the annual mortality rate is *D/N*. If it is known from other studies (for example, a follow-up study of a cohort of users) that a fraction *d* of HRDU dies annually, then equating the fractions *d* and *D/N* can be used as above to give the *mortality multiplier 1/d* and the final estimator

$$\hat{N}_D = \frac{D}{d}$$

In Greece, drug-related deaths have fallen from a peak of D = 343 in 2005 to only 77 in 2012. Assuming a value of 1.5% for d , which is comparable to values that have been reported from other countries, would give an estimated HRDU population of 22867 in 2005. This is broadly compatible with other estimates. However, the corresponding estimate of 5133 for 2012 is unbelievable, so consistency can be obtained only if *d* has fallen substantially. This is probably true, because of the effect of methadone substitution programmes, for example, but no current estimate of *d* is known. Therefore this method cannot be applied in Greece. Furthermore, the low frequencies involved would lead to large standard errors of estimation. The problem would become even worse in subgroups, such as the older users.

Another method which has the potential to overcome deficiencies in data is the *multiple indicator method* (EMCDDA [6]).This regression method can be used to obtain estimates of the number of HRDU in cities or other geographical areas for which capture-recapture or other estimates have not been obtained, as long as they have been obtained in some places and given that there exists a set of predictors that are expected to be correlated geographically with high-risk drug use (for example, the unemployment rate and other socio-economic indicators, and crime rates). Regressing the rates of HRDU on the predictors in the set of places with known rates, gives an equation which can be used to predict HRDU rates in the places with unknown rates. This method could potentially be applied in Greece to provide estimates for cities or regions. The problem is that, so far, separate estimates have been obtained only for Greater Athens and Thessaloniki, which is insufficient for the application of the method. Attempts to estimate HRDU numbers in, say, Iraklion and elsewhere have not yet been successful, because of the problem of low frequencies as mentioned earlier.

Conclusions

Estimating the size of the population of HRDU is a matter of great practical importance to which statistical modelling makes an essential contribution. The relevant data are not only difficult to collect, but are often sparse, especially

when the focus falls on particular subgroups of the population, such as HDRU in a particular city or in older age groups. Although a wide variety of statistical methods has been proposed in the literature, the lack of data may make them unusable or lead to very imprecise estimates.

The capture-recapture modelling employed in the present paper produced reasonable estimates for the older HDRU who have not previously been considered much but are becoming increasingly important. The method adopted here enabled results to be derived for the 60+ age group, which could not have been obtained otherwise. The results indicate that there are likely to be at least 2000 HRDU over the age of 50 years in Greece. They represent more than 10% of the total population and can be expected to continue to increase substantially in the next few years.

Acknowledgment

Professor Richardson's research was supported by the THALIS research programme "ICILAS: Investigating Crucial Interdisciplinary Linkages in Ageing Societies" in Panteion University, co-funded by the European Union and the Hellenic Ministry of Education.

References

1. J.B. Lang. On the comparison of multinomial and Poisson log-linear models. Journal of the Royal Statistical Society, Series B, 58, 253-266, 1996.
2. R.R. Regal and E.B. Hook. Goodness-of-fit based confidence intervals for estimation of the size of a closed population. Statistics in Medicine 3, 287-291, 1984.
3. A.M. Overstall and R. King. Conting: An R package for Bayesian analysis of complete and incomplete contingency tables. Journal of Statistical Software, 58(7), 1-27, 2014.
4. D. Zelterman. Robust estimation in truncated discrete distributions with applications to capture-recapture experiments. Journal of Statistical Planning and Inference, 18, 225-237, 1988.
5. D. Bohning and P.G.M. van der Heijden. A covariate adjustment for zero-truncated approaches to estimating the size of hidden and elusive populations. Annals of Applied Statistics, 3(2), 595-610, 2009.
6. EMCDDA. Guidelines for the prevalence of problem drug use (PDU) key indicator at national level. EMCDDA, Lisbon, 2004.

Decision trees as a Classification Technique in Manpower Planning

Evy Rombaut[1] and Marie-Anne Guerry[2]

[1] Department of Business Operations and Technology, Faculty of Economic and Social Sciences & Solvay Business school, Vrije Universiteit Brussel, Pleinlaan 2, 1050 Etterbeek, Belgium. (E-mail: erombaut@vub.ac.be)
[2] Department of Business Operations and Technology, Faculty of Economic and Social Sciences & Solvay Business school, Vrije Universiteit Brussel, Pleinlaan 2, 1050 Etterbeek, Belgium. (E-mail: maguerry@vub.ac.be)

Abstract. In manpower planning mathemathical models, based on estimations of transition probabilities between groups of employees, are used to predict future staff compositions. Although the quality of the model depends on the division of the staff in groups, this classification has been neglected in literature.
The present paper investigates whether decision tree learning can be used as a classification technique in manpower planning. The paper presents a method for dividing the population according to the available data in the HR database. The approach will improve predictions and validity of the model. Another advantage of our developed method is that it can be automated and implemented in software.
Implementation of the method will make it possible for HR departments in a company to use the models in practice. The approach will be illustrated on a real life human resources database using statistical software such as R and WEKA.
Keywords: Decision trees, Manpower Planning, Homogeneity in groups, Human Resources.

1 Introduction

In the domain of Human Resources transition behavior of employees is an important topic of study. In [12] two different approaches from Schneider and Pfeffer are being discussed on how to analyze behaviour of employees. Schneider's emphasis is on using an understanding of individuals as a route to explaining phenomena in a company. Other theorists, like Pfeffer, say that the demographic compositions of organizations influence many behavioural patterns such as job transfers and promotions. Pfeffer considers that explanatory factors are age, sex, race, socio-economic background and religion. Pfeffer provides a discussion of the organization-level constructs of homogeneity and cohesiveness and patterns of employee flows. In psychological and sociological studies the total population is divided in groups, according to various characteristics, e.g. grade, age, sex,... For example, the population can first be split in men and women, afterwards different categories can be made according to age. It is said that these groups are homogeneous because of personal attributes of the members [12]. In manpower planning aggregate analyses are made as well, the definition of homogeneity in the context of manpower planning is however different.

16th ASMDA Conference Proceedings, 30 June – 4 July 2015, Piraeus, Greece

Manpower planning is a facet of Human Resources Management based on mathematical models which are used to analyze staff within a certain firm. It provides long term decision support regarding recruitments, redundancies and internal staff mobility [1]. These mathematical models are used to predict future staff compositions and make an aggregate analysis based on distinctive groups in a company. In manpower planning these groups are called states.
A distinction is made between a push and a pull model since there can be several underlying reasons why an employee would transfer to an other state. For example, an employee can transfer to an other state because of a vacancy. Here the employee is pulled towards another state, hence the name pull model. On the other hand, if the transfer is due to for example an automatical flow such as tranferring to a higher category because of seniority of the employee, whether or not there is a vacant position, we say that the employee is pushed towards an other state. In practice, a mix of push and pull transitions might occur in the same personnel system [9]. Therefore De Feyter [8] introduced the mixed push-pull manpower model, which allows modelling both types of flows within a firm.
In the present paper we will restrict us to push models that are also time-homogeneous, i.e. the flows among groups are characterized by time independent transition probabilities. In these models the expected number of employees at a certain time depends on the estimated transition probabilities.
For each state in the system transition probabilities are estimated. A division of the personnel system in grades might not be sufficient to lead to a 'good' estimator. The goal is to get homogeneity with respect to the considered flows. Several approaches to obtain homogeneity are discussed in literature [1,3,7,9,17]. Homogeneity can also be obtained by dealing with heterogeneity. There are two types of heterogeneity which should be considered: heterogeneity within a group and heterogeneity between groups. Ugwuowo and McClean give a review of methods that incorporate population heterogeneity into manpower modelling in [17]. They put forward that it is not always possible nor convenient to use a method of disaggregation. Since we may not know what the individual causal factors are and even if we do know, we may not have the proper data on each subgroup. Therefore they apply a semi-Markov model to examine sources of heterogeneity within groups.
The problem arises of how to deal with heterogeneity due to latent sources, i.e. sources for which there are no observations available. Guerry [9] introduces a hidden Markov model that takes into account the specificity of a manpower system and the fact that there are both observable and latent sources of heterogeneity in such a system. A distinction is made between deterministic and stochastic variables, the first kind are variables that do not change over time or that are determined by their evolution over time such as gender or age, the second are variables based on probabilities such as position in the company. To make an accurate prediction for the stochastic variables the population should be divided in homogeneous subgroups in order to increase intra-homogeneity and inter-heterogeneity.
In the present paper we will focus on dividing the population in homogeneous subgroups as proposed by De Feyter [7], we will not deal with the latent sources

of heterogeneity but use the observable data to reach homogeneity.
The division in subgroups in manpower planning mostly follows a certain scheme which is explained accurately in [7]. First it is important to look at the characteristic we are interested in. If predictions are to be made about e.g. grade or salary, this has to be taken into account in the division in distinctive groups. The second stage goes further into transitions between subgroups and flows out of the system. Every introduction of an additional subdivision brings the need for a new investigation of the degree of heterogeneity. In the third and following stages the homogeneity of the created subgroups so far is investigated. Clearly homogeneity in manpower planning depends on similarity in transition probabilities.
The splitting process goes on until homogeneity is reached for all possible transitions in all created subgroups. However, a very important trade-off should be taken into account. The final homogeneous subgroups need to be large enough to make reliable estimations and predictions. At some point a choice has to be made between accepting a degree of heterogeneity in a subgroup or further division with the risk of creating subgroups that are too small. The challenge is to find an equilibrum between homogeneity and group size. Therefore De Feyter proposed a stepwise splitting-up approach [7]. An advantage of this approach is that it keeps an eye on the size of the subgroups, so a good balance between homogeneity and group size can be reached. Also the method avoids making unnecessary splits when certain variables are correlated and one variable might prove to be sufficient for a split. The biggest disadvantage of the approach is that for each possible split, every variable and transition is investigated seperately.

In the present paper we will examine decision tree learning as a methodology to classify personel in homogeneous subgroups with the advantages that the most explanatory variables are selected in the dataset, and that the selection of the variables and the division according to the variables is not biased by prior information. Moreover the tree will result in a division of the staff in subgroups by a procedure that can be automated.

2 Push model

The push model was founded by Bartholomew and thoroughly described in [1]. Consider a population where the members are divided in k homogeneous groups, for example according to the grades in a company. Let $n_j(t)$ denote the stock of people in grade j at time t, so the initial number of members in grade j is $n_j(0)$. The number of new recruited employees in grade j at time $t+1$ will be denoted as $R_j(t+1)$. A member of grade i moves to grade j within one time interval with probability p_{ij}. The expected number of employees $\bar{n}_j(t+1)$ present in grade j at time $t+1$ can be expressed as

$$\bar{n}_j(t+1) = \sum_{i=1}^{k} p_{ij}\bar{n}_i(t) + R_j(t+1).$$

Better estimations for the transition probabilities will result in better estimations for the flows and stocks. We will focus on a hierarchical, time-homogeneous push model with at most one transition for every member in every time interval. The aim is to determine the homogeneous subgroups that define the states of the Markov model.

3 Split in manpower systems

When constructing a Markov model we typically use a Human Resources database consisting of data from several years. In every year we have information on every employee in the system and whether or not the employee was promoted from grade i to $i+1$ during this year. We are interested in

Year	ID	Sex	Marital Status	Age	Seniority	Grade	Work%	Promotion
2012	135	Male	Single	41	15	2	100	No
2013	135	Male	Single	42	16	2	100	Yes
2014	135	Male	Single	43	17	3	100	No
2012	136	Female	Divorced	35	9	1	80	No
2013	136	Female	Divorced	36	10	1	80	No
2014	136	Female	Divorced	37	11	1	80	No

Table 1. HR database example.

which characteristics are of influence on this promotion and how we can split the population according to these characteristics. This type of problem led us to the theory of decision trees. Decision trees were introduced in the area of data mining and are used as a classification technique for all types of data. A detailed outline on how a decision tree works is given in [15]. A decision tree will not only select the most explanatory characteristics but will also give the best possible split according to this characteristic. Note that for every $i = 1, \ldots, k-1$, transitions from i to $i+1$ might have other explanatory variables for promotion. So we will use the decision tree splitting technique for transition flows from i to $i+1$ for every $i = 1, \ldots, k-1$.

4 Decision trees

In this section we will give an overview of the basic principles of decison tree learning and the applicability in manpower planning is presented. A decision tree consists of nodes where the root node is the entire dataset, this root node has branches to childnodes, which form a partition of the root node. If a childnode has no outgoing branches, the child is called a leaf, otherwise the child has outgoing branches to children that again form a partition of this node [13]. The branches of the tree are created by making decisions based on the available variables. About 30 years ago Breiman [5] introduced the CART

(classification and regression trees) algorithm, which is a technique of recursive partioning that consists of a two step search procedure [4]. In the first step of the procedure the best split is selected for each variable. Secondly, after the best split is determined for each characteristic, the best split is selected overall which results in a first split of the dataset according to the best predicting characteristic [4]. Many decision tree algorithms are based on CART. CART itself still remains a very popular data analysis tool and has a high practical value [4]. We will provide some details on both steps of the procedure in the following two sections.
In the domain of data mining many classification techniques have been developed, among others CART, C4.5 and MLP [16], which have been implemented in software tools such as WEKA. WEKA is an open source software which has achieved widespread acceptance within academia and business circles and has become a widely used tool for data mining research [10]. We will use the WEKA software and choose the popular CART algorithm for our classification problem.

4.1 Measures for selecting the best split

An important issue in choosing group divisions is looking at how to make a 'best' split. If we want to split a group according to for example sex the split is straightforward: we make a binary split in men and women. The split is far less evident if we want to split a group according to a continuous characteric, for example, according to wages, age, etc. There exist two types of decision trees: binary and non-binary. In a binary tree every node that is not a leaf has two children. A non-binary tree might get complex really fast when characteristics have many values, and every value leads to a branch. Researchers therefore mostly prefer binary trees [5,6,15] (e.g CART and ID3 are binary split methods). When the characteristic is binary, the split is evident. However if we consider **nominal** characteristics such as marital status which has three distinct values (e.g. single, married, divorced), we need to group certain values together. It becomes even more difficult when we consider **continuous** characteristics.
In general a characteristic with k values leads to $2^{k-1} - 1$ ways to create a binary partition. For a continuous characteristic C the binary split can be defined as $C < v$ and $C \geq v$. The decision tree should consider all possible values for v and choose the one that leads to the best split. Which gives rise to the following question. How can we obtain the best split?
In the theory of decision trees a split is based on predefined classes. In the context of manpower planning we have a dataset of records where every record consists of characteristics of an employee which belongs either to the class promoted or the class non-promoted. We give an overview of the most used split measures as described in [15]. We define $p(i|t)$ to be the fraction of records belonging to class i at a given node t. The measures for selecting the best split are often based on the degree of impurity of the child nodes. The smaller the degree of impurity, the better. Consider we have l classes, examples of impurity

measures are

$$\text{Entropy}(t) = -\sum_{i=1}^{l} p(i|t) \log_2 p(i|t)$$

$$\text{Gini}(t) = 1 - \sum_{i=1}^{l} p(i|t)^2$$

$$\text{Classification error}(t) = 1 - \max_i p(i|t)$$

When all records belong to the same class we get the impurity measures result in 0. The highest value for these functions is 0.5 for Gini and the classification error, and 1 for Entropy. The CART algorithm is based on the Gini measure. After the suitable impurity measure is chosen, a splitting criterion for the decision tree can be defined. We denote $i(N)$ as the impurity of the node N. We can calculate the gain Δ of making a split in the partition $\{C_1, C_2, \ldots, C_k\}$ by

$$\Delta = i(N) - \sum_{j=1}^{k} \frac{|C_j|}{|N|} i(C_j),$$

where N is the parent node with children C_j. For a binary split $k = 2$. Decision tree induction algorithms often choose a test condition that maximizes the gain Δ [15]. Maximizing the gain is obviously equivalent to minimizing the weighted average impurity measures of the child nodes because $i(N)$ is the same for all test conditions.

Example 1. We made a small dataset which might be extracted from an HR database, on which we will illustrate the use of the splitting criterion.

Sex	Marital Status	Age	Promotion
Male	Single	23	No
Female	Married	35	No
Male	Married	27	No
Female	Single	45	Yes
Female	Married	38	No
Female	Divorced	48	No
Male	Single	47	Yes
Male	Divorced	36	No
Male	Single	22	No
Male	Married	50	Yes

Table 2. HR dataset example.

In the example each record contains the personal information of a staff member with in the last column the characteristic *promotion* which gives a

'yes' if the employee has received a promotion from i to $i+1$ within a year, a 'no' if the employee hasn't. We construct a decision tree where every leaf contains only employees who belong to the same class according to the latter characteristic. Therefore when we calculate an impurity measure, it will be based on the number of promoted and non-promoted employees. A first split can be made according to the characteristic marital status which has 3 values: single(S), married(M) and divorced (D). Since the aim is to make a binary split we can do this in 3 $(= 2^{3-1} - 1)$ possible ways as described above.

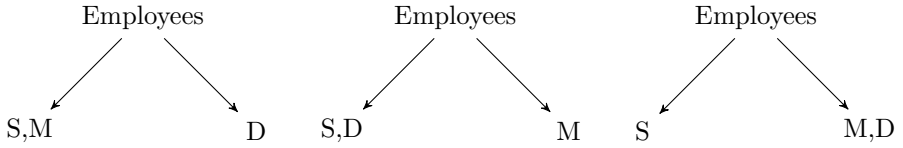

We choose the Gini impurity measure in our example. First we calculate the impurity measure of the parent node, which is the entire dataset

$$i(\text{employees}) = 1 - \left(\frac{3}{10}\right)^2 - \left(\frac{7}{10}\right)^2 = 0.42.$$

Next we calculate the gains for the different splits.

$$\Delta_1 = 0.42 - \left[\frac{8}{10}\left(1 - 0.75^2 - 0.25^2\right) + \frac{2}{10}\left(1 - 0.5^2 - 0.5^2\right)\right] = 0.02$$
$$\Delta_2 = 0.42 - \left[\frac{6}{10}\left(1 - 0.83^2 - 0.17^2\right) + \frac{4}{10}\left(1 - 0.5^2 - 0.5^2\right)\right] = 0.05$$
$$\Delta_3 = 0.42 - \left[\frac{4}{10}\left(1 - 1^2 - 0^2\right) + \frac{6}{10}\left(1 - 0.5^2 - 0.5^2\right)\right] = 0.12$$

Since Δ_3 is the biggest gain, we choose to make the third split.

In the previous example we needed to consider 3 possible splits, however if we would like to split the dataset according to a continuous characteristic C, it might take a lot of computations to consider every value v for making a binary split $C < v$ and $C \geq v$. To reduce complexity we can first sort the dataset according to the continuous characteristic. For example if we would like to make a split according to the age in the previous example. We would first order the data increasingly based on the age of the employees. Candidate split positions are identified by taking the midpoints between two adjacent sorted values [15], e.g. $v = 22.5, 25, 31, \ldots$. But to reduce possible values even more, we will only consider candidate split positions located between two adjacent records with different class labels (in our example Yes or No for the characteristic Promotion). So the only possible candidate split positions are $v = 41.5$ or $v = 47.5$ or $v = 49$. We consider the splits where $v = 41.5$, $v = 47.5$,

Sex	Marital Status	Age	Promotion
Male	Single	22	No
Male	Single	23	No
Male	Married	27	No
Female	Married	35	No
Male	Divorced	36	No
Female	Married	38	No
Female	Single	45	Yes
Male	Single	47	Yes
Female	Divorced	48	No
Male	Married	50	Yes

Table 3. HR dataset example sorted according to age.

$v = 49$ and calculate the gain respectively.

$$\Delta_1 = 0.42 - \left[\frac{6}{10}\left(1 - 1^2 - 0^2\right) + \frac{4}{10}\left(1 - 0.75^2 - 0.25^2\right)\right] = 0.27$$
$$\Delta_2 = 0.42 - \left[\frac{8}{10}\left(1 - 0.75^2 - 0.25^2\right) + \frac{2}{10}\left(1 - 0.5^2 - 0.5^2\right)\right] = 0.02$$
$$\Delta_3 = 0.42 - \left[\frac{9}{10}\left(1 - 0.78^2 - 0.22^2\right) + \frac{1}{10}\left(1 - 0^2 - 1^2\right)\right] = 0.11$$

Again we select the biggest gain, thus $v = 41.5$, resulting in the age partition $C_1 = [22, 41]$ and $C_2 = [42, 50]$.
We now know how to select the best split for a characteristic. However in a dataset there is often more than one characteristic present. As in the example we gave above there are 3 different characteristics which might have an influence on promotion. In the next section we discuss how the characteristic for the first split is chosen.

4.2 Selecting the characteristic

When more than one characteristic is present, we need to select the variable for the first split. In the example from the previous section we considered a split according to marital status and a split according to age. For these characteristics the biggest gain was 0.12 and 0.27 respectively. For the characteristic sex only one split is possible, here the gain is 0.003. This means we will decide on making a first split according to age which results in two nodes. For every node we then consider the number of members in each class: non-promoted(NP), promoted (P). The left node results in NP:6,P:0 and an impurity score of 0, thus will turn into a leaf of the tree. The right node has NP:1,P:3, and an impurity score of 0.375.
Since the left node is a leaf, we will now only investigate the right node and calculate the impurity scores for possible splits. Splitting according to sex will

give a gain of 0.125, to marital status will give 3 possible splits with gains 0.375 (SM and D), 0.125 (SD and M), 0.125 (S and MD), to age will give 2 possible splits with gains 0.041 ($v = 47.5$) and 0.041 ($v = 49$). So we decide to split according to marital status and put single and married employees together in a node. After this last split, all nodes are pure, i.e. all records in a leaf belong to the same class.

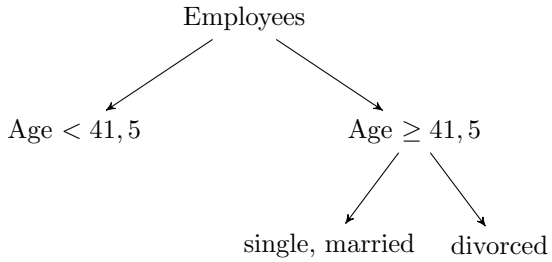

The splitting procedure will stop when all records in a leaf belong to the same class. This might not always be a good criterion, especially when we want to use the resulting groups of records we retrieve in a leaf in manpower planning. In manpower planning we want a group to be homogeneous but also we want a group to be large enough to make good estimations for transition probabilities. So in our case we will predefine a minimum number of objects we want in every leaf. The splitting procedure will stop if this minimum is reached or if a next split would imply that the leafs turn out to be too small.
Note that the technique of decision trees is focused on trying to classify cases according to a chosen characteristic. The highest gain will be reached when a split is conducted that gives leafs that are most homogeneous according to the chosen characteristic. In other words the maximal gain for a split will reach the maximal intra homogeneity inside the leaf. In the case of manpower planning we also want the resulting subgroups to be inter-heterogeneous as well. Thus if the decision tree will provide us subgroups where the estimated transition probabilities lie close together, we could merge the groups again.

5 Estimating probabilties depending on the sample size

We use a time-homogeneous Markov model i.e. the transition probabilities will be constant over time. An estimator for the transition probability to transfer from grade i to grade j will be

$$\hat{p}_{ij} = \frac{\sum_{t=0}^{T-1} n_{ij}(t)}{\sum_{t=0}^{T-1} n_i(t)}, \tag{1}$$

where $n_{ij}(t)$ denotes the number of people who moved from grade i to j in the time interval $[t, t+1]$ and T the number of years of available data [1]. In order to make a reliable estimation the sample size $\sum_{t=0}^{T-1} n_i(t)$ should be big enough. For every grade i we consider the probability of promoting to grade $i+1$ or staying in grade i. Let $\hat{p}_{i,i+1}$ be the probability of promoting to grade $i+1$.

Then $1 - \hat{p}_{i,i+1}$ is the probability of staying in grade i. This is a binomial experiment that is conducted n times, with $n = \sum_{t=0}^{T-1} n_i(t)$.
If n is 'large enough' a confidence interval for the true probability $p_{i,i+1}$ is given by

$$\hat{p}_{i,i+1} \pm z_{\frac{\alpha}{2}} \sqrt{\frac{\hat{p}_{i,i+1}(1-\hat{p}_{i,i+1})}{n}},$$

where $z_{\frac{\alpha}{2}}$ is the critical value of the normal distribution for a given error level α [18]. For example if $\alpha = 0.05$, then the critical value $z_{0.025}$ will be 1.96. The meaning of this critical value is that if the data is normally distributed and $\alpha = 0.05$, 95% of the data will be within the confidence interval and only 2.5% will be in each of the 'tails' outside [18]. From this confidence interval Cochran's sample size formula is derived [2] which gives a minimal value for the sample size n for a reliable estimation. The sample size n should be at least

$$n^* = \left(\frac{z}{m}\right)^2 \times \hat{p}_{i,i+1}(1-\hat{p}_{i,i+1}),$$

where z is a critical value (mostly 1.96 or 2.58 corresponding with an error level of respectively 0.05 or 0.01) and m is the radius of the confidence interval and thus the margin of error the researcher is willing to except (usually 0.025 or 0.01) [2]. Note that n^* depends on the estimated probability, however the estimated probability is unknown upfront and depends on the sample. We could choose to set $\hat{p}_{i,i+1} = \frac{1}{2}$, which results in the upper bound of n^*. However, promotion probabilities are usually pretty small so this would result in a value of n^* that is unnecessary large.
Depending on the data we can calculate $\hat{p}_{i,i+1}$ for the entire grade i. This is an average probability for every employee in grade i to transfer to $i+1$, thus we will choose to base the minimal number of members in the subgroups of grade i on the probability $\hat{p}_{i,i+1}$. So the minimal number of members in the subgroups of grade i will be

$$n_s(i) = \left(\frac{z}{m}\right)^2 \hat{p}_{i,i+1}(1-\hat{p}_{i,i+1}). \tag{2}$$

We will choose common values for z and m: $z = 1.96$ and $m = 0.025$. However, if the sample is big (*e.g.* > 10000) and the probability $p_{i,i+1}$ small (*e.g.* $< 4\%$) the value 0.025 for m might not be a good choice for two reasons. First of all choosing a margin of error to be 2,5% for a probability smaller than 4 % doesn't seem quite right. Secondly, if the sample is big and the probability small this will lead to many subgroups with small differences in transition probabilities. So in the case of a big sample and low probability, we set $m = 0.01$ [2].

6 Illustration

We use a real life database that contains the information on academic staff from our university for the period of 1993-2013. There are 6 different grades: the first grade consists of Phd researchers, the second of Post Doctoral Researchers, the third till the sixth grade consist of different hierarchical grades

of Professors (grade 3: assistent professor, grade 4: associate professor, grade 5: professor, grade 6: full professor). Every record in the dataset represents one year for one employee (cfr. example in section 3). The dataset consists of 46317 cases from 1993 till 2013 and contains the following variables for every employee on annual base: sex, age, seniority (sen), workpercentage, faculty (fac), grade in the beginning of the year, grade at the end of the year, promotion. There are 8 faculties in our university: ES, WE, IR, LW, LK, PE, RC, GF.

For each grade i we will construct a decision tree, where the tree will be sorted according to the characteristic *promotion* having values 0 and 1, a 0 means that the employee stayed in grade i (we do not consider employees who left the company for making the split), a 1 means that the employee transfered to grade $i+1$. First we will apply the sample size formula (2) for every grade, we present the results for the first and second grade. To create homogeneous groups for grade 1, we need to look at the promotion probability from grade 1 to grade 2. In the first grade there are 21539 cases with 794 promotions, so $\hat{p}_{1,2} = 3.69\%$. Since this is a small probability and a large sample, we will choose m to be 0.01. The minimum size for the subgroups will be

$$n_s(1) = \left(\frac{1.96}{0.01}\right)^2 0.0369(1-0.0369) = 1365.$$

In the second grade there are 4149 cases with 738 promotions, so $\hat{p}_{2,3} = 17.79\%$, resulting in a minimum subgroupsize

$$n_s(2) = \left(\frac{1.96}{0.025}\right)^2 0.1779(1-0.1779) = 899.$$

Other minimal sizes in our example are: $n_s(3) = 288$, $n_s(4) = 360$, $n_s(5) = 379$. Next we construct a decision tree using the CART algorithm. This results in the following tree for grade 1. In the tree 'fac1' stands for the group of employees of faculties WE, IR and LW, 'fac2' are the other faculties.

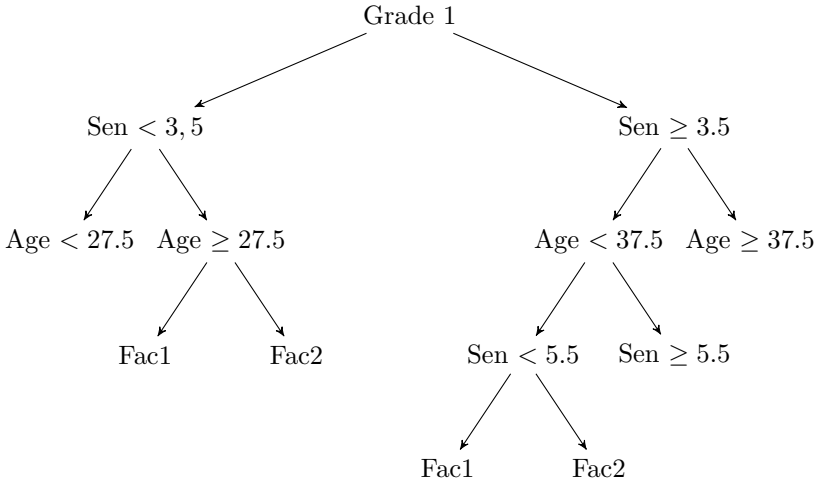

The decision tree results in 7 leafs, from the outer left leaf to outer right leaf: NP:6936,P:19 (0.27%), NP:2658,P:86 (3.13%), NP:3140,P:34 (1.07%), NP:1472,P:153 (9.42%), NP:1572,P:61 (3.74%), NP:2374,P:339 (12.5%), NP:2620,P:74 (2.75%). Between brackets we find the transition probability for each leaf, i.e. for each homogeneous subgroup. Note that some leafs have similar transition probabilties e.g. the second, fifth and last leaf, so we could decide to take these leafs together to form one subgroup. We decide not to do so, we will only take adjacent leafs together, since the results can be more easily interpreted this way.
For the second grade we get the following tree.

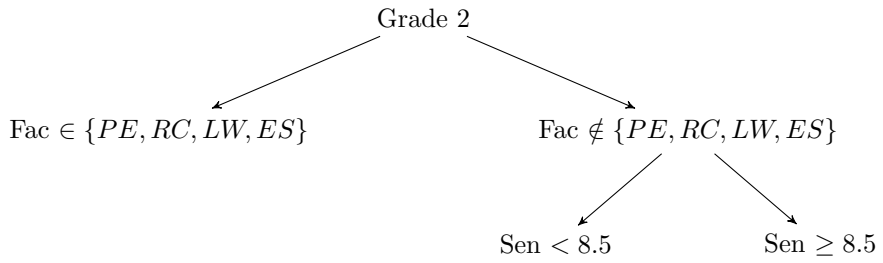

The decision tree gives us 3 leafs, with from the outer left leaf to the outer right leaf: NP:774,P:295 (27.6%), NP:1808,P:216 (10.67%), NP:829,P:227 (21.5%). We did the same procedure for every grade, but will only give the results for the first two.
The leafs of the decision trees result in homogeneous subgroups of employees. A Markov model is built with these subgroups as states. This model will be referred to as the 'tree-method-model'. The goodness of fit of the model is examined by an internal validation method [1]. The transition probabilities are based on the dataset and equation (1). Next we use the Markov model to predict the stocks for the time span of the dataset starting from the initial stocks $n(0)$ and compare the predicted stocks to the real stocks. The tree-model-method is compared with the grade-only-model in wich the staff is only divided according to grade (without considering any further split). In figure 1, the lowest blue curve represents the real evolution of the stock in grade 1 and 2. The middle curve is the result from the tree-method-model and the upper curve the result from the grade-only-model. Clearly the tree-method-model gives better predictions. Finally we compute the AGFI (Adjusted Goodness-of-Fit Index) measure to compare the goodness of a more complex model to a base model. This value ranges between 0 and 1 with larger values indicating a better fit [14]. It is computed by the formula

$$AGFI = 1 - \frac{\chi_t^2/df_t}{\chi_g^2/df_g}.$$

Where χ_g^2 (resp. χ_t^2) is the chi-square of the grade-only-model (resp. tree-method-model), and df_g and df_t are the degrees of freedom of the corresponding models [14], in our dataset this results to $AGFI = 0.79$.

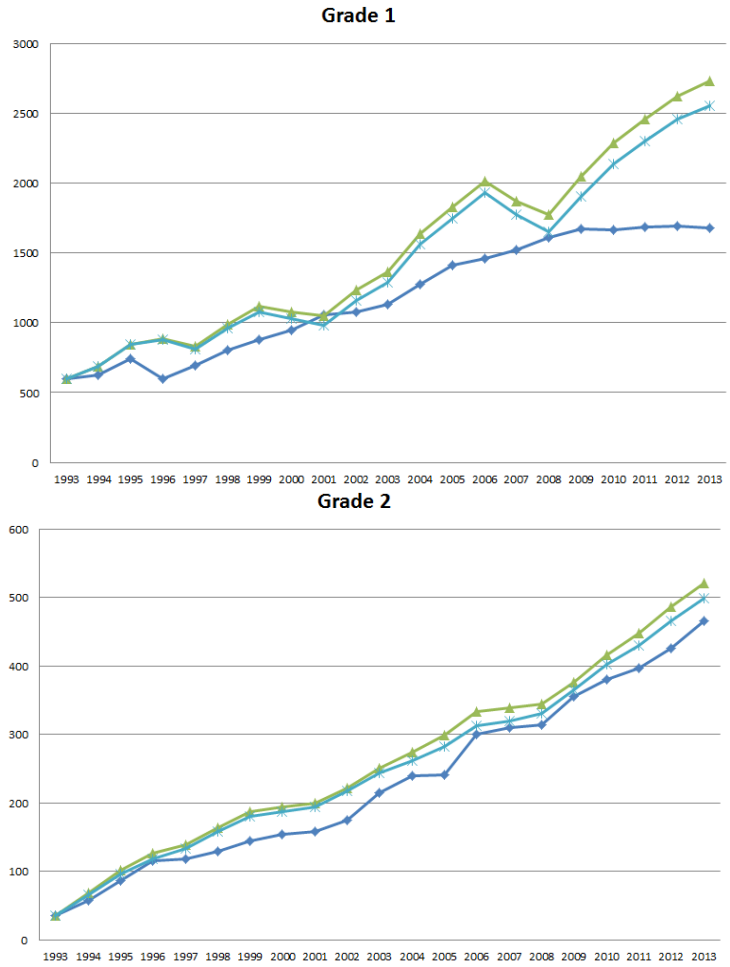

Fig. 1. Evolution of the stocks.

7 Future research

De Feyter [7] provided some preliminary ideas on techniques that could be used for group division such as cluster analysis and logistic regression. Regression methods have become an integral component of any data analysis concerned with describing the relationship between a response variable and one or more explanatory variables [11]. So regression analysis can be a key in searching which characteristics have an influence on transition behavior of employees in a company. Logistic regression can detect the importance of variables for promotion and can be used to calculate an individual promotion probability for all employees in a company. This technique will however not provide a division of the staff in groups. So, more usefull would be to look at the use of multinomial logistic regression, this way we can take wastage probabilities and non hierarchical probabilities into account and estimate the transition probabilities on an

individual level instead of making an aggregate analysis. The predictions will then be based on the estimations from the regression.

References

1. Bartholomew, D.J., Forbes, A.F., McClean, S.I. (1991). Statistical Techniques for manpower Planning, second ed. John Wiley & Sons, Chichester.
2. Bartlett, J.E., Kotrlik, J. W., Higgins, C. H. (2001). Organizational research: Determining appropriate sample size in survey research appropriate sample size in survey research. Information technology, learning, and performance journal, 19(1), 43.
3. Belhaj, R., Tkiouat, M. (2013). A Markov Model for Human Resources Supply Forecast Dividing the HR System into Subgroups. Journal of Service Science and Management 6, 211-217.
4. Berk, R.A. (2008). Statistical Learning from a Regression Perspective, Springer Science Business Media.
5. Breiman, L. et al (1984). Classification and Regression Trees. Wadsworth & Brooks/Cole advanced books & software, California.
6. Boley, D.L (1998). Principal direction divisive partitioning. Data Mining and Knowledge Discovery, vol.2, n.4, p325 -344.
7. De Feyter, T. (2006). Modelling heterogeneity in manpower planning: dividing the personnel system into more homogeneous subgroups. Applied Stochastic Models in Business and Industry 22 (4), 321-334.
8. De Feyter, T. (2007). Modelling mixed push and pull promotion flows in manpower planning. Ann. Oper. Res. 155, 25-39.
9. Guerry, M.A. (2011). Hidden heterogeneity in manpower systems: A Markov-switching model approach. European Journal of Operational Research 210, 106-113.
10. Hall, M., Frank, E., Holmes, G., Pfahringer, B., Reutemann, P., Witten, I. H. (2009). The WEKA data mining software: an update. ACM SIGKDD explorations newsletter, 11(1), 10-18.
11. Hosmer, D.W., Lemeshow, S. (2000). Applied Logistic Regression, second ed. John Wiley & Sons, Inc.
12. Jackson, S.E et al (1991). Some Differences Make a Difference: Individual Dissimilarity and Group Heterogeneity as Correlates of Recruitment Promotions, and Turnover. Journal of Applied Psychology 76/5, 675-689.
13. Rutkowski, L. Jaworski, M., Pietruczuk, L., Duda, P. (2014). The CART decision tree for mining data streams. Information Sciences 266, 1-15.
14. Schermelleh-Engel, K., Moosbrugger, H., Muller, H. (2003). Evaluating the fit of the structural equation models: tests of significance and descriptive goodness-of-fit measures. Methods of Psychological Research Online, 8, 23-74.
15. Tan, P., Steinbach, M., Kumar, V. (2006). Introduction to Data Mining. Pearson Education, Inc.
16. Tsoi, A. C., Pearson, R. A. (1991). Comparison of Three Classification Techniques: CART, C4. 5 and Multi-Layer Perceptrons. In Advances in neural information processing systems, p 963-969.
17. Ugwuowo, F.I., McClean, S.I. (2000), Modelling heterogeneity in a manpower system: a review. Applied Stochastic Models in Business and Industry 16, 99-110.
18. Wallis, Sean A. (2013). Binomial confidence intervals and contingency tests: mathematical fundamentals and the evaluation of alternative method. Journal of Quantitative Linguistics 20 (3), 178-208.

Modeling a warm standby system with corrective and preventive maintenance

Ruiz-Castro, Juan Eloy

Department of Statistics and Operational Research, Faculty of Science, Campus Fuentenueva s/n. University of Granada, Granada, Spain
(E-mail: jeloy@ugr.es)

Abstract. A complex warm standby system, subject to repairable and non-repairable failures, that evolves in discrete time, is modeled through a Markov process. The system is composed of one online unit and the rest in warm standby. The online unit can fail due to wear or external shocks. In both cases the failure can be repairable or non-repairable. The rest of the units can fail due to wear, all of them repairable failures. When the online unit undergoes a non-repairable failure, this one is replaced by a new and identical one. If any unit suffers a repairable failure, this one goes to the repair facility for corrective repair. The corrective repair time depends on the type of unit (online or warm standby unit). The online unit passes through several degradation levels while it is working on. This one is observed when a random inspection occurs. If the degradation level observed is major, then preventive maintenance is carried out. Interesting measures such as reliability and some conditional probabilities are worked out. The modeling has been calculated in an algorithmic form through matrix algebraic expressions.
Keywords: Preventive maintenance, phase type distributions, Marked Markovian Arrival Processes.

1 Introduction

Redundant systems and preventive maintenance are of considerable research interest. Serious damage, financial losses and, possibly, total system failure can be provoked by poor reliability. Two approaches can be adopted to improve the reliability of a complex system: standby systems and preventive maintenance.

Preventive maintenance is intended to improve system reliability and to increase profits. Nakagawa [3] studied standard and advanced problems of maintenance policies for system reliability. Preventive maintenance has also been described for use in complex systems, with either a multi-state unit or with a general set of cold standby multi-state units (Ruiz-Castro [7],[8]).

Nowadays, multi-state systems are of particular importance in ensuring reliability. Many real-life systems, termed multi-state systems, are composed of multiple components with different performance levels and incorporating several failure modes. Lisnianski et al. [2] has studied multi-state systems, presenting a variety of significant cases of interest to engineers and industrial

16th ASMDA Conference Proceedings, 30 June – 4 July 2015, Piraeus, Greece

managers. Lisnianski and Frenkel [1] included Markov processes in the analysis of multi-state systems, highlighting the benefits of their application.

When complex systems are modelled, intractable expressions are often encountered. Several methodologies have been proposed to analyse the behaviour of a multi-state system, and one such method is that of Markov process theory. One class of distributions that makes it possible to model complex systems with well structured results, thanks to its matrix-algebraic form, is the phase-type distribution, which was introduced and analysed in detail by Neuts [6]-[5], who pointed out its useful algorithmic properties.

Many stochastic systems have inputs to the system over time that can be counted to control events, e.g. electrical systems at which electric shock waves arrive at random intervals. Multi-state systems that evolve over time may be subject to different types of failures, whether repairable or non-repairable, and benefit from measures such as preventive maintenance to enhance performance and economic results. The analysis of these systems requires a mathematical tool that can describe the input analytically and give rise to anumerically tractable model. The Markovian arrival process (MAP) class that was introduced by Marcel Neuts [4] counts the number of events in an underlying Markov chain.

The aim of the present paper is to model a warm standby complex system that evolve in discrete time, is subject to different types of failure (repairable and non-repairable) and are protected by means of preventive maintenance. The evolution is analysed using a Markov model and a marked, batch-arrival MAP. A numerical example shows the versatility of the modelling, comparing two similar complex systems with and without preventive maintenance.

2 The system

We assume a system with N components, the online unit and the rest in warm standby, that evolves in discrete time. The online unit is subject to internal failures due to wear out and to external shocks (both repairable or non-repairable). When an internal failure or an external shock is produced, this one can be repairable with probability p_{in_re} and p_{ex_re}, respectively. Any warm standby unit can undergo only repairable failures due to wear. When one failure occurs, the unit goes to the repair facility with a single repairman for corrective repair. The online unit is a multi-state one where it passes through several performance states which are partitioned in minor (the first n_1 states) and major (the rest). Preventive maintenance over the online unit is carried out as response to random inspections. The online unit goes to preventive maintenance only when one major state is observed under inspection. Corrective repair times and preventive maintenance are different according to the type of failure, from either the online place or standby. The order of the type of failure in queue keeps in memory. The system is subject to the following assumptions.

***Assumption* 1.**The internal operational time of the online unit is *PH*-distributed with representation ($\boldsymbol{\alpha}$, $\mathbf{T}$). The number of operational states is equal to n, and

these are partitioned in minors (the first n_1 states) and majors states (states n_1+1, …, n). The internal failure is repairable.

***Assumption* 2.** Internal failures are repairable with probability p_{in_re} and non-repairable with probability $p_{in\_nre}= 1 - p_{in\_re}$. The type of failure is independent of the failure time.

Assumption 3. Events that produce failures of the online unit due to external shocks occur according to a phase type renewal process. If the online place is busy, this event produces the failure of the unit. The time between two consecutive events is *PH* distributed with representation ($\boldsymbol{\gamma}$, **L**). The order of the matrix *L* is equal to *t*.

Assumption 4. External failures are repairable with probability p_{ex_re} and non-repairable with probability $p_{ex\_nre}= 1 - p_{ex\_re}$. The type of failure is independent of the failure time.

Assumption 5. When the online unit undergoes a non-repairable failure then it is replaced by a new and identical one in a negligible time.

Assumption 6. Any warm standby can fail at any time with probability *p*.

Assumption 7. While the online place is busy by a unit, random inspections can occur. The time between two consecutive inspections is *PH* distributed with representation ($\boldsymbol{\eta}$, **M**). The order of the matrix **M** is equal to ε.

Assumption 8. The corrective repair time for any warm standby that fails is *PH* distributed with representation ($\boldsymbol{\beta_0}$, $\mathbf{S_0}$). The order of this matrix is equal to z_0.

Assumption 9. The corrective repair time when the online unit fails is *PH* distributed with representation ($\boldsymbol{\beta_1}$, $\mathbf{S_1}$). The order of this matrix is equal to z_1.

Assumption 10. The preventive maintenance time is *PH* distributed with representation ($\boldsymbol{\beta_2}$, $\mathbf{S_2}$). The order of this matrix is equal to z_2.

Assumption 11. The random times defined above are independent.

The system is modelled through a marked Markovian arrival process with state-space formed of macro-states, $E = \{E^0, E^1, \ldots, E^N\}$, where E^k contains the phases when there are *k* units in the repair facility, for k=0,…N. The macro-state E^k is partitioned in several macro-states depending on the order of the units in the repair facility. Thus, $E^k = \left\{E_{i_1,i_2,\ldots,i_k}; i_l = 0,1,2, l = 1,\ldots,k\right\}$, k =1,…N, contains the phases when there are *k* units in the repair facility and the order of these units to repair is given by $i_1,\ldots,i_k$ in lexicographical order; where 0 indicates that the unit comes from warm standby, 1 indicates that the online unit undergoes a repairable failure and 2 indicates that the online unit is in the repair facility for preventive maintenance. The state-space by considering the different phases are given by

$$E^0 = \left\{(i, j, m); 1 \le i \le n, 1 \le j \le t, 1 \le m \le \varepsilon\right\},$$

$$E_{i_1,\ldots,i_k} = \left\{(i, j, m, a); 1 \le i \le n, 1 \le j \le t, 1 \le m \le \varepsilon, 1 \le a \le z_{i_1}\right\} \text{ for, } k = 1,\ldots, K-1,$$

and $$E_{i_1,\ldots,i_K} = \left\{(j, a); 1 \le j \le t, 1 \le a \le z_{i_1}\right\},$$

where *i* denotes the phase of the operational time of the online unit, *j* is the phase of the external shock time, *m* the phase of the inspection time and finally, *r* is the phase of the repair time.

3 The Modeling: Marked Markovian Arrival Process with arrivals in batch

The system is modelled through a MMAP with arrivals in batch. Four types of events are distinguished:
O: only warm standby units can fail at a certain time.
A: the online unit undergoes a repairable failure (any unit in warm standby can fail).
B: the online unit undergoes a major inspection (any unit in warm standby can fail).
C: the online unit undergoes a non-repairable failure (any unit in warm standby can fail).

When the events *A*, *B* and *C* have place at a certain time, the number of warm standby units that fail can vary from 0 to the total units in standby at the previous moment. We defined $\mathbf{D}^{Or}$, $\mathbf{D}^{Ar}$,$\mathbf{D}^{Br}$ and $\mathbf{D}^{Cr}$, for $r = 0,\ldots, N-1$, as the matrices that contain the transition probabilities between any two phases described in the state space when the event *O*, *A*, *B* or *C* occurs, respectively, and *r* standby units fail.

The system is modelled by the following *MMAP*,
$\left(\mathbf{D}^{O0},\mathbf{D}^{O1},\ldots,\mathbf{D}^{O,N-1},\mathbf{D}^{A0},\mathbf{D}^{A1},\ldots,\mathbf{D}^{A,N-1},\mathbf{D}^{B0},\mathbf{D}^{B1},\ldots,\mathbf{D}^{B,N-1},\mathbf{D}^{C0},\mathbf{D}^{C1},\ldots,\mathbf{D}^{C,N-1}\right)$.

3.1 The matrix blocks

The matrices defined above are built in this section. Previously several vectors and matrices are defined. We denote by $\mathbf{e}_a$ a column vector containing all 1 of order *a* (if the subscript is not noted, then the order of **e** is the appropriate for a correct product). Also, we denote as $\mathbf{e}_{a:b}$ to the column vector composed of zeros excepting the range given (*a:b*) where the values are ones. The following auxiliary matrices, used when one inspection occurs, are defined as $\mathbf{U_1}$ and $\mathbf{U_2}$, and the element (*i, j*) of these matrices is given by

$$U_1(i,j)=\begin{cases}1 & ; \quad i=j\le n_1\\ 0 & ; \quad \text{otherwise}\end{cases},\ U_2(i,j)=\begin{cases}1 & ; \quad i=j\ge n_1+1\\ 0 & ; \quad \text{otherwise.}\end{cases}.$$

Blocks for the online unit
While the online unit is operational, it can undergo internal failure, external shock and/or one inspection. These possibilities are considered in the definition of the following matrices that describe different transition probabilities for the online unit.

The transition probability when the online unit changes of phase without failure or preventive maintenance by considering the corresponding phases is given by $\mathbf{H}_0=\mathbf{T}\otimes\mathbf{L}\otimes\mathbf{M}+\mathbf{U}_1\mathbf{T}\otimes\mathbf{L}\otimes\mathbf{M}^{\mathbf{0}}\boldsymbol{\eta}$. If a repairable failure on the online unit takes place, it is given by

$$\mathbf{H}_1 = \mathbf{T}^0 \boldsymbol{\alpha} p_{in\_re} \otimes \left(\mathbf{L} + \mathbf{L}^0 \boldsymbol{\gamma} p_{ex\_re}\right) \otimes \left(\mathbf{M}^0 \boldsymbol{\eta} + \mathbf{M}\right) + \left(\mathbf{e}_n - \mathbf{T}^0\right) \boldsymbol{\alpha} \otimes \mathbf{L}^0 \boldsymbol{\gamma} p_{ex\_re} \otimes \left(\mathbf{M}^0 \boldsymbol{\eta} + \mathbf{M}\right).$$

The latter case when the only operational unit is the online, and at same transition time a repaired is not produced is given by $\mathbf{H}_1^{'} = \mathbf{T}^0 p_{in\_re} \otimes \left(\mathbf{L} + \mathbf{L}^0 \boldsymbol{\gamma} p_{ex\_re}\right) \otimes \mathbf{e}_{\varepsilon} + \left(\mathbf{e}_n - \mathbf{T}^0\right) \otimes \mathbf{L}^0 \boldsymbol{\gamma} p_{ex\_re} \otimes \mathbf{e}_{\varepsilon}$.

When one inspection occurs and a major state is observed then the unit goes to the repair facility to preventive maintenanceand it is given by $\mathbf{H}_2 = \mathbf{U}_2 \left(\mathbf{e}_n - \mathbf{T}^0\right) \boldsymbol{\alpha} \otimes \mathbf{L} \otimes \mathbf{M}^0 \boldsymbol{\eta}$. When there is only one operational unit and a repaired is not produced at a certain time, the latter expression is given by $\mathbf{H}_2^{'} = \mathbf{U}_2 \mathbf{T} \otimes \mathbf{L} \otimes \mathbf{M}^0 \boldsymbol{\eta}$. Finally, if a non-repairable failure on the online unit takes place then it is equal to

$$\mathbf{H}_3 = \mathbf{T}^0 \boldsymbol{\alpha} p_{in\_nre} \otimes \left(\mathbf{L} + \mathbf{L}^0 \boldsymbol{\gamma}\right) \otimes \left(\mathbf{M}^0 \boldsymbol{\eta} + \mathbf{M}\right) + \left(\mathbf{e}_n - \mathbf{T}^0\right) \boldsymbol{\alpha} \otimes \mathbf{L}^0 \boldsymbol{\gamma} p_{ex\_nre} \otimes \left(\mathbf{M}^0 \boldsymbol{\eta} + \mathbf{M}\right).$$

The warm standby units are introduced in the modelling in the following way. If r indicates the number of standby units which are broken at a certain time and l the number of units in the repair facility before that time, then we define the matrix whose elements are the transition probabilities among phases as

$$\mathbf{H}_{c,l,r} = \binom{K-l-1}{r} p^r (1-p)^{K-l-1-r} \mathbf{H}_c ,$$

where c = 0,1,2 depending on the type of event (0: the online keeps on working; 1: the online undergoes a repairable failure; 2: the online unit goes to preventive maintenance) and for $l = 0,\ldots, N-1$; $r \le N-l-1$.

If the online unit goes to repair facility, all warm standby units fail and a repair does not occur then

$$\mathbf{H}_{c,l,K-l-1}^{'} = p^{K-l-1} \mathbf{H}_c^{'}, \text{ for } c = 1, 2.$$

The matrix blocks of the MMAP that models the system have been built by considering the matrices described above. Next, the matrix $\mathbf{D}^{Or}$ is shown. This matrix contains the transition probabilities when the online unit keeps on working and r warm standby units fail at a certain time. This fact depends on the number of units in the repair facility before and after the transition time. The block (l, k) of the following matrix corresponds to this transition between the macro-states E^l and E^k. This matrix is given by

$$\mathbf{D}^{O0} = \begin{pmatrix} \mathbf{D}_{00}^{O0} & \mathbf{0} & \mathbf{0} & \cdots & \mathbf{0} & \mathbf{0} \\ \mathbf{D}_{10}^{O0} & \mathbf{D}_{11}^{O0} & \mathbf{0} & \cdots & \mathbf{0} & \mathbf{0} \\ \mathbf{0} & \mathbf{D}_{21}^{O0} & \mathbf{D}_{22}^{O0} & \cdots & \mathbf{0} & \mathbf{0} \\ \vdots & & \ddots & \ddots & & \vdots \\ \mathbf{0} & & & \mathbf{D}_{K-1,K-2}^{O0} & \mathbf{D}_{K-1,K-1}^{O0} & \mathbf{0} \\ \mathbf{0} & \cdots & & & \mathbf{D}_{K,K-1}^{O0} & \mathbf{D}_{KK}^{O0} \end{pmatrix},$$

$r = 1,\ldots, K-2,$

$$\mathbf{D}^{Or} = \begin{pmatrix} \mathbf{0} & \cdots & \mathbf{0} & \mathbf{D}_{0r}^{Or} & \mathbf{0} & \mathbf{0} & \cdots & & & \mathbf{0} \\ \mathbf{0} & \cdots & \mathbf{0} & \mathbf{D}_{1r}^{Or} & \mathbf{D}_{1,r+1}^{Or} & \mathbf{0} & \cdots & & & \mathbf{0} \\ \vdots & & \vdots & \mathbf{0} & \mathbf{D}_{2,r+1}^{Or} & \mathbf{D}_{2,r+2}^{Or} & \mathbf{0} & \cdots & & \vdots \\ & & & \vdots & \ddots & \ddots & \ddots & & & \\ & & & & & \mathbf{0} & \mathbf{D}_{K-r-2,K-3}^{Or} & \mathbf{D}_{K-r-2,K-2}^{Or} & & \\ & & & & & & \mathbf{0} & \mathbf{D}_{K-r-1,K-2}^{Or} & \mathbf{D}_{K-r-1,K-1}^{Or} & \mathbf{0} \\ \mathbf{0} & & \mathbf{0} & \mathbf{0} & \cdots & \cdots & \mathbf{0} & \mathbf{0} & \mathbf{0} & \mathbf{0} \\ \vdots & & \vdots & \vdots & & & & & & \vdots \\ \mathbf{0} & \cdots & \mathbf{0} & \mathbf{0} & \cdots & & & & \cdots & \mathbf{0} \end{pmatrix},$$

and $\mathbf{D}^{O,K-1} = \begin{pmatrix} \mathbf{0} & \cdots & \mathbf{0} & \mathbf{D}_{0,K-1}^{O,K-1} & \mathbf{0} \\ \mathbf{0} & \cdots & \mathbf{0} & \mathbf{0} & \mathbf{0} \\ \vdots & & \vdots & \vdots & \vdots \\ \mathbf{0} & \cdots & \mathbf{0} & \mathbf{0} & \mathbf{0} \end{pmatrix}.$

The matrices $\mathbf{D}_{lk}^{Or}$ are composed by matrix blocks corresponding to the transition between macro-states $E_{i_1,\ldots,i_l}$ and $E_{i_1,\ldots,i_k}$. The matrix block $\mathbf{D}_{lk}^{Or}(i_1,\ldots,i_k \mid i_1,\ldots,i_l)$ contains the transition probabilities described by considering the order in queue of failure types before and after transition. Then,

$\mathbf{D}_{00}^{O0} = \mathbf{H}_{0,0,0}$,

$\mathbf{D}_{0r}^{Or}(i_1,\ldots,i_r) = \left(\mathbf{H}_{0,0,r} + \mathbf{H}_{2,0,r}^{'} I_{\{r=N-1\}}\right) \otimes \boldsymbol{\beta}^{i_1}$; $i_s = 0, s = 1,...,r$; $r = 1,...,N-1$,

$\mathbf{D}_{l,l+r}^{Or}(i_1,\ldots,i_{l+r} \mid j_1,\ldots,j_l) = \left[\mathbf{H}_{0,l,r} + \mathbf{H}_{2,l,r}^{'} I_{\{r=N-l-1\}}\right] \otimes \mathbf{S}_{j_1}$; $l = 1,\ldots,N-1$, $r = 0,\ldots,N-l-1$, $i_s = j_s, s = 1,...,l$, $i_{l+s} = 0, s = 1,...,r,$

$\mathbf{D}_{l,l+r-1}^{Or}(i_1,\ldots,i_{l+r-1} \mid j_1,\ldots,j_l) = \mathbf{H}_{0,l,r} \otimes \mathbf{S}_{j_1}^{0} \left(I_{\{l>1 \text{ or } r\neq 0\}} \boldsymbol{\beta}^{i_1} + I_{\{l=1,r=0\}}\right)$; for $l = 1,\ldots,N-1$, $r = 0,\ldots,N-l-1$, $i_{s-1} = j_s, s = 2,...,l$, $i_{l+s} = 0, s = 0,...,r-1,$

and

$\mathbf{D}_{N,N-1}^{Or}(i_1,\ldots,i_{N-1} \mid j_1,\ldots,j_N) = \boldsymbol{\alpha} \otimes \left(\mathbf{L} + \mathbf{L}^0 \boldsymbol{\gamma}\right) \otimes \boldsymbol{\eta} \otimes \mathbf{S}_{j_1}^{0} \boldsymbol{\beta}^{i_1}$; $i_{s-1} = j_s, s = 2,...,N$,

$\mathbf{D}_{K,K}^{Or}(i_1,\ldots,i_N \mid j_1,\ldots,j_N) = \left(\mathbf{L} + \mathbf{L}^0 \boldsymbol{\gamma}\right) \otimes \mathbf{S}_{j_1}$; $i_s = j_s, s = 1,...,N$,

where $I_{\{\}}$ is the indicatory function.

The rest of the matrices can be worked out in a similar way.

Given the MMAP that governs the behavior of the system, the transition probability matrix associated to the Markov process is given as the addition of the matrices built above. Thus,

$$\mathbf{P} = \sum_{r=0}^{K-1} \left(\mathbf{D}^{Or} + \mathbf{D}^{Ar} + \mathbf{D}^{Br} + \mathbf{D}^{Cr} \right).$$

The transient distribution of the model can be worked out from the transition probability matrix by considering the different matrix blocks. The probability that at time ν the system is in the different states of the macro-state E^k is given by

$$p_{E^k}^{\nu} = \sum_{l=0}^{K} \boldsymbol{\omega}_l \mathbf{D}_{lk}^{(\nu)},$$

where $\boldsymbol{\omega} = \left(\boldsymbol{\omega}_0, \boldsymbol{\omega}_1, \ldots, \boldsymbol{\omega}_K \right)$ is the initial distribution.

4 Performance measures

Some performance measures have been calculated in an algorithmic form for the system described in this work. I focus on the mean times in each macro-state and on the mean number of events up to a certain time.

4.1 Mean times

Mean sojourn time in macro-state k up to a certain time

It is well-known that the sojourn mean time at any macro-state *k* up to time ν can be worked out as

$$\psi_k^{\nu} = \sum_{m=0}^{\nu} p_{E^k}^m \mathbf{e}, \quad \text{for } k = 0, 1, \ldots, N.$$

Mean working time on standby repairable failures up to a certain time

The mean time that the repairman is working on standby repairable failures from the beginning up to time ν is given by

$$\psi_{stby}^{\nu} = \sum_{m=0}^{\nu} \sum_{k=1}^{N-1} p_{E^k}^m \mathbf{e}_{1:3^{k-1} nt\varepsilon z_0} + \sum_{m=0}^{\nu} p_{E^K}^m \mathbf{e}_{1:2\cdot 3^{N-2} tz_0}.$$

Mean working time on online repairable failures up to a certain time

The mean time that the repairman is working on repairable failures of online units from the beginning up to time ν is given by

$$\psi_{online}^{\nu} = \sum_{m=0}^{\nu} \sum_{k=1}^{N-1} p_{E^k}^m \mathbf{e}_{3^{k-1} nt\varepsilon z_0 + 1:3^{k-1} nt\varepsilon (z_0 + z_1)} + \sum_{m=0}^{\nu} p_{E^K}^m \mathbf{e}_{2\cdot 3^{N-2} tz_0 + 1:2\cdot 3^{N-2} t(z_0 + z_1)}.$$

Working mean time on preventive maintenance up to a certain time

The mean time that the repairman is working on preventive maintenance from the beginning up to time ν is given by

$$\psi_{pm}^{\nu} = \sum_{m=0}^{\nu} \sum_{k=1}^{N-1} p_{E^k}^m \mathbf{e}_{3^{k-1} nt\varepsilon (z_0 + z_1) + 1:3^{k-1} nt\varepsilon (z_0 + z_1 + z_2)} + \sum_{m=0}^{\nu} p_{E^K}^m \mathbf{e}_{2\cdot 3^{N-2} t(z_0 + z_1) + 1:2\cdot 3^{N-2} t(z_0 + z_1 + z_2)}.$$

4.2 Mean number of events

The system is subject to several types of events; repairable and non-repairable failures and preventive maintenance. These events are happening by time and it is interesting to analyse the mean number of these ones up to a certain time.

Thus, the mean number of repairable failures of the online unit up to a certain time ν is

$$\Gamma_{re}^{\nu} = \boldsymbol{\omega} \sum_{m=1}^{\nu} \mathbf{P}^{m-1} \mathbf{D}^{A} \mathbf{e} ,$$

where $\mathbf{D}^{A} = \sum_{r=0}^{N-1} \mathbf{D}^{A,r}$.

Analogously, the mean number of non-repairable failures and major revisions of the online unit up to a certain time ν is equal to these expressions respectively,

$$\Gamma_{nre}^{\nu} = \boldsymbol{\omega} \sum_{m=1}^{\nu} \mathbf{P}^{m-1} \mathbf{D}^{C} \mathbf{e} \text{ and } \Gamma_{pm}^{\nu} = \boldsymbol{\omega} \sum_{m=1}^{\nu} \mathbf{P}^{m-1} \mathbf{D}^{B} \mathbf{e} ,$$

where $\mathbf{D}^{B} = \sum_{r=0}^{N-1} \mathbf{D}^{B,r}$ and $\mathbf{D}^{C} = \sum_{r=0}^{N-1} \mathbf{D}^{C,r}$.

Finally, the mean number of warm standby units that fail up to a certain time ν is equal to

$$\Gamma_{stby}^{\nu} = \boldsymbol{\omega} \sum_{m=1}^{\nu} \mathbf{P}^{m-1} \sum_{r=1}^{N-1} r \left[\mathbf{D}^{Or} + \mathbf{D}^{Ar} + \mathbf{D}^{Br} + \mathbf{D}^{Cr} \right] \mathbf{e} .$$

5 Numerical example

We assume a system with 3 units, the online one and the rest in warm standby. The objective of this study is to analyze the effectiveness of preventive maintenance in the behavior of the reliability system. The lifetime distribution for the online unit, the time distributions between two external shocks and two inspections, the preventive maintenance time distribution and the repair time distributions according to the types of failures are given in tables 1 and 2. When an internal failure occurs, this one is repairable with probability $p_{\text{in\_re}}$ =0.8 and non-repairable with probability $p_{\text{in\_nre}}$=0.2. Any standby unit can undergo a repairable failure at any moment with probability p = 0.001 and a failure due to external shock is repairable with probability $p_{\text{ex\_re}}$=0.7.

The internal behavior of the online unit is composed of three phases (good, fair, poor). The inspections over this unit occur randomly with a mean time between two consecutive inspections equal to 10 units of time. In this case, the online unit is inspected and if phase three (poor) is observed then the unit goes to repair facility for preventive maintenance. The online unit is subject to external shocks. The mean time between two consecutive shocks is equal to 143.16 units of time.

Lifetime distribution online unit	Time distribution between two external shocks	Time distribution between two consecutive inspections
$\boldsymbol{\alpha} = (1,0,0)$	$\boldsymbol{\gamma} = (1,0)$	$\boldsymbol{\eta} = (1,0)$
$\mathbf{T} = \begin{pmatrix} 0.995 & 0.005 & 0 \\ 0 & 0.95 & 0.05 \\ 0 & 0 & 0.95 \end{pmatrix}$	$\mathbf{L} = \begin{pmatrix} 0.987 & 0.006 \\ 0.995 & 0.0005 \end{pmatrix}$	$\mathbf{M} = \begin{pmatrix} 0.8 & 0.1 \\ 0.5 & 0.4 \end{pmatrix}$

Table 1. Time to events distributions

Corrective repair distribution warm standby unit	Corrective repair distribution on line unit	Preventive maintenance time distribution
$\boldsymbol{\beta}_0 = (1,0)$	$\boldsymbol{\beta}_1 = (1,0)$	$\boldsymbol{\beta}_2 = (1,0)$
$\mathbf{S}_0 = \begin{pmatrix} 0.05 & 0.45 \\ 0.4 & 0.15 \end{pmatrix}$	$\mathbf{S}_1 = \begin{pmatrix} 0.7 & 0.26 \\ 0.6 & 0.1 \end{pmatrix}$	$\mathbf{S}_2 = \begin{pmatrix} 0.005 & 0.002 \\ 0.001 & 0.002 \end{pmatrix}$

Table 2. Time to repair and preventive maintenance distributions

Some measures associated to both systems, with and without preventive maintenance, have been compared to analyze the effectiveness of preventive maintenance. Table 3 shows the mean number of events occurred up to a certain time for both systems, with and without preventive maintenance, respectively.

Time (ν)	Γ^{ν}_{re}	Γ^{ν}_{nre}	Γ^{ν}_{pm}	Γ^{ν}_{stby}
50	0.2739 (0.3004)	0.1122 (0.1188)	0.0699 (-----)	0.0974 (0.0974)
100	0.5686 (0.6682)	0.2206 (0.2546)	0.1894 (-----)	0.1940 (0.1935)
1000	5.8910 (7.4237)	2.3473 (2.7328)	2.3804 (-----)	1.9308 (1.9199)
5000	29.5461 (37.4496)	11.7594 (13.7474)	12.1188 (-----)	9.6501 (9.5932)
10000	59.1150 (74.9819)	23.5245 (27.5155)	24.2918 (-----)	19.2991 (19.1848)
20000	118.2528 (150.0466)	47.0548 (55.0519)	48.6378 (-----)	38.5973 (38.3680)

Table 3. Mean number of events (repairable and non-repairable failures of the online unit, major revisions inspected and standby failures) for both systems (without preventive maintenance between parentheses) up to a certain time

Acknowledgements

This paper is partially supported by the Junta de Andalucía, Spain, under the grant FQM-307 and by the Ministerio de Economía y Competitividad, España, under Grant MTM2013-47929-P.

References

1. Lisnianski, A. and Frenkel, I. (2012) *Recent Advances in System Reliability: Signatures, Multi-state Systems and Statistical Inference*. Springer-Verlag London Limited.
2. Lisnianski, A.; Frenkel, I. and Ding, Y. (2010) *Multi-state System Reliability Analysis and Optimization for Engineers and Industrial Managers*. Springer-Verlag London Limited.
3. Nakagawa, T. (2005) *Maintenance Theory on Reliability*. Springer Series in Reliability Engineering series. Springer-Verlag London Limited.
4. Neuts, M.F. (1979) A versatile Markovian point process. *Journal of Applied Probability*, **16**, 764-779.
5. Neuts, M.F. (1981). *Matrix geometric solutions in stochastic models. An algorithmic approach*. Baltimore, John Hopkins, University Press.
6. Neuts, M.F. (1975) Probability Distributions of Phase Type. *Liber Amicorum Prof. Emeritus H. Florin*, Belgium: Department of Mathematics, University of Louvain, pp. 183–206.
7. Ruiz-Castro, J.E. (2013) A preventive maintenance policy for a standby system subject to internal failures and external shocks with loss of units. *International Journal of Systems Science*. DOI: 10.1080/00207721.2013.827258.
8. Ruiz-Castro, J.E. (2014) Preventive maintenance of a multi-state device subject to internal failure and damage due to external shocks. *IEEE Transactions on Reliability*, 63, 2, 646-660.

American-style Asian Options Under Jump-diffusion Processes with Geometric Average

Stefane Saize[1] and Johan Tysk[2]

[1] Eduardo Mondlane University, Maputo, Mozambique
(E-mail: Email: stefanesaize@gmail.com)
[2] Uppsala University, Uppsala, Sweden
(E-mail: Email: johan.tysk@math.uu.se)

Abstract. In this paper we derive the analytical solutions to the American-style Asian Options under jump-diffusion processes. The similar problem was studied by Hansen and Jorgensen[4], but they studied the diffusion case. First of all we transform the problem into one-state variable problem (the dual problem). To this new problem, we find its general analytical solution by using theories from Hansen and Jorgensen [4], Merton [8] and H. Pham [10]. Also we derive the analytical solutions to the particular case, when the average is geometric. At the end of this paper we have some numerical results comparing the earlier exercise boundaries in diffusion and jump-diffusion cases.
Keywords: Dual problem, Diffusion processes, Jump-diffusion processes, Equivalent measure, Lognormal jump sizes, American option, Asian option. .

1 Introduction

An Asian option is a financial derivative for which its payoff function is characterized by involvement of a stock price average. These types of options reduce the risk of manipulations of the stock price at maturity and they are cheaper than standard European and American options. In this paper we will consider the contract function with so called floating strike price i.e, the strike price is an average of the stoke price. In addition we will consider the discontinuous stoke price. Merton[8] studied the case of European call option for a simple contract function (vanilla option) under jump-diffusion processes and he stablished the general form of the solution for vanilla option and the particular case, when the jump sizes follow the lognormal distribution. In a paper Huên Pham[10], is studied the American put option for a simple contract function under jump-diffusion model and there is stated the analytical solution to the problem, the exercise boundary and their properties. Also Gukal[3] has considered the problem of option pricing under jump diffusion model using the idea of Merton[8], and stated its analytical solutions.
In this paper, we will study the same problem as in Hansen and Jorgensen [4], but considering it under jump-diffusion process, instead. So, to achieve our results, we will use the results in a paper of Hanssen and Jorgensen[4], the theory established by Merton[8] and the result of Pham[10] and other references. Here we will find the general analytical solution of American-style Asian option

16th ASMDA Conference Proceedings, 30 June – 4 July 2015, Piraeus, Greece

under jump diffusion process, for the case of floating strike. Also we will study the particular case, when the average is geometric. At the end we have some numerical results.

2 The basic model

Let us consider a financial market consisting on two assets, the bond $B(t)$ which is a risk free asset, and a stock with price process $S(t)$, defined by the dynamics

$$dB(t) = rB(t)dt, \tag{1}$$
$$B(0) = 1, \tag{2}$$

where r is the risk free rate. Then $B(t) = e^{rt}$, and $S(t)$ satisfies following stochastic differential equation,

$$dS(t) = \mu S(t)dt + \sigma S(t)dW(t) + (X-1)S(t)dN_t, \quad S(0) = s, \tag{3}$$

where,

1. μ is a drift of the process;
2. σ the volatility of the stock price;
3. $W(t)$ is a standard Brownian motion;
4. N_t is a Poisson process with parameter λt;
5. X is a jump size in stock, if the a jump in the process N_t occurs;
6. X are *i.i.d.* random variables and $X-1$ is an impulse function producing a finite jump in S to XS ;
7. $W(t),\ N(t),\ X$ are mutually independent.

Therefore, $S(T) = S(t)\exp\left\{(\mu - \frac{1}{2}\sigma^2)(T-t) + \sigma(W(T) - W(t))\right\} \prod_{k=N_t+1}^{N_T} X_k.$

Before we consider the problem, when the average is geometric, let us first give the general solution for any tipe of average. So, in the next section we will discuss about the geral valuation of tyhe problem.

3 General valuation of the American-style Asian options under jump-difusion processes

As in Hansen and Jorgensen[4], our goal is to give an analytical solution $V(t,s)$ to the Americas-style Asian options, where the contract function is given by,

$$pay - off = [\rho(S(t) - A(t)]^+, \tag{4}$$

where $\rho = \pm 1$ and,

$$A(t) = exp\{\frac{1}{t}\int_0^t \ln S(\tau)d\tau\} \text{ the geometric average.}$$

But in in this paper we will consider this problem when the stock return are descontinuous. In a paper of Merton[8] is provided a method to solve the option pricing problems when the underlying stock returns are discontinuous for the the vanila option. In a paper of Hansen and Jorgensen[4] is given an analytical valuation for American-style Asian options. So, we will connect these theories and the results from Pham[10] in order to find an analytical valuation of American-style Asian options when underlying stock returns are discontinuous .
By the result from Karout and Karatzas[6] and Pham[10], we have that the solution of the free boundary problem is given

$$V(t) = ess \sup_{\tau \in \Gamma_{t,T}} E_t^Q \left\{ [\rho(S(\tau) - A(\tau))]^+ \right\}, \tag{5}$$

$$\tag{6}$$

where $\Gamma_{t,T}$ is a set of all stopping times taking values in $[t, T]$.
Now let

$$\xi(t) = e^{-rt}\frac{S(t)}{S(0)} = exp\{-\frac{1}{2}\sigma^2 t + \sigma W(t) - \lambda E[X-1]t\}\prod_{k=1}^{N_t} X_k. \tag{7}$$

Therefore, using Girsanov's theorem (see T. Björk[1] p. 164), let us introduce a new equivalent measure Q' such that $dQ' = \xi(T)dQ$, thus, the process $W^{Q'} = W^Q - \sigma t$ (see Hansen and Jorgensen[4] or Karout and Karatzas[6]), is a standard Brownian motion under Q' and the stock price satisfies the stochastic differential equation

$$dS(t) = (r + \sigma^2 - \lambda K)Sdt + \sigma dW^{Q'}(t) + (X-1)dY(t), \tag{8}$$

where $K = E[X-1]$.

As in Hansen and Jorgensen[4] let us transform (5) changing the measure Q into the equivalent measure Q'. Whence,

$$V(t) = ess \sup_{\tau \in \Gamma_{t,T}} E_t^Q \left\{ e^{-r(\tau-t)}[\rho(S(\tau) - A(\tau))]^+ \right\} = ess \sup_{\tau \in \Gamma_{t,T}} E_t^{Q'} \left\{ \frac{\xi(t)}{\xi T} e^{-r(\tau-t)}[\rho(S(\tau) - A(\tau))]^+ \right\}$$

$$= ess \sup_{\tau \in \Gamma_{t,T}} E_t^{Q'} \left\{ \frac{S(t)}{e^{rt}} e^{-r(\tau-t)}[\rho(S(\tau) - A(\tau))]^+ E_\tau^{Q'} \left[\frac{e^{rT}}{S(T)} \right] \right\}$$

$$= ess \sup_{\tau \in \Gamma_{t,T}} E_t^{Q'} \left\{ \frac{S(t)}{e^{rt}} e^{-r(\tau-t)} [\rho(S(\tau) - A(\tau))]^+ E_\tau^{Q'} \left[\frac{e^{rT}}{S(T)} \right] \right\}$$

$$= ess \sup_{\tau \in \Gamma_{t,T}} E_t^{Q'} \left\{ \frac{S(t)}{e^{rt}} \frac{e^{\tau}}{S(\tau)} e^{-r(\tau-t)} [\rho(S(\tau) - A(\tau))]^+ \right\} = ess \sup_{\tau \in \Gamma_{t,T}} E_t^{Q'} \left\{ S(t) [\rho(1 - \frac{A(\tau)}{S(\tau)})]^+ \right\}.$$

Therefore, we have reduced (5) into

$$V(t) = ess \sup_{\tau \in \Gamma_{t,T}} E_t^{Q'} \left\{ S(t) [\rho(1 - x(\tau))]^+ \right\} \tag{9}$$

where $x(\tau) = \frac{A(\tau)}{S(\tau)}$. According to Harrisson and Kreps[5], $\frac{V(t)}{S(t)}$ is a martingale.

Now let us derive the dynamics of $x(t)$. Applying the Ito's formula for a jump-diffusion process given by Proposition 8.14 from Cont and Tankov [2]:

$$dx(t) = \frac{dA(t)}{S(t)} - \frac{(r + \sigma^2 - \lambda K) A(t)}{S^2(t)} dt + \frac{\sigma^2 A(t)}{S^2(t)} dt - \sigma \frac{A(t)}{S(t)} dW^{Q'} + \left[\frac{A(t_- + \Delta t)}{S(t_- + \Delta t)} - \frac{A(t_-)}{S(t_-)} \right]$$

$$dx(t) = x(t) \left[\left(\frac{d \ln A(t)}{dt} - r - \sigma^2 + \lambda K \right) dt - \sigma dW^{Q'}(t) + \sigma^2 dt + \frac{\Delta[A(t)] + (1 - X) A(t)}{X S(t)} \right].$$

$$dx(t) = x(t) \left[\mu(t, x(t)) dt - \sigma dW^{Q'}(t) + \frac{1 - X}{X} dN_t \right],$$

where $\mu(t, x(t)) = \left(\frac{d \ln A(t)}{dt} - r + \lambda K \right)$. Hence,

$$dx(t) = x(t) \left[\mu(t, x(t)) dt - \sigma dW^{Q'}(t) + \frac{1 - X}{X} dN_t \right]. \tag{10}$$

Denote by $\widetilde{V}(t)$ the expression $\frac{V(t)}{S(t)}$, then problem (5) is reduced to the following one-state variable problem (lets call it a **dual problem**) with strike price 1,

$$\widetilde{V}(t) = ess \sup_{\tau \in \Gamma_{t,T}} E_t^{Q'} \left\{ [\rho(1 - x(\tau))]^+ \right\}, \tag{11}$$

The optimal stopping time for this problem is τ_t^* such that $\tau_t^* = \inf\{\tau \in [t, T] : x(\tau) = b(\tau)\}$, where $b(\tau)$ is a boundary of the continuation (or the exercise) region. The regions has the following presentations:

1. Continuation region: $C = \{t \in [0, T] : \ \rho x(t) > \rho b(t)\}$;
2. Stopping region: $D = \{t \in [0, T] : \ \rho x(t) \leq \rho b(t)\}$.

From now on, we will study the dual problem (11), since $V(t) = S(t)\widetilde{V}(t)$. Then, by Theorem 1 in Hansen and Jorgengen[4], using the results of Merton[8] and the results in Gukhal[3] or Pham[10], the solution of the dual problem (11) will be given as follow

$$\begin{aligned}\widetilde{V}(t) = \sum_{n=0}^{\infty} \int \left[\frac{e^{-\lambda(T-t)}(\lambda(T-t))^n}{n!} \widetilde{v}(t, x(t)Z_n e^{\lambda K t}) + \widetilde{e}_J(t, x(t)Z_n e^{\lambda K t}) \right] F_n(dz) - \\ - \lambda E_t^{Q'} \left\{ \int_t^T E\left[g(J, x(s), b(s)) \right] ds \right\},\end{aligned} \tag{12}$$

where,

$$\begin{aligned}&\widetilde{e}_J(t, x(t)Z_n e^{\lambda K t}) = \int_t^T \frac{e^{-\lambda(\tau - t)}(\lambda(\tau - t))^n}{n!} E^{Q'}_{t, x(t)Z_n e^{\lambda K t}} \left\{ \rho \mu_1(\tau, x(\tau)) x(\tau) \mathbf{1}_D \right\} d\tau, \\ &g(J, x(s), b(s)) = \widetilde{V}(Jx(s), s) - (1 - Jx(s)) 1_{\rho\{x(s) \le \rho b(s), \rho J x(s) > \rho b(s)\}}\end{aligned},$$

and $\widetilde{v}(t)$ is defined in Theorem 1 in [4], F_n is a distribution function of

$$Z_n = \prod_{k=1}^{n} \frac{1}{X_k} = \prod_{k=1}^{n} J_k.$$

Let us adopt the following notation,

$$\int \widetilde{v}(t, x(t)Z_n e^{\lambda K t}) F_n(dz) = E_n[\widetilde{v}(t, x(t)Z_n e^{\lambda K t})]$$

and

$$\int \widetilde{e}_J(t, x(t)Z_n e^{-\lambda K t}) F_n(dz) = E_n[\widetilde{e}_J(t, x(t)Z_n e^{\lambda K t})].$$

So we have the following result:

Theorem 31 *The solution to the dual problem* (11) *when the underlying stock returns are discontinuous, is given by*

$$\begin{aligned}\widetilde{V}(t) = \sum_{n=0}^{\infty} \left[\frac{e^{-\lambda(T-t)}(\lambda(T-t))^n}{n!} E_n[\widetilde{v}(t, x(t)Z_n e^{\lambda K t})] + E_n[\widetilde{e}_J(t, x(t)Z_n e^{\lambda K t})] \right] - \\ - \lambda E_t^{Q'} \left\{ \int_t^T E\left[g(J, x(s), b(s)) \right] ds \right\}.\end{aligned} \tag{13}$$

where the first part in the right hand side, is the value of the corresponding European option with jumps, the second two terms correspond to the earlier exercise premium (the bonus by exercising the option before the maturity time T). The earlier exercise premium is composed by two terms, the first of the last two terms is a current value of the premium and the last one is the rebalancing cost due to jumps from the exercise region into continuation region (see Gukhal[3]). The last part of the right hand side, there is no an explicit form of it.

Proof: Since we know that $\widetilde{V}$ is a martingale under the measure Q', then in

the continuation region $C = \{t \in [0,T] : \ \rho x(t) > \rho b(t)\}$ the function $\widetilde{V}$ must satisfy the equation

$$d\widetilde{V} = \widetilde{V}_t dt + \widetilde{V}_x dx + \widetilde{V}_{xx}(dx)^2. \tag{14}$$

Therefore, from H. Pham [10] it is shown that, in a continuation region,

$$\widetilde{V} = \sum_{n=0}^{\infty} \frac{e^{\lambda(T-t)}(\lambda(T-t))^n}{n!} E_n[\widetilde{v}(t, x(t)Z_n e^{\lambda K t})], \tag{15}$$

and, Merton[8], have proved that the expression (15) is a solution to the problem, and by the martingale property in the continuation region

$$d\widetilde{V} = dM_1^{Q'}, \tag{16}$$

where M_1 is a martingale under measure Q'.
In other hand, if x belongs to the stopping region $D = \{t \in [0,T] : \ \rho x(t) \leq \rho b(t)\}$, then $\widetilde{V}(t) = \rho(1 - x(t))$, hence by Pham[10],

$$d\widetilde{V} = -\rho\mu_1(x(t),t)x(t)dt + \lambda E[\widetilde{V}(Jx,t) - (1 - Xx)1_{\{Jx > b(t)\}}]dt. \tag{17}$$

From (16) and (17) we have

$$d\widetilde{V} = \{-\rho\mu_1(x(t),t)x(t)dt + \lambda E[\widetilde{V}(Jx,t) - (1 - Jx)1_{\{\rho Jx > \rho b(t)\}}]dt\}_{\{\rho x(t) \leq \rho b(t)\}} + dM^{Q'}, \tag{18}$$

where $M^{Q'}$ is a martingale part under measure Q', and then the result follows.□

From Peskir[9] or Björk[1], we know that in the exercise region we have $\widetilde{V}(t) = \rho(1 - x(t))$, then the the exercise boundary must satisfy the following free boundary equation:

$$\begin{aligned} \rho(1 - b(t)) = \sum_{n=0}^{\infty} \left[\frac{e^{-\lambda T(-t)}(\lambda(T-t))^n}{n!} E_n[\widetilde{v}(t, b(t)Z_n e^{\lambda K t})] + E_n[\widetilde{e}_J(t, b(t)Z_n e^{\lambda K t})] \right] - \\ - \lambda E_{t,b(t)}^{Q'} \left\{ \int_t^T E\left[g(J, x(s), b(s))\right] ds \right\}. \end{aligned} \tag{19}$$

When the jump intensity λ is small enough or if the jump sizes have a small mean then, it will cause very small chances in the American option. So, the cost term in the solution of American option should be very small (see Kou et all[7]). Therefore, in this circumstances, the cost term is negligenciable.

4 American-style Asian options under jump-diffusion processes, when the average is geometric

To study this case, we will follow the previous theory taking in account that $A(t) = e^{\frac{1}{t}\int_0^t \ln S(\tau)d\tau}$.

In this case, $\frac{dA(t)}{A(t)} = \left(-\frac{1}{t^2}\int_0^t \ln S(\tau)d\tau - \ln S(t)\right) = -\frac{1}{t}\ln x(t)dt$. Therefore, the dynamics of the underlying asset $x(t)$ will be defined by

$$dx(t) = x(t)\left[\mu_g(t,x(t))dt - \sigma dW^{Q'}(t) + (J-1)dN_t\right], \tag{20}$$

where $[\mu_g(t,x(t)) = -\frac{1}{t}\ln x(t) - r + \lambda K$. Now, using Lemma 1 and Lemma A3 from Hansen and Jorgensen[4] and Theorem 31 with strike price $L = 1$ we prove the following Theorem:

Theorem 41 *In the geometric average case, the solution to the problem* (11)*, is given by*

$$\widetilde{V}(t) = \sum_{n=0}^{\infty} E_n\left\{\frac{e^{-\lambda(T-t)}(\lambda(T-t))^n}{n!}\widetilde{v}_n(t) + \widetilde{e}_{Jgn}(t, xZ_n e^{\lambda K(\tau-t)})\right\} - \lambda E_{t,x}^{Q'}\left\{\int_t^T E\left[g(J,x(\tau),b(\tau))\right]d\tau\right\},$$

where,

$\widetilde{v}_n(t) = \widetilde{v}(t, xZ_n e^{\lambda K(\tau-t)})$ *and*

$\widetilde{e}_{Jgn}(t, xZ_n e^{\lambda K(\tau-t)}) =$

$$= \int_t^T \frac{e^{-\lambda(\tau-t)}(\lambda(\tau-t))^n}{n!}\rho e^{\alpha_g(t,\tau)+\frac{1}{2}\beta_g^2(t,\tau)}[-(\frac{\alpha_g(t,\tau)+\beta_g^2(t,\tau)}{\tau}+r)\Phi(-\rho\frac{\alpha_g(t,\tau)+\beta_g^2(t,\tau)-\ln b(\tau)}{\beta_g(t,\tau)})$$
$$+\frac{\beta_g(t,\tau)}{\tau}\phi(\frac{\alpha_g(t,\tau)+\beta_g^2(t,\tau)-\ln b(\tau)}{\beta_g(t,\tau)})]d\tau,\ \textit{with}\ x(t) = xZ_n e^{\lambda K(\tau-t)}$$

4.1 The case when jumps sizes are i.i.d. lognormal random variables

Here we will give the solution for the case of geometric average under lognormal jump sizes. Let

$$S(T) = S(t)\exp\{(r+\lambda K - \frac{1}{2}\sigma^2)(T-t) + \sigma(W(T)-W(t)) + \sum_{k=1}^{N_t}\ln X_k\}, \tag{21}$$

where $\ln X_k \sim N(a, b^2)$, , $k = 1, 2, \ldots, N_t$. So, if in the interval $[t, T]$ we have exactly n jumps, then we know that

$$(r + \frac{1}{2}\sigma^2 - \lambda K)(T-t) + na + \sqrt{\sigma^2 + \frac{nb^2}{T-t}}(W(T) - W(t)) \sim$$
$$N((r + \frac{1}{2}\sigma^2 - \lambda K)(T-t) + na, \sigma^2(T-t) + nb^2).$$
Whence,

$$S(T) = S(t)\exp\{(r + \frac{1}{2}\sigma^2 - \lambda K)(T-t) + na + \sqrt{\sigma^2 + \frac{nb^2}{T-t}}(W(T) - W(t))\} \tag{22}$$

and hence

$$\ln S(T) \sim N(\ln S(t) + (r + \frac{1}{2}\sigma^2 - \lambda K)(T-t) + na, (\sigma^2 + \frac{nb^2}{T-t})(T-t). \tag{23}$$

Therefore, given $A(T) = e^{\frac{1}{T}\int_0^T \ln S(u)du}$. Then,

$$\ln A(T) = \frac{1}{T}\int_0^T \ln S(u)du = \frac{1}{T}\int_0^t \ln S(u)du + \frac{1}{T}\int_t^T \ln S(u)du$$

$$= \frac{t}{T}\ln A(t) + \frac{1}{T}\int_t^T \left(\ln S(t) + (r + \frac{1}{2}\sigma^2 - \lambda K)(u-t) + na + \sqrt{\sigma^2 + \frac{nb^2}{u-t}}\int_t^T dW(\tau)\right)du$$

$$= \frac{t}{T}\ln A(t) + \frac{T-t}{T}\ln S(t) + ((r + \frac{1}{2}\sigma^2 - \lambda K)\frac{(T-t)^2}{2T} + \frac{na(T-t)}{T}$$
$$+ \frac{1}{T}\int_t^T \sqrt{\sigma^2 + \frac{nb^2}{u-t}}\int_t^u dW(\tau)du$$

$$= \frac{t}{T}\ln A(t) + \frac{T-t}{T}\ln S(t) + ((r + \frac{1}{2}\sigma^2 - \lambda K)\frac{(T-t)^2}{2T} + \frac{na(T-t)}{T}$$

$$+ \frac{1}{T}\int_t^T \int_\tau^T \sqrt{\sigma^2 + \frac{nb^2}{u-t}}dudW(\tau)$$

$$= \frac{t}{T}\ln A(t) + \frac{T-t}{T}\ln S(t) + ((r + \frac{1}{2}\sigma^2 - \lambda K)\frac{(T-t)^2}{2T} + \frac{na(T-t)}{T}$$

$$+\frac{1}{T}\int_t^T \left(\theta(T,\tau,t)+T\sqrt{\sigma^2+\frac{nb^2}{T-t}}\right)dW(\tau),$$

where,

$\theta(T,\tau,t)=\int_\tau^T \sqrt{\sigma^2+\frac{nb^2}{u-t}}du - T\sqrt{\sigma^2+\frac{nb^2}{T-t}}$. Hence it leads us to the following result,

Lemma 42 *Let $S(t)$ satisfying the jump diffusion equation*

$$dS(t)=(r+\lambda K+\sigma^2)S(t)dt+\sigma S(t)dW(t)+S(t)(X-1)dY_t,$$

with $\ln X \sim N(a,b^2)$ and define $A(t)=e^{\frac{1}{t}\int_0^t \ln S(\tau)}$. Then for $T>t$, $\ln A(T)$ conditioned to F_t and n jumps follows a normal distribution with mean and variance given by

$$E[\ln A(t)]=\frac{t}{T}\ln A(t)+\frac{T-t}{T}\ln S(t)+((r-\frac{1}{2}\sigma^2-\lambda K)\frac{(T-t)^2}{2T}+\frac{na(T-t)}{T}$$

and

$$Var[A(t)]=\frac{1}{T^2}\int_t^T \left(\theta(T,\tau,t)+T\sqrt{\sigma^2+\frac{nb^2}{T-t}}\right)^2 d\tau.$$

Now let us find the distribution of $\ln X(T)$. Since $X(T)=\frac{A(T)}{S(T)}$ then,

$\ln X(T)=\ln A(T)-\ln S(T)=\frac{t}{T}\ln A(t)+\frac{T-t}{T}\ln S(t)+((r-\frac{1}{2}\sigma^2-\lambda K)\frac{(T-t)^2}{2T}+\frac{na(T-t)}{T}$

$$+\frac{1}{T}\int_t^T \left(\theta(T,\tau,t)+T\sqrt{\sigma^2+\frac{nb^2}{T-t}}\right)dW(\tau)-\ln S(t)-(r+\frac{1}{2}\sigma^2-\lambda K)(T-t)$$

$$-na-\sqrt{\sigma^2+\frac{nb^2}{T-t}}\int_t^T dW(\tau)$$

$$=\ln x(t)-\left(r-\lambda K+\frac{\sigma^2}{2}\right)\frac{(T^2-t^2)}{2T}-\frac{nat}{T}+\frac{1}{T}\int_t^T \theta(T,\tau,t)dW(\tau).$$

And so, we have proved the following lemma,

Lemma 43 *Let $T > t$ then $\ln x(T)|(\boldsymbol{F}_t \wedge N_t = n)$, follows a normal distribution with mean and variance given by*

$$\alpha_n(T,t) = E[x(T)] = \ln x(t) - \left(r - \lambda K + \frac{\sigma^2}{2}\right)\frac{(T^2 - t^2)}{2T} - \frac{nat}{T}$$

and

$$\beta_n^2(T,t) = Var[x(T)] = \frac{1}{T^2}\int_t^T \theta^2(T,\tau,t)d\tau.$$

According to Lemma 43 and Lemma A3 from Hansen and Jorgensen[4],

Theorem 44 *The solution to the problem* (11)*, in the geometric average case, under lognormal jump sizes, is given by* $\widetilde{V}(t) = \sum_{n=0}^{\infty}\left\{\frac{e^{-\lambda(T-t)}(\lambda(T-t))^n}{n!}\widetilde{\overline{v}}_n(t) + \widetilde{\overline{e}}_{Jgn}(x,t)\right\} -$
$\lambda E_t^{Q'}\left\{\int_t^T E\left[g(J,x(\tau),b(\tau))\right]d\tau\right\}$,
where,

$$\widetilde{\overline{v}}_n(t) = \rho\left\{\Phi\left(-\rho\frac{\alpha_{g,n}(t,T)}{\beta_{g,n}}\right) - e^{\alpha_{g,n}(t,T)+\frac{1}{2}\beta_{g,n}^2(t,T)}\Phi\left(-\rho\frac{\alpha_{g,n}(t,T)+\beta_{g,n}^2(t,T)}{\beta_{g,n}(t,T)}\right)\right\},$$

and,

$$\widetilde{\overline{e}}_{Jgn}(t) = \int_t^T \frac{e^{-\lambda(\tau-t)}(\lambda(\tau-t))^n}{n!}\exp\{\alpha_{g,n}(t,\tau) + \frac{1}{2}\beta_{g,n}^2(t,\tau)\}\times$$
$$\times[-\rho\left(\frac{\alpha_{g,n}(t,\tau)+\beta_{g,n}^2(t,\tau)}{\tau} + r\right)\Phi\left(-\rho\gamma_{g,n}(t,\tau)\right) + \frac{\beta_{g,n}}{\tau}\phi\left(\gamma_{g,n}(t,\tau)\right)]d\tau.$$

5 Free boundary and stopping region

The free boundary $b(t)$ is a smooth function (see Pham[10]) satisfying the following properties,

1. $\widetilde{V}(t,b(t)) = \rho(1-b(t)), \quad \forall t \in (0,T]$;
2. If $\rho x(t) \leq \rho b(t)$ (stopping region) then $\widetilde{V}(t,x(t))) = \rho(1-x(t))$;
3. If $\rho x(t) > \rho b(t)$ then solution $\widetilde{V}(t,x(t))$ satisfies the partial differential equation in the free boundary problem and $\widetilde{V}(t,x(t)) > \rho(1-x(t))$;

4. For a fixed time t, for all $\lambda_1, \lambda_2 \geq 0$ such that, $\lambda_1 < \lambda_2$ then $\rho b_{\lambda_1}(t) \geq \rho b_{\lambda_2}(t)$ (see for example, Figure (a));
5. For a fixed time t, for all a_1, a_2 such that, $a_1 < a_2$ then $\rho b_{a_1}(t) \geq \rho b_{a_2}(t)$ (see for example, Figure (b));
6. Contrary to the standard American options, in the American-style Asian options, $b(t)$ can be greater than the strike price (see Hansen and Jorgensen[4]).

6 Numerical results

Here we will get some numericall results for the free boundary $b(t)$. Hour goal here is to comprare the results from the diffusion and jump-diffusion cases. So, let us consider the case when jump intensity (λ) is small anough. So, we can negligenciate the cost term. Therefore, to solve the equation (19), we use the trapezoidal rule for the integral part.

In general for American-style Asian put options (call options) with floating

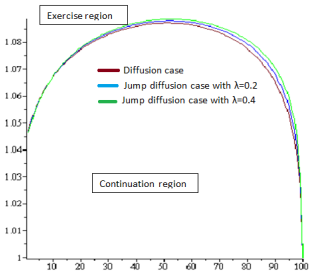

(a) Exercise boundary for diffusion and jump diffusion cases, for an American-style Asian put option with $\sigma = 0.2$, $T = 7/12$, $r = 0.05$.

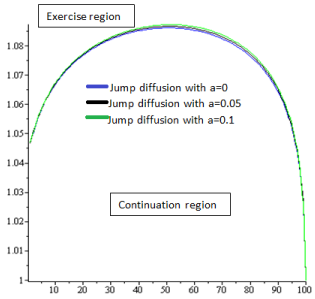

(b) Exercise boundary for jump diffusion case, for an American-style Asian put option with $\sigma = 0.2$, $T = 7/12$, $r = 0.05$.

strike, the exercise boundary in a jump-diffusion process is greater or equal (less or equal) to the exercise boundary in a diffusion process case. This property gives the investor to have no much hope to get good profit at the start of time, but the hope increases when the time increase and from certain time, the investor starts again to lose a hope of getting a good profit.

The picture above is the result from the simulation of $b(t)$, by setting ρ to be equal to -1. In this case we have a call option for the dual problem (11) which corresponds to the American-style Asian put option with floating strike, under diffusion processes. It shows us the behaviour of the earlier exercise boundary when the values of the parameter λ (figure (a)) and the average of jump sizes (figure (b)) change. So it is possible to see that, the exercise boundary as a function of jump intensity λ (figure (a)), is a nondecreasing function in the case of American-style Asian put option and nonincreasing function for an American-style Asian call option, with floating strike price.

From picture (b) we can see that, the exercise boundary as a function of the jump-size is nondecreasing (nonincreasing) function for the American-style Asian put (call) option with floating strike price.

7 Conclusion

In this paper we extend the Analytical valuation of American-style Asian option studied by Hansen and Jorgensen[4], to the case of jump-diffusion processes. This extension have never been considered anywhere before.
In our studies we derive the general solution for the American-style Asian options under jump-diffusion processes by solving the dual problem (the one-state variable problem). In a geometric average case we find that the one-state variable is a geometric Brownian motion and directly using the results of Merton[8], Hansen and Jorgensen[4], and Pham[10], we derive its analytical solution. And in the case of lognormal jumps, we derive a simplified solution to the problem. At the end we have some numerically results for the early exercise boundary in a diffusion as well as jump-diffusion processes cases. We find that the continuation region increases in jump-intensity λ and jump-size.

References

1. *Björk, T., Arbitrage Theory in contiuous time, third edition. New York, (2009)*
2. *Cont, R., Tankov, P., Financial modelling with jump processes. Chapman & HallICRC, USA (2004)*
3. *Gukhal, C. R., Analytical Valuation of American Options on Jump-Diffusin Pprocesses. Mathematical Finance, Vol. 11, No. 1 (January 2001), p.97-115.*
4. *Hansen, A.T., Jorgensen, P.L., Analytical Valuation of American-style Asian Options. Management Science, Vol. 46, No. 8 (Aug., 2000), pp. 1116-1136 .*
5. *Harrison and Kreps, Martingales and Arbitradge in Multperiod Securities Markets. Jornal of economic theory, 20:381-408.*
6. *Karout, N.E., Karatzas, I., The Optimal Stopping Problem for a General American Option*
7. *Kou, S., Petrella, G., Wang, H., Pricing Path-dependent Options With Jump Risk Via Laplace Transform. The Tokyo Economic Review, 74(1):1-23 (June 2005)*
8. *Merton, R. C., Option Pricing when the underlying Stock Returns are Discontinuous.* Journal of Financial Economics 3 125-144 (1976).
9. *Peskir, G., and Shiryaev, A., Optimal Stopping and Free-Boundary Problems. Birkhauser Verlag, Switzerland (2006)*
10. *Pham, H., Optimal Stopping, Free Boundary, and American Option in a Jump-Diffusion Model. Appl Math Optim 35:145-164 (1997).*